Simulation-Based Analysis of a Smart Heat Transfer Station

Enhancing Grid Stability and Energy Efficiency through Local Solar-to-Heat Conversion

M.R.W. van Hal



Simulation-Based Analysis of a Smart Heat Transfer Station

Enhancing Grid Stability and Energy Efficiency through Local Solar-to-Heat Conversion

by

M.R.W. van Hal

to obtain the degree of Master of Science
at the Delft University of Technology,
to be defended publicly on Thursday 24 July, 2025 at 3:00 PM.

Student number: 4915100

Project duration: November, 2024 – July, 2025

Thesis committee: Dr. ir. M. (Martin) Bloemendal, TU Delft

Prof. dr. P. (Phil) Vardon, TU Delft

Dr. ir. I. (Ivo) Pothof, Deltares, TU Delft

Ir. C. (Christiaan) van Soest, De WarmteTransistieMakers

Cover: "How Do District Heating Systems Work?", Water Treatment Ser-

vices (UK)

An electronic version of this thesis is available at http://repository.tudelft.nl/.





Preface

This thesis wraps up my time as a master's student at TU Delft, and it's the last chapter I'll write before my friends can officially call me Ir. It has been a valuable and sometimes intense journey, filled with countless learning moments. Writing this thesis turned out to be one of the most interesting parts of my studies. Although the beginning was challenging, figuring out the exact scope of my thesis, I found a rhythm and was able to really dive into the topic. It felt incredibly rewarding to explore such a relevant subject in depth.

With a background in Mechanical Engineering, I've always been interested in thermodynamics and energy systems. This thesis allowed me to apply that interest in a broader context, combining system design with themes like the energy transition, environmental responsibility, and real-world implementation.

I would like to thank Christiaan and everyone at De WarmteTransitieMakers for giving me the opportunity to work on such a meaningful project. Your guidance, trust, and clear feedback helped me grow, not only in knowledge, but also on a personal level.

A big thanks also to Martin for your constructive input, quick responses, and the freedom you gave me to steer this thesis in the direction I found most interesting. I would also like to thank Ivo and Phil for taking part in the thesis committee and providing valuable feedback.

A special thanks to Barbara, thank you for always being there, for listening, encouraging, and occasionally letting me blow off steam. Thank you as well for reading through my report and giving feedback, even when I didn't always show how much I appreciated it. Your patience and steady support were all that I needed. I couldn't have done this without you.

To my family: your support means a lot. From practical stuff to just being around, you were there when it counted. As a base in Utrecht to save travel time, a place to vent and reset, or just knowing you were there, it was always appreciated. To my mom, sorry for pushing you a bit too hard to get a heat pump in your new house. I guess that's what happens when your son writes a thesis about them.

M.R.W. van Hal Delft, July 2025

Abstract

Solar panel adoption increases in residential areas, so electricity grids face growing pressure from peak feed-in, especially during hours with high radiation during summer months. In this thesis, the potential of a Smart Heat Transfer Station (SHTS) to alleviate these challenges by converting surplus solar-generated electricity into usable heat for district heating networks (DHN) is investigated. The SHTS aims to improve local energy system performance by enhancing flexibility, reducing grid feed-in congestion, and increasing renewable self-consumption.

A Python-based simulation model is developed to evaluate the technical and economic performance of the SHTS under realistic conditions. The model integrates solar panels, a heat pump, an electric boiler, and a tank thermal energy storage system (TTES).

The strategy proved robust enough to perform effectively under varying solar radiation and thermal demand conditions. Simulation results show that the SHTS can significantly reduce electricity feed-in, by using up to 86% of generated solar electricity internally, and lower CO_2 emissions by replacing district heating demand with local heat production. Optimal configurations depend on a trade-off between system efficiency, emissions, and cost. High solar availability, a well-sized TTES, and a balanced combination of heat pump and electric boiler capacities are found to be critical for the performance of the SHTS.

Despite spatial constraints and regulatory uncertainties, the SHTS presents a promising, scalable solution for energy systems with high solar panel integration. It offers grid operators relief from feed-in congestion without reinforcements in the electricity grid and behavioral change from end users. Additionally, this allows heat providers to increase the share of renewable heat in their supply, while ensuring the service remains both affordable and reliable for end users.

This study presents a practical, simulation-based framework with rule-based control for evaluating and optimizing innovative systems, such as the SHTS, providing insights into how SHTSs can enhance the utilization of locally generated energy. By identifying the key technical and economic conditions for successful implementation, it lays the groundwork for real-world deployment. Future research should focus on integrating predictive control algorithms, which can improve system responsiveness by anticipating solar availability and demand patterns. Additionally, future work should examine regulatory and spatial constraints and analyze the aggregated behavior of multiple SHTS units.

Contents

Pr	eface	9	i
Αb	strac	ct	ii
No	men	clature	viii
1		oduction	1
	1.1	The Challenge of Grid Congestion	1
	1.2	Current Research and Knowledge Gaps	1
	1.3	De WarmteTransitieMakers	2
	1.4	The Potential of SHTS	2
	1.5	Research questions	3 3
	1.6	Structure of the thesis	3
2	Lite	rature	4
	2.1	Energy demand	4
		2.1.1 Heat demand	4
		2.1.2 Electricity demand	5
	2.2	District Heating Networks	7
		2.2.1 Heating systems	7
		2.2.2 Technical aspects	7
		2.2.3 Innovations and Trends	8
	2.3	Electricity Grid	9
		2.3.1 Grid congestion	9
	2.4	Energy storage	12
		2.4.1 Thermal storage	12
		2.4.2 Electrical storage	13
	2.5	Heat pumps	14
		2.5.1 Types of Heat Pumps	14
		2.5.2 Technical Aspects	14
		2.5.3 Market Trends and Policy Implications	16
	2.6	Conventional heat transfer station	17
		2.6.1 Components	17
	0.7	2.6.2 Thermal Demand and Capacity	18
	2.7	Smart Technologies for Energy Systems	19
	2.8	CO ₂ emissions	21
	2.9	Electricity and heat pricing	24
	2.10	Key Components SHTS	25
3	Meth	hod	27
	3.1	Modes of operation	27
		3.1.1 Heat pump	29
		3.1.2 E-boiler	32
		3.1.3 Tank thermal energy storage	33
	3.2	Input Variables	36
	3.3	Asset Optimization	38
	3.4	Assessment Framework	39
		3.4.1 Technical metrics	39
		3.4.2 Greenhouse Gas Emissions	40
		3.4.3 Economic Evaluation	41
	3.5	Model Verification	43

Contents

4	Results	44
	4.1 Sensitivity Analysis	44
	4.2 Assessment Parameters	46
	4.3 Operational Behavior	48
	4.4 Economic Benefit	57
	4.5 Optimal Configurations	59
	4.5.1 Technical Performance Evaluation	59
	4.5.2 Economic Performance Analysis	63
	4.6 SHTS Design Trade-offs	66
5	Discussion	68
	5.1 Model Limitations	68
	5.2 System Design Considerations and Sensitivity	69
	5.3 Strategic, Social, and Policy Implications	
	5.4 Real-Life Implementation Challenges	71
6	Conclusion	73
7	Recommendations	75
Re	eferences	76
Δ	Thermal Stratified Tank Model	82

List of Figures

2.1	Daily heat demand profile [87]	4
2.2	Yearly heat demand profile [87]	5
2.3	Daily electricity demand [21]	5
2.4	Yearly electricity demand [21]	6
2.5	Daily profile of EV charging [90]	6
2.6	Heat generation sources [24]	7
2.7	High voltage grid congestion map (electricity consumption)[76]	10
2.8	High voltage grid congestion map (electricity feed-in)[76]	10
2.9	Medium-voltage grid congestion map (electricity consumption)[76]	10
2.10	Medium-voltage grid congestion map (electricity feed-in)[76]	10
	Latent heat storage [55]	12
2.12	Vapor compression cycle used in heat pumps [83]	15
2.13	Forecast of the number of installed residential HPs (excluding air-to-air HPs) [68]	16
	Schematic set up Heat Transfer Station	17
2.15	A Heat Transfer Station in Amsterdam [56]	18
2.16	The EU ETS carbon price evolution until 2030 [54]	21
2.17	The EU ETS carbon price evolution after 2030 [54]	21
	Average life-cycle CO_2 equivalent emissions [92]	22
	Electricity produced by energy source [73]	23
	Average electricity price per hour per month (2024)	24
	Reproduction of the schematic Heat Transfer Station, see figure 2.14, for clarity	25
2.22	A schematic view of an SHTS	26
3.1	Mode of operation during summer months	28
3.2	Mode of operation during spring and autumn months	28
3.3	Mode of operation during winter months	29
3.4	COP at different outside temperatures	30
3.5	COP at different partial load ratios	31
11	Thermal energy in the TTEC during the first two weeks of June	48
4.1 4.2	Thermal energy in the TTES during the first two weeks of June	40 49
4.2 4.3	Thermal energy in the TTES during the first two weeks of February	49 49
4.3 4.4	Thermal energy in the TTES during the first two weeks of March	49
4.4	in table 4.3	50
4.5	Solar and grid consumption of the HP and e-boiler	51
4.5 4.6	Smoothed daily electricity input into the SHTS, split by grid and solar	51
4.0 4.7	Cumulative electricity input into the SHTS, split by grid and solar	52
4.7 4.8	Total and feed-in solar electricity in the first two weeks of June	52
	Total and feed-in solar electricity in the whole year 2024	53
	Heat covered during the first two weeks of June	53
	Direct heat supply during the first two weeks of June	54
	Heat covered during the whole year (2024)	54
	COP of the heat pump during the first two weeks of June	55
	COP of the heat pump during the whole year (2024)	55
	NPV of the SHTS as a function of the system lifetime	58
	SCOP vs. heat coverage, colored by E-boiler capacity	60
	SCOP vs. heat coverage, colored by HP capacity	60
	SCOP vs. heat coverage, colored by TTES capacity	60
	Grid feed-in vs. heat coverage, colored by E-boiler capacity	61
	Grid feed-in vs. heat coverage, colored by HP capacity	61

List of Figures vi

4.21	Grid feed-in vs. heat coverage, colored by TTES capacity	61
4.22	CO_2 emission savings vs. heat coverage, colored by E-boiler capacity	62
	2 2 2	62
		62
4.25		63
4.26		63
4.27		63
		64
		64
		64
	Optimal configurations per performance indicator, plotted by system SCOP and heat coverage	
	71 75	66
		67
		67
4.35	Optimal configurations per performance indicator plotted by NPV and heat coverage	67
۸ 1	Multi Nada madaling of stratified thermal aparay storage tank [6]	82
	5 · · · · · · · · · · · · · · · · · · ·	-
	, , , , , , , , , , , , , , , , , , , ,	84
A.3	Energy and mass flows within the tank model, during charging and discharging	85

List of Tables

2.1	Temperatures of DHN	8
	Legend for grid congestion maps	
3.1	TTES volume corresponding to capacity at $\Delta T=30^{\circ} {\rm C}$ (based on 300 households)	34
3.2	Model Input Data	36
3.3	Overview of Key Model Assumptions	37
3.4	Parameter Ranges for Asset Optimization	38
3.5	Validation of model outputs against reference data	43
4.1	Base configuration of the SHTS	44
4.2	Sensitivity analysis for the SHTS components	45
4.3	Performance metrics of the SHTS for the base scenario	46
4.4	Impact metrics of the SHTS	47
4.5	Economic performance metrics of the SHTS for the base scenario	57
	Parameter Ranges for Asset Optimization	59
4.7	Optimal SCOP parameters	60
4.8	Optimal grid feed-in parameters	61
	Optimal CO_2 emission saving parameters	62
4.10	Optimal LCOH parameters	63
4.11	Optimal NPV parameters	64
	Summary of optimal configurations per performance indicator	66

Nomenclature

Abbreviations

Abbreviation	Definition
ATES	Aquifer Thermal Energy Storage
AWHP	Air-to-Water Heat Pump
BESS	Battery Energy Storage System
BTES	Borehole Thermal Energy Storage
CapEx	Capital Expenditure
CF	Cash Flow
COP	Coefficient of Performance
DHN	District Heating Network
DHW	Domestic Hot Water
DWTM	De WarmteTransitieMakers
EHP	Electric Heat Pump
EV	Electric Vehicle
FLH	Full Load Hours
HP	Heat Pump
HTS	Heat Transfer Station
IRR	Internal Rate of Return
LCOH	Levelized Cost of Heat
LHS	Latent Heat Storage
NMDA	Niet Meer Dan Anders
NPV	Net Present Value
OpEx	Operational Expenditure
PCM	Phase Change Material
PHH	Prosumer Heat Hub
PLR	Partial Load Ratio
RES	Renewable Energy Sources
PV	Photovoltaic
SCOP	Seasonal Coefficient of Performance
SDHN	Smart District Heating Network
SHS	Sensible Heat Storage
SHTS	Smart Heat Transfer Station
TES	Thermal Energy Storage
TOU	Time-of-Use
TTES	Tank Thermal Energy Storage
V2G	Vehicle-to-Grid
VPP	Virtual Power Plant
WCW	Wet Collectieve Warmte

List of Tables ix

Symbols

Symbol	Definition	Unit
\overline{A}	Area	[m ²]
C_w	Specific heat capacity of water	[J/(kg·K)]
E	Electricity or Energy	[kWh]
h	Heat transfer coefficient	[W/m ² K]
I	Absolute sensitivity index	[-]
m	Mass	[kg]
\dot{m}	Mass flow rate	[kg/s]
P	Power	[W]
Q	Thermal capacity	[kWh]
r	Discount rate	[-]
t	Time	[s or years]
T	Temperature	$[^{\circ}C$ or K $]$
T_{source}	Supply temperature from HP/E-boiler	$[^{\circ}C$]
T_{return}	Return temperature to the source	$[^{\circ}C$]
T_{top}	Top layer temperature in TTES	$[^{\circ}C$]
Tamb	Ambient temperature	$[^{\circ}C\]$
ΔT	Temperature difference	$[^{\circ}C$ or K $]$
U	Heat transfer coefficient	[W/(m ² ·K)]
V	Volume	$[m^3]$
Δ	Difference or change	[-]
ho	Density of water	[kg/m³]
$\overset{\cdot}{\eta}$	Efficiency factor	[-]
λ_{eff}	Effective thermal conductivity	[W/(m·K)]
$\epsilon_{el,grid}$	Emission factor of grid electricity	[kgCO ₂ /kWh]
€heat,DHN	Emission factor of district heating	[kgCO ₂ /kWh]

1 Introduction

1.1. The Challenge of Grid Congestion

The Dutch energy network is undergoing a significant transformation due to the shift toward renewable energy sources and decentralized energy technologies. This transition has introduced new complexities, particularly in preventing grid congestion, which occurs when the network's capacity cannot accommodate peak supply. Grid congestion is a critical bottleneck in integrating renewable energy and achieving energy sustainability. Consumers who also produce electricity using solar panels, known as prosumers, supply excess electricity to the grid or ideally adapt their consumption to manage surplus energy. This electricity feed-in further exacerbates grid congestion. If unaddressed, it is projected to result in an annual loss of 310 TWh in the EU by 2040 [30]. This is almost triple the total annual electricity consumption in the Netherlands. The issue is particularly severe in densely populated areas, where high peaks in both energy demand and electricity surplus hinder the widespread adoption of technologies such as solar panels and heat pumps [64].

The primary causes of grid congestion include peak overload, limited flexibility, and transmission losses [42]. These inefficiencies hinder the integration of renewable energy, leading to higher costs, environmental degradation, and reduced energy reliability.

Thermal energy accounts for nearly half of global energy consumption, with 44 % used for space heating and water [43]. The increasing adoption of district heating networks (DHN) offers a promising pathway to decarbonize thermal demand, particularly in urban areas. However, the integration of DHNs into broader energy systems remains limited. Meanwhile, increasing electricity demand, driven by the growing adoption of heat pumps (HPs) and electric vehicles (EVs), is contributing to grid congestion. In addition, the use of HPs and the charging of electric vehicles often coincides with the household's peak electricity use at a specific time of day.

Demand for electricity increases due to electrification and digitization. Alongside the integration of renewable energy, the existing grid operators struggle to balance supply and demand. This results in inefficiencies, unreliability, and higher costs. Conventional systems lack the flexibility to optimize energy flows, leading to wasted renewable energy during excess supply, feed-in congestion, or even curtailment.

1.2. Current Research and Knowledge Gaps

Current research extensively covers district heating systems and energy modeling in built environments. Furthermore, traditional studies often focus on single energy carriers, such as electricity or heating networks, without fully exploring the integration potential throughout the energy system [69]. This includes interactions at multiple levels, such as heat transfer stations (HTSs), network infrastructures, and end-user systems, which collectively could contribute to optimizing energy efficiency and flexibility.

Recent studies emphasize the importance of integrated energy systems that combine electricity and heat to enhance flexibility and efficiency. For example, research on congestion management through integrated electrical and thermal infrastructures highlights the potential of district heating networks and combined heat and power plants to alleviate electrical grid congestion [36]. Existing models often address these systems in isolation, overlooking the potential of an SHTS. An SHTS can optimize the local balance between energy supply and demand by dynamically managing energy flows.

In addition to integrated electric and thermal infrastructures, multi-energy virtual power plants (VPPs) play

a role in enhancing system flexibility. A VPP is a network of distributed energy resources, such as solar panels, batteries, and electric vehicles, managed through advanced software to balance energy supply and demand, improve grid stability, and support renewable energy integration. Today, VPPs are often combined with HPs or thermal storage.

Recent studies tend to neglect the financial and social dimensions of SHTSs, which are essential to understanding their feasibility and scalability in real-world applications. SHTS requires a multidisciplinary approach, incorporating engineering, energy modeling, and economics to design and implement solutions that are both technically and economically viable.

Addressing grid congestion and promoting sustainable energy systems requires the active participation of prosumers. Prosumers play a crucial role in balancing energy supply and demand. While heat demand remains relatively stable, electricity usage may increase, and consumption patterns will change.

1.3. De WarmteTransitieMakers

This thesis is being conducted in collaboration with De WarmteTransitieMakers, which is a Dutch consultancy that specializes in speeding up the heat transition in the built environment. They are involved in developing strategic plans, conducting technical and spatial analyses, and guiding municipalities and utilities in the implementation of sustainable heating solutions. Throughout this thesis project, De WarmteTransitieMakers provided access to knowledge, data sources, and expert insights. Their experience has helped to define the scope of this study and has ensured its practical relevance within the overall context of the energy transition.

1.4. The Potential of SHTS

To address the challenges of grid congestion and inefficiencies, SHTSs present a promising solution. SHTSs act as HTS, which also convert and store energy. Capable of dynamically managing the storage, conversion, and distribution of heat and electricity at the local level. By converting locally solar-generated electricity surplus to thermal energy and storing this, the SHTS reduces the heat demand from the DHNs, alleviates peak loads, and minimizes grid feed-in. These benefits enhance grid stability, improve energy efficiency, and facilitate the integration of decentralized renewable energy sources, such as solar panels.

This thesis develops a simulation model of an SHTS that integrates thermal storage, a heat pump, and an electric boiler to manage local solar electricity surpluses flexibly. The model emphasizes dynamic control at the substation level, using demand and weather data. The novelty lies in combining these assets with local control strategies with detailed system simulations to assess both technical and economic performance.

1.5. Research questions

Given the potential of SHTS and renewable goals, the following research question is defined for this study:

Under what conditions does the implementation of a smart heat transfer station (SHTS) improve the performance of energy supply systems in neighborhoods?

To answer this main research question, the following sub-questions will be answered:

- 1. What are the key differences between a conventional HTS and an SHTS?
- 2. What assessment parameters objectively describe the performance and impact of the SHTS?
- 3. How does the SHTS operate under varying heat demand and solar energy conditions?
- 4. How can the potential economic benefits for the system operators of the SHTS be quantified?
- 5. What is the optimal configuration of the SHTS components to maximize performance under a consistent and suboptimal control strategy?

1.6. Structure of the thesis

This thesis is logically structured to answer the general research question in a stepwise manner. Chapter 2 consists of a literature review of the fields relevant to this study, including energy demand profiles, district heating systems, grid congestion, energy storage, heat pumps, conventional heat transfer stations, and innovative energy system technologies.

Chapter 3 explains the methodology used to build and analyze the smart HTS. It describes the system components, input data, assumptions, optimization methods, and how the environmental and economic impacts are quantified. This serves as the basis for the simulations conducted to assess the feasibility of the proposed system.

Chapter 4 presents the validation process and the findings based on the main and sub-questions. It demonstrates how the smart HTS operates in terms of energy balancing, grid congestion alleviation, CO_2 emission impact, and economic viability under various configurations and operational strategies. These results are discussed in chapter 5, followed by the associated limitations and challenges.

Chapter 6 provides the overall conclusions of the study. It summarizes the key findings obtained from the model results and addresses the main research question, exploring the potential of SHTS in contributing to neighborhood-level energy systems.

Finally, chapter 7 highlights areas for potential further research in the development of SHTS.

Literature

This chapter presents a comprehensive literature review on energy systems, with a focus on key aspects that contribute to the development and operation of smart heat transfer stations. Section 2.1 explores both heat and electricity demand. Section 2.2 delves into district heating networks, highlighting their technical aspects and recent innovations shaping their future development.

Section 2.3 shifts the focus to the electricity grid. In Section 2.4, energy storage is discussed in detail, with a focus on thermal and electrical storage technologies and their role in balancing supply and demand. Heat pumps are the subject of Section 2.5, which examines various types and technical aspects. Section 2.6 provides an overview of conventional HTS. Section 2.7 introduces smart technologies for energy systems, including energy management systems and electric vehicle (EV) integration. Section 2.8 discusses the CO_2 emissions associated with electricity and district heating, as well as the emission trading system. Section 2.9 focuses on electricity and heat pricing. Chapter 2 wraps up with the answer to the first sub-question in section 2.10, highlighting the key differences between a conventional HTS and an SHTS.

2.1. Energy demand

2.1.1. Heat demand

Heat demand in households is driven by two primary components: space heating and hot tap water demand, each with distinct consumption patterns and seasonal variations.

Household heat demand varies significantly based on factors such as insulation quality, building age, and household size. For daily patterns, heat demand typically peaks in the early morning and late evening when occupants are at home, indoor temperatures require adjustment, and hot tap water is being used, illustrated in figure 2.1.

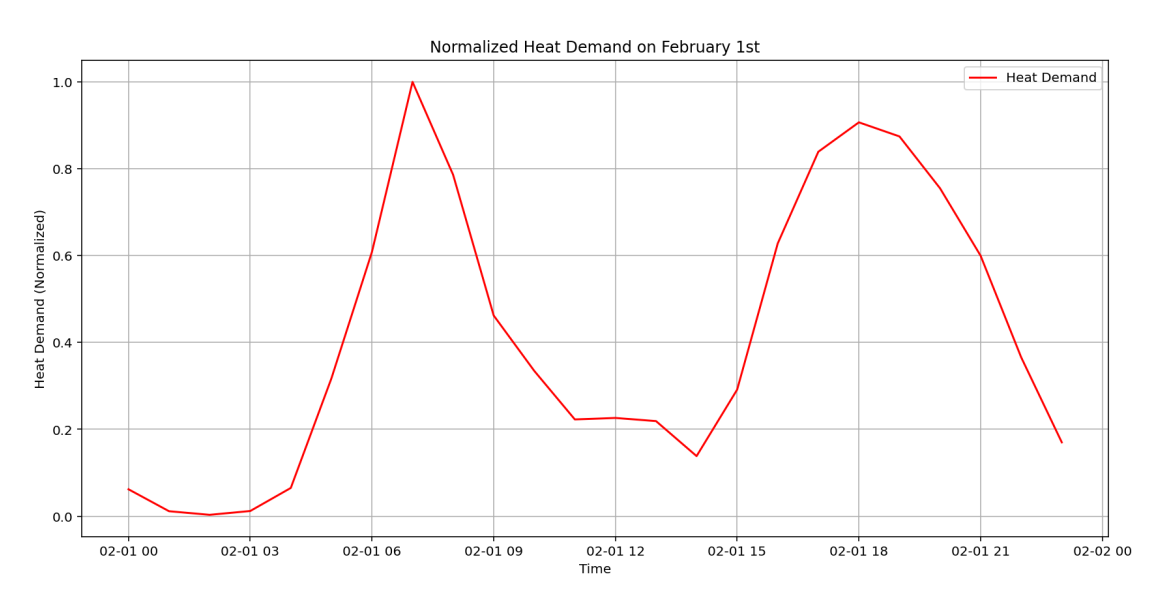


Figure 2.1: Daily heat demand profile [87]

Figure 2.2 shows fluctuations during the year for heating peaks during winter, driven by colder temperatures, while hot tap water demand remains relatively stable throughout the year. Space heating is responsible for 60.6%, and hot tap water is responsible for 19.04% of the total energy use in the residential area [31]. While space heating is highly seasonally dependent, hot tap water consumption remains more consistent, influenced by household actions rather than external conditions [71].

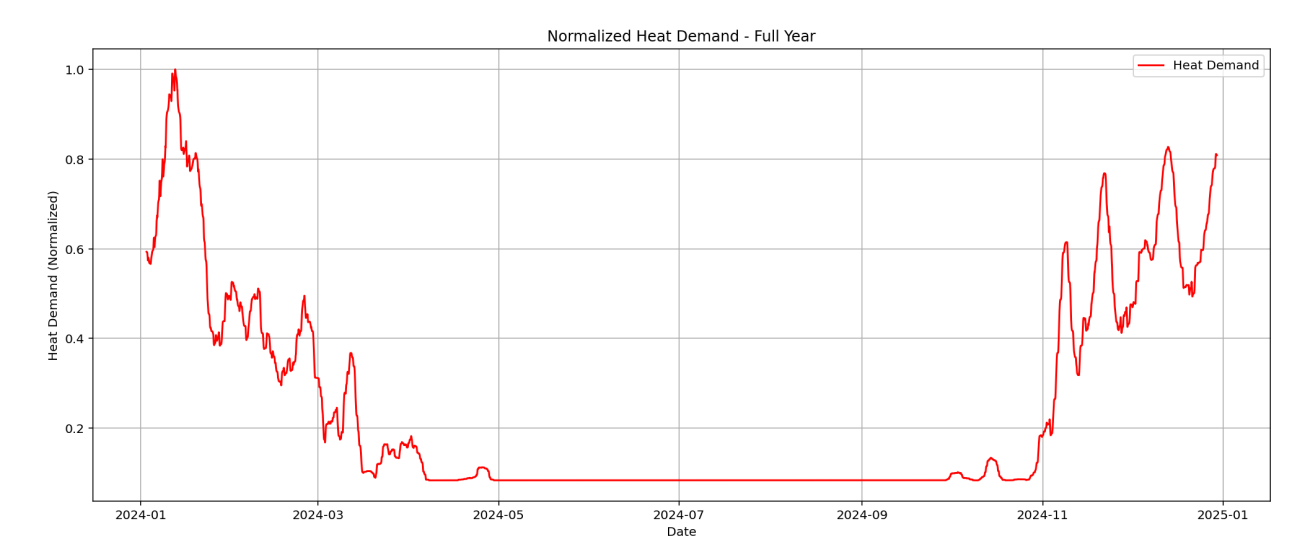


Figure 2.2: Yearly heat demand profile [87]

2.1.2. Electricity demand

Understanding electricity demand in houses is crucial for designing integrated energy systems that balance supply and demand effectively. Various factors, including appliance usage, household size and behavior, building characteristics, and seasonal and weather variations, influence household electricity consumption. The adoption of technologies such as EVs and HP, as well as the increasing use of smart appliances, also plays a significant role [38].

Daily and yearly electricity demand patterns provide valuable insights into how households consume energy. Figure 2.3 illustrates the daily electricity demand fluctuation, reflecting household activities such as electric cooking and heating, and appliance use [46].

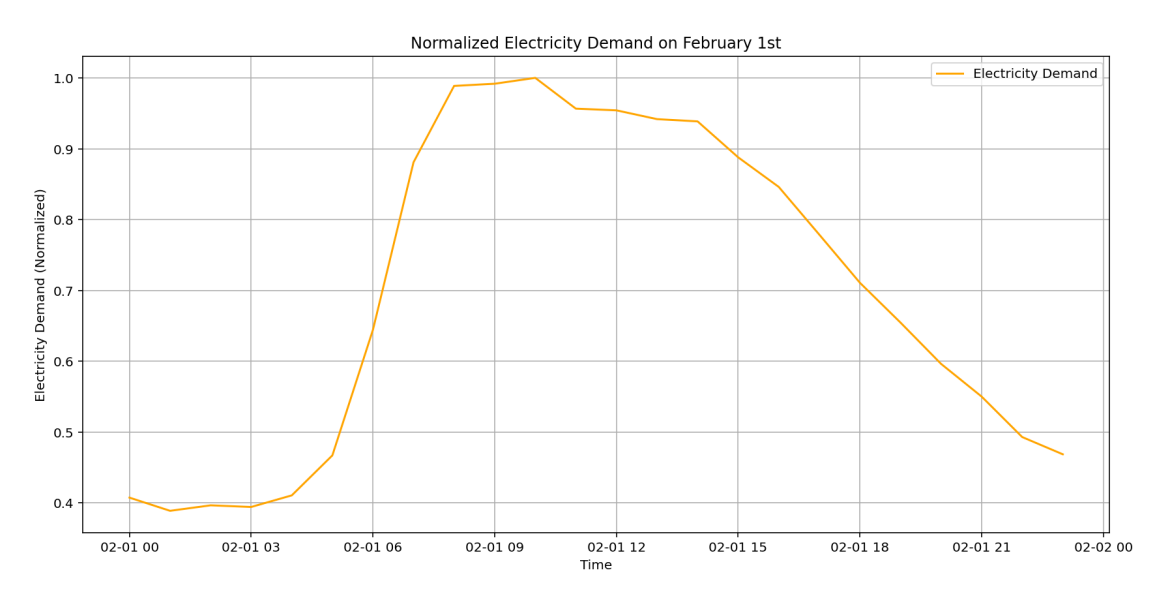


Figure 2.3: Daily electricity demand [21]

Seasonal variations also influence the yearly electricity demand pattern. In colder and darker months, higher electricity usage is due to electrical heating demand and extended use of lighting, while during summer months, a minimum occurs, see figure 2.4. However, with the current air-conditioning trend [77], the electricity consumption in the summer months will likely increase. These variations contribute to growing pressure on the grid, which will be further discussed in section 2.3.1.

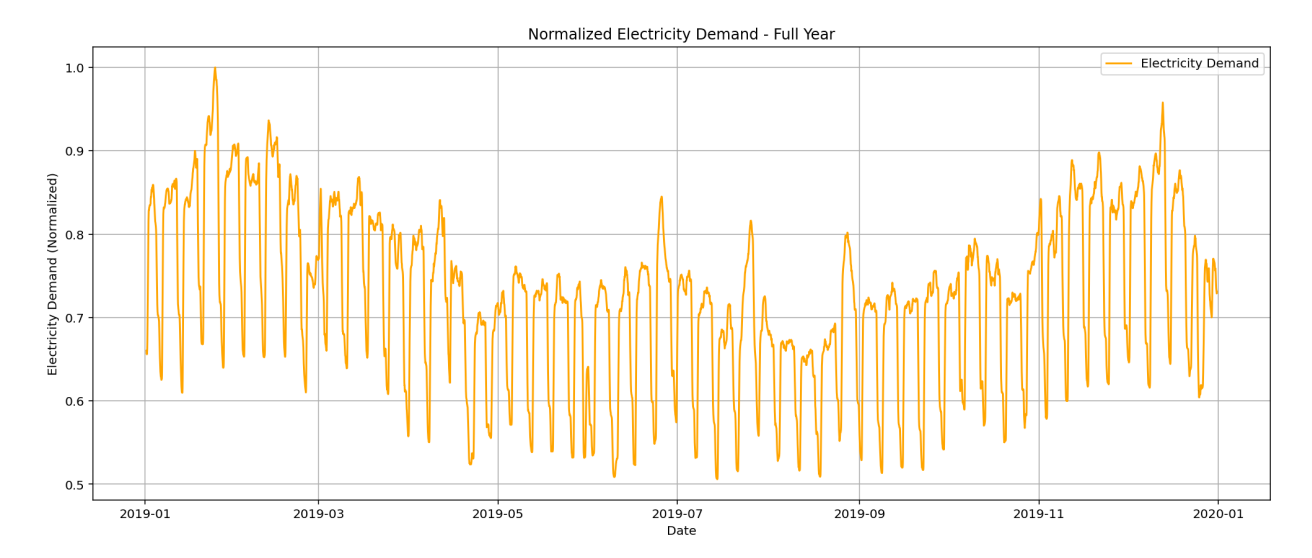


Figure 2.4: Yearly electricity demand [21]

Impact of Increasing Use of EVs and HPs

Electrification through the adoption of EVs and HPs significantly impacts electricity demand. EV charging typically adds substantial load hours when demand is already high, further increasing peak loads on the grid [90]. In figure 2.5, it is shown that on weekdays, a peak in the morning at work, and at home at the end of the day occurs. Similarly, heat pumps, while energy-efficient, contribute to higher electricity consumption, especially in winter when they are used for space heating [85]. Simultaneous peaks are lower due to diversified usage patterns, but still represent critical stress points for the grid [11]. The combined impact of these technologies has been shown to strain local grid infrastructure, requiring upgrades or alternative energy solutions, further elaborated in section 2.7.

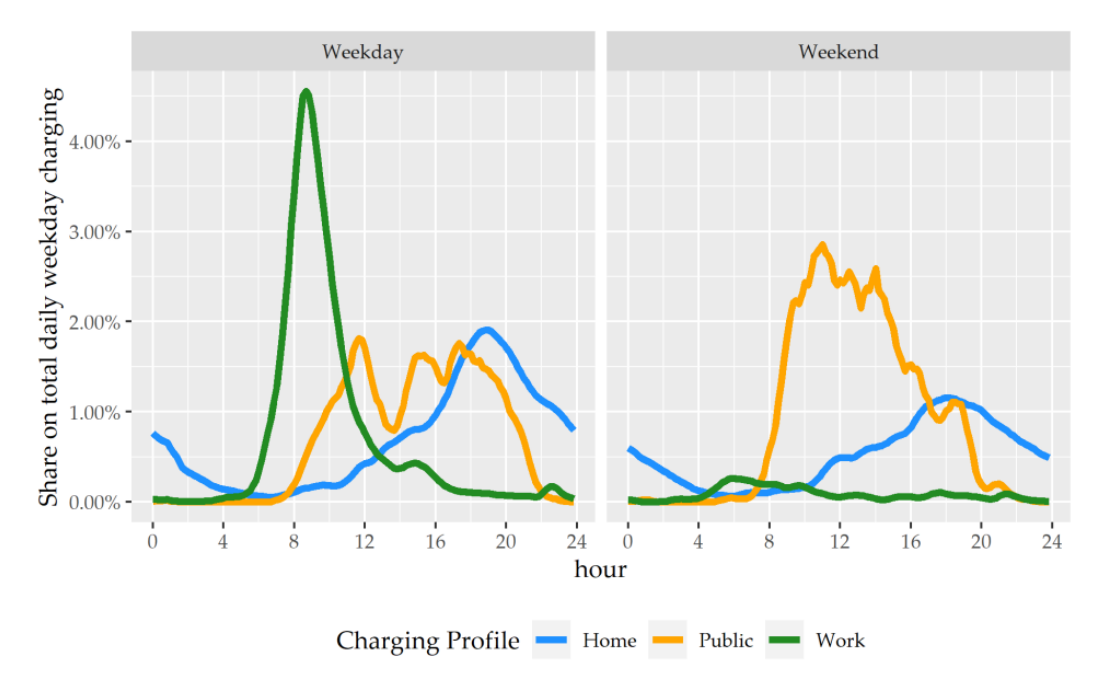


Figure 2.5: Daily profile of EV charging [90]

2.2. District Heating Networks

2.2.1. Heating systems

The choice of heating systems in Dutch households depends on factors such as the building's age and the availability of local infrastructure. It has been government policy during the 60's to connect households to a national gas network. Currently, over 90% of all households are connected to natural gas.

Heating systems can be categorized based on where the heat is produced: either individually at each household or through centralized systems.

Most individual households currently rely on gas-fired boilers for heating and hot water due to their affordability and reliability, as figure 2.6 shows. With the Netherlands' goal to phase out natural gas by 2050 [62], alternative systems like electric boilers and heat pumps are gaining popularity. However, this is by far not enough. These systems reduce reliance on fossil fuels but face challenges such as high upfront costs, building insulation requirements, and retrofitting complexities in older homes [27]. Solar thermal collectors are not gaining popularity, according to the Warmtepomp Trendrapport 2025 [68]. The solar energy sector is more focused on PV panels than solar thermal collectors.

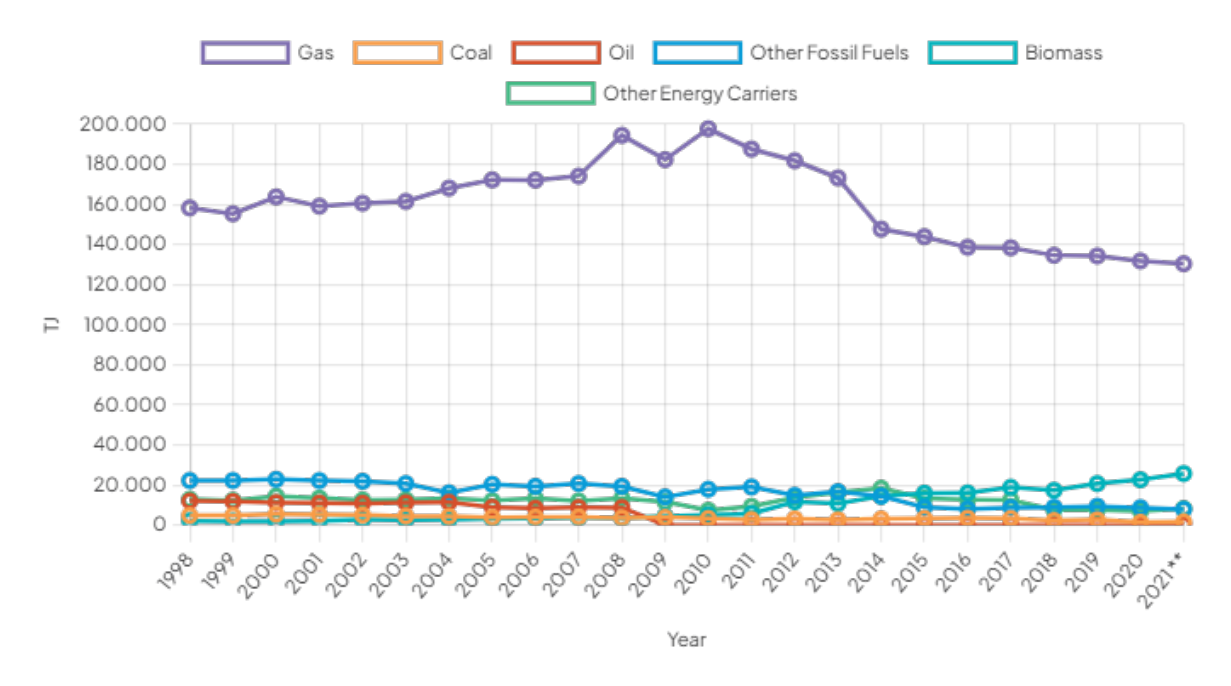


Figure 2.6: Heat generation sources [24]

Centralized heating systems, such as district heating networks, are increasingly common in urban areas like Amsterdam, Rotterdam, and Utrecht [60]. These systems often use residual heat from industrial processes or waste incineration, reducing the need for individual household connections. Although infrastructure costs and heat losses during transport pose challenges, district heating is a vital part of the Netherlands' transition to sustainable energy, despite the limited choice for customers [82].

2.2.2. Technical aspects

The technical design of district heating networks relies on several key infrastructure components. Insulated pipes are essential for minimizing heat losses during transport, particularly over long distances [16]. At the same time, pumping systems maintain the required pressure and flow rate to distribute heat evenly across the network. The pumping systems are responsible for a significant part of the electricity used in a DHN [70], making it necessary to minimize this energy consumption. Heat exchangers, located at the HTS and between the distribution network and the consumer's building, are essential for ensuring efficient and reliable heat transfer. They prevent the district heating water from mixing with the building's internal heating system, maintaining stable temperatures, providing a pressure break, and minimizing the risk of a system-wide failure in the event of a localized issue [19].

2.2.3. Innovations and Trends

A significant trend in district heating networks is the shift from old-fashioned high-temperature systems, sometimes operating above $100^{\circ}C$, to middle-temperature (50-80°C), low-temperature (35–50°C), and ultra-low temperature (20–35°C) district heating networks, see table 2.1.

Middle-temperature systems $(50-80^{\circ}C)$ offer improved energy efficiency by reducing heat losses during distribution and enabling better integration with renewable energy sources in comparison with high temperature DHN. Furthermore, systems with lower temperatures are more compatible with modern, well-insulated buildings that require lower temperature heat [37]. However, retrofitting older buildings to connect to lower temperature district heating systems could be a feasible option [84].

Table 2.1: Temperatures of DHN

DHN Type	Temperature Range
High-temperature (HT) DHN	$> 80^{\circ}C$
Middle-temperature (MT) DHN	$50 – 80^{\circ}C$
Low-temperature (LT) DHN	$35-50^{\circ}C$
Ultra-low-temperature (ULT) DHN	$20 35^{\circ} C$

As district heating networks expand, concerns about consumer rights emerge. Households in connected areas often have limited options to opt out, raising questions about fair competition and pricing [79].

2.3. Electricity Grid 9

2.3. Electricity Grid

The electricity grid in the Netherlands plays a critical role in supporting residential and industrial energy demand, with power generated from wind, solar, gas, coal, biomass, and waste heat incinerating power plants [2]. This vast and complex network is maintained by regional grid operators, who manage the transmission and distribution lines to ensure a stable and efficient energy supply across the country.

The electricity grid operates across three voltage levels, each of which faces unique challenges related to electricity distribution and congestion [57]:

- (Extra) High-Voltage Grid: Responsible for the long-distance transport of electricity and connecting large-scale renewable energy sources such as offshore wind and solar farms (above 35 kV).
- Medium-voltage Grid: Acting as the intermediary between high-voltage transmission lines and low-voltage networks, the medium-voltage grid connects industrial zones and decentralized energy generation (1-35 kV).
- Low-Voltage Grid: Supplying electricity directly to households and small businesses, serving as the final link in the electricity distribution system (below 1 kV).

In addition to rising demand, the increasing reliance on decentralized renewable energy generation introduces complexities. Medium- and low-voltage grids must handle bidirectional electricity flows, balancing the delivery of electricity to consumers with the feed-in of surplus electricity back into the grid [4]. This variability increases congestion and highlights the need for infrastructure upgrades [4].

As the energy transition progresses, the Dutch electricity grid must evolve to support sustainable energy goals. TenneT, which is responsible for the high-voltage grid in the Netherlands, is investing to meet growing demand and integrate renewable energy sources, ensuring a stable and resilient energy system [75].

2.3.1. Grid congestion

Grid congestion occurs when the electricity grid reaches its full capacity, hindering the efficient transmission of electricity. As electricity demand increases, grid congestion becomes an increasing problem. It can occur at low, medium, and high voltage levels, particularly in areas with an increase in electrification in industry and the built environment [74].

Grid congestion poses a significant challenge to the electricity system. The rapid expansion of renewable energy sources, combined with increasing electricity demand, has led to constraints in transmission and distribution capacity. This has resulted in delays in connecting new renewable energy projects, limiting the effective utilization of clean energy resources [3]. To address these challenges, expanding grid infrastructure and implementing flexibility solutions, such as energy storage and demand-side management, are critical for ensuring a stable and resilient energy system [3].

Recent studies further emphasize the importance of congestion management strategies, such as flexible grid operation, dynamic tariffing, and local energy balancing, to mitigate the impact of grid constraints in both urban and rural areas [35][40].

A visual representation, as the high-voltage congestion map of the Netherlands shown in figure 2.7, high-lights the areas where grid capacity issues are most critical for electricity consumption. Similarly, figure 2.9 illustrates the medium-voltage electricity consumption congestion map, focusing on regional grid challenges.

Table 2.2 explains the different colors used in figures 2.7, 2.8, 2.9, and 2.10, where red and orange areas indicate regions with waiting lists for new grid connections.

Grid congestion in the feed-in market is depicted in figure 2.8 for the high-voltage grid and in figure 2.10 for the medium-voltage grid. These maps show where the grid has reached its capacity to transport surplus electricity generated by renewable energy sources, such as solar panels and wind turbines, back to the grid [76]. Grid congestion occurs during both the morning and afternoon peaks, as well as during feed-in peaks when wind generation is high and the sun is shining.

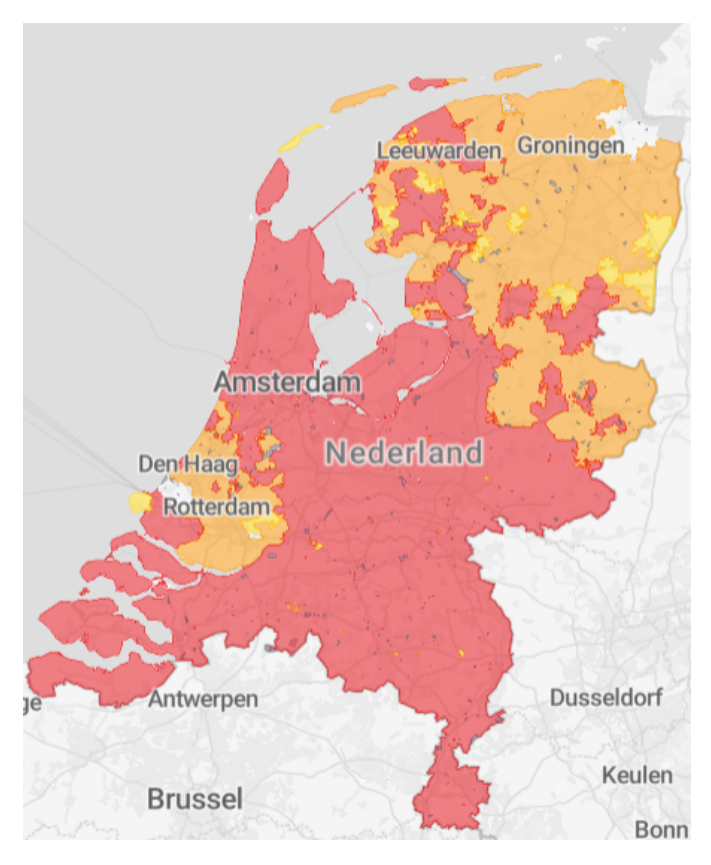


Figure 2.7: High voltage grid congestion map (electricity consumption)[76]

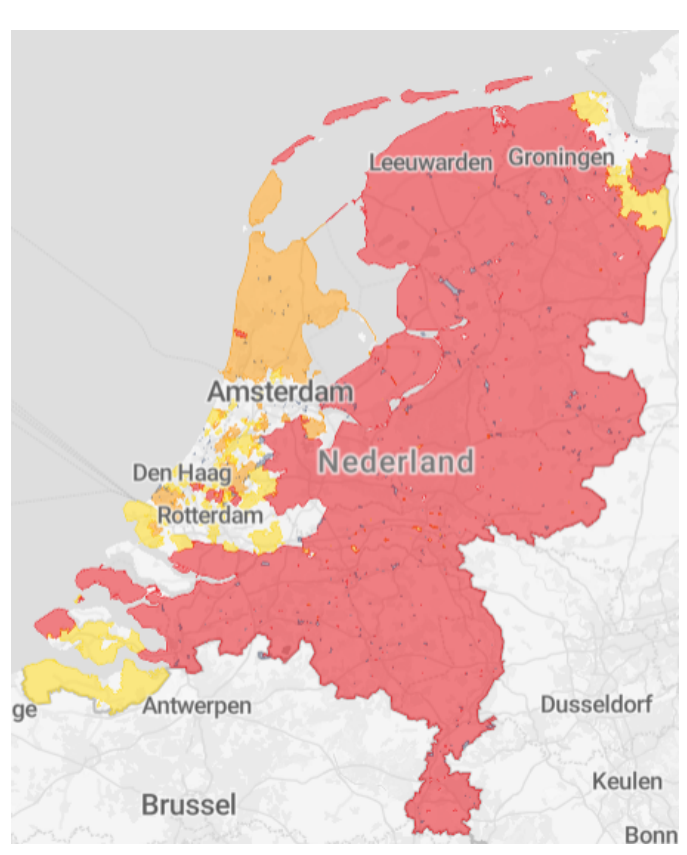


Figure 2.8: High voltage grid congestion map (electricity feed-in)[76]

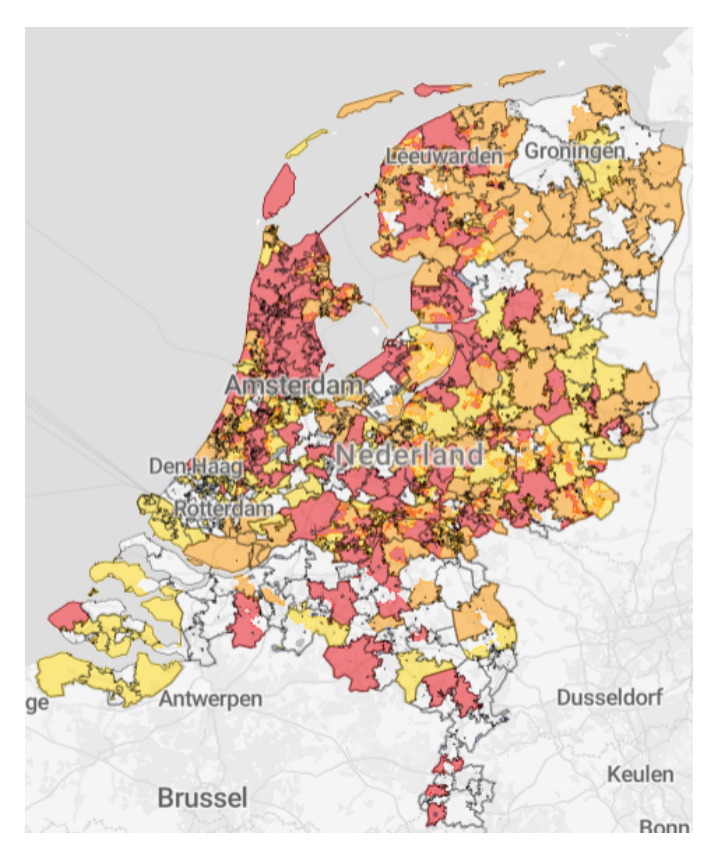


Figure 2.9: Medium-voltage grid congestion map (electricity consumption)[76]

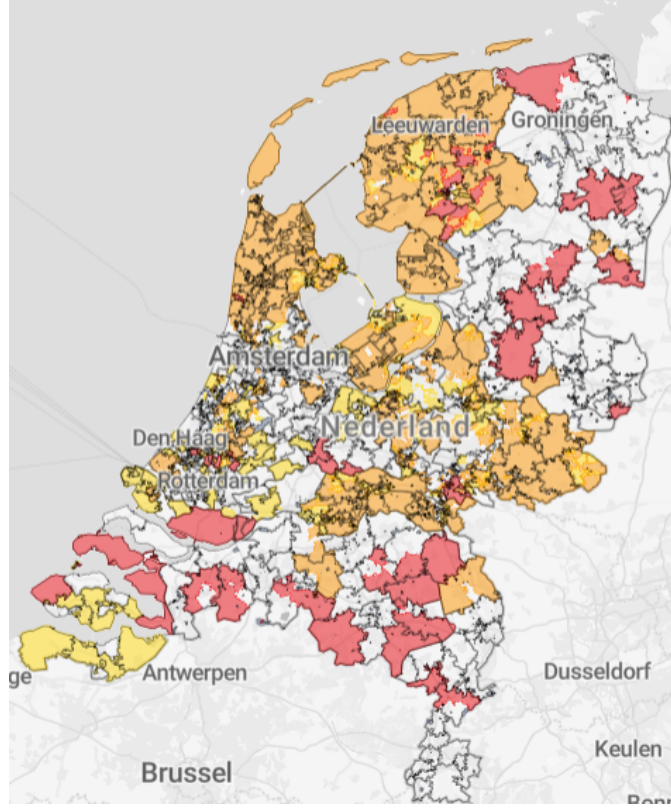


Figure 2.10: Medium-voltage grid congestion map (electricity feed-in)[76]

2.3. Electricity Grid

Color	Meaning	
	Transport capacity available without waiting list	
	Transport capacity limitedly available without waiting list	
	Area under investigation with a waiting list	
	Shortage of transport capacity with a waiting list	
	Color will be added later	

Table 2.2: Legend for grid congestion maps

The large amount of red areas in both maps highlights the severity of grid congestion in the Netherlands, affecting both electricity consumption and feed-in. This indicates significant capacity constraints in the grid, posing a major challenge for the energy transition and the integration of renewable energy sources.

2.4. Energy storage

2.4. Energy storage

The variability in energy demand and supply, driven by the rise of renewable energy sources, requires effective storage solutions. Energy storage stabilizes the grid, enhances efficiency, and reduces reliance on fossil fuels. Thermal and electrical storage are important for managing fluctuations in supply and demand.

Energy storage covers the gap between energy availability and consumption, addressing daily and seasonal mismatches in energy demand. Day-to-day storage smooths daily peaks by storing surplus energy for later use. Seasonal storage leverages summer energy surpluses to meet winter demands, both reducing strain on the grid and reducing carbon emissions [15].

Thermal storage technologies, including sensible, latent, and thermochemical storage, as well as electrical storage options such as batteries and hydrogen, offer flexible and scalable solutions.

2.4.1. Thermal storage

Sensible heat storage

Sensible Heat Storage (SHS) is one of the simplest and most widely used forms of Thermal Energy Storage (TES). It involves storing heat by raising the temperature of a storage medium, typically water or solid materials such as concrete or stone. The storage capacity depends on the medium's specific heat capacity, mass, and temperature difference. The most common storage for daily use is Tank Thermal Energy Storage (TTES) [47], due to their relative affordability compared to latent or chemical heat storage. Aquifer Thermal Energy Storage (ATES) and Borehole Thermal Energy Storage (BTES) are typically used for seasonal storage [12][81]. As this model focuses on daily storage, a TTES is a plausible choice.

Latent heat storage

Latent Heat Storage (LHS) utilizes Phase Change Materials (PCMs) to store energy during phase transitions, such as the solid-to-liquid transition. Figure 2.11 shows that PCMs can store and release energy at nearly constant temperatures [14]. LHS is only economically viable when charging and discharging as frequently as possible, making it unsuitable for seasonal storage [14].

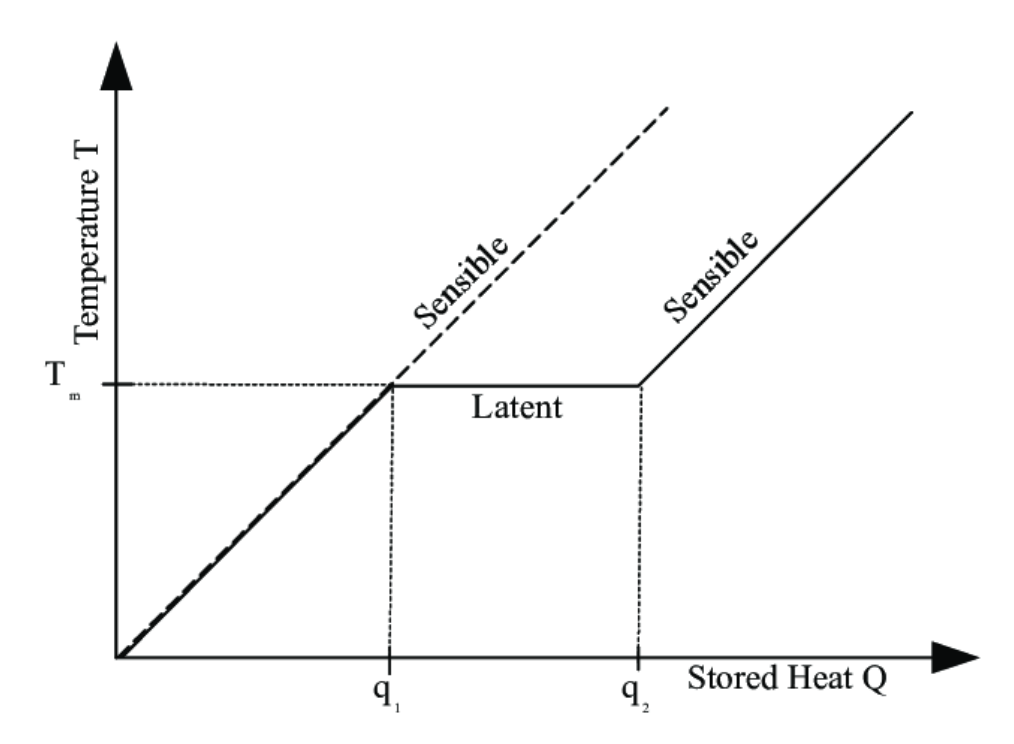


Figure 2.11: Latent heat storage [55]

2.4. Energy storage

Thermochemical heat storage

Thermochemical heat storage involves reversible chemical reactions to store and release heat. These systems offer high energy densities and can store heat for extended periods without high thermal losses [63]. This is because the storage occurs near ambient temperature, resulting in only a small temperature gradient and thus low thermal losses.

2.4.2. Electrical storage Battery energy storage systems

Battery Energy Storage Systems (BESS) store electrical energy chemically and release it when needed. Lithium-ion batteries are popular due to their high energy density, efficiency, response time, high number of life cycles, and relatively low energy losses over time [52]. BESS supports grid stability and renewable integration [52]. However, BESS has relatively high costs, which can limit its widespread adoption despite its advantages [52]. Additionally, safety issues for large BESS should be considered, as battery fires are difficult to extinguish and control.

Hydrogen Storage

Hydrogen storage involves converting excess electricity into hydrogen through processes such as electrolysis or steam methane reforming. Storing it in tanks or underground caverns for later use in fuel cells or gas turbines. It enables large-scale, long-duration energy storage [34]. However, high infrastructure costs limit its competitiveness in other energy storage applications [34].

2.5. Heat pumps 14

2.5. Heat pumps

Heat pumps are increasingly essential components in district heating networks. Utilizing renewable or ambient heat sources such as air, water, or the ground. Depending on the application, heat pumps can be used centrally or installed individually in households.

Centralized Heat Pumps

Centralized heat pumps are typically installed at the source of heat production. These systems distribute heat via a DHN to multiple houses or a large building [28]. Although centralized systems are efficient for large-scale applications, they require significant upfront investments in infrastructure, such as distribution pipelines. Additionally, centralized heat pumps can pose challenges for a building's owners' association, including issues related to noise, aesthetics, and conflicting financial capacities or priorities among owners [59]. For the SHTS, a centralized heat pump would be a viable option. This way, it will be possible to combine the system with a TTES. The HP en TTES will need to be the property of the network operators, rather than being shared between homeowners, to prevent conflicts.

Individual Heat Pumps

In contrast, individual heat pumps are installed in households, allowing homeowners to independently manage their heating and, in some cases, cooling needs. According to recent research, individual heat pumps tend to be more cost-effective and energy-efficient compared to centralized neighborhood heat pump systems. They also eliminate the need for extensive piping networks, reducing overall infrastructure costs [86]. It provides the option to lower the temperature from the HTS to the houses, as they will be boosted locally. However, making an SHTS with individual heat pumps will be complex and will take a lot of space in each house [39].

2.5.1. Types of Heat Pumps

Heat pumps are classified based on their heat source and heat sink. The five main types are described below:

- Air-to-Water Heat Pumps: Air-to-water heat pumps extract heat from the outside air and transfer it
 to a water-based heating system. These are the most common type of heat pump, widely used in
 residential and commercial buildings due to their relatively low installation costs and adaptability to
 various climates, and also capable of cooling [89].
- Air-to-Air Heat Pumps: Air-to-air heat pumps extract heat from the outside air and directly transfer it
 to the indoor air. These are typically used for space heating and cooling, but they are not suitable for
 providing hot water [26]. An air conditioner is comparable to an air-to-air heat pump.
- Water-to-Water Heat Pumps: These systems extract heat from water sources, such as rivers, lakes, or groundwater, and transfer it to a water-based heating system. They are highly efficient but depend on the availability of suitable water resources [8].
- Geothermal Heat Pumps: Also known as ground source heat pumps, extract heat from a stable underground temperature. It has a high efficiency. However, the installation is more complex than others, and the costs are high. There are two versions: closed-loop systems (buried pipes with circulating fluid) and open-loop systems (using groundwater directly) [25].
- Water-to-Air Heat Pumps: These systems extract heat from water sources and release it as warm air.
 These can be combined with geothermal energy.

Air-to-Water Heat Pumps (AWHPs) are highly versatile, seamlessly integrating with systems such as radiant floor heating and cooling [18]. This adaptability provides a comprehensive solution for modern heating needs. Furthermore, air-source heat pumps are the most commonly used option [53], making the AWHP the preferred choice for modeling the SHTS.

2.5.2. Technical Aspects

The vapor-compression cycle is the fundamental thermodynamic process that enables AWHPs to efficiently transfer heat from the outdoor air to a water-based system. This cycle is widely used in heat pump technology due to its ability to deliver high efficiency and reliability across various heating and cooling applications. This closed-loop process consists of four stages: compression, condensation, expansion, and evaporation [83]:

2.5. Heat pumps 15

1. Compression: In the compressor, the gaseous refrigerant is compressed to a higher pressure, which significantly increases its temperature.

- 2. Condensation: The high-temperature, high-pressure refrigerant moves into the condenser, where it releases heat to the circulating water. This heat transfer warms the water for space heating or domestic hot water applications.
- Expansion: The liquid refrigerant then passes through an expansion valve, also known as a throttling device. Here, the pressure and temperature drop significantly, ensuring it is in the correct state for effective heat absorption in the next stage.
- 4. Evaporation: In the evaporator, the low-pressure refrigerant absorbs heat from the surrounding air and undergoes phase change from liquid to gas.

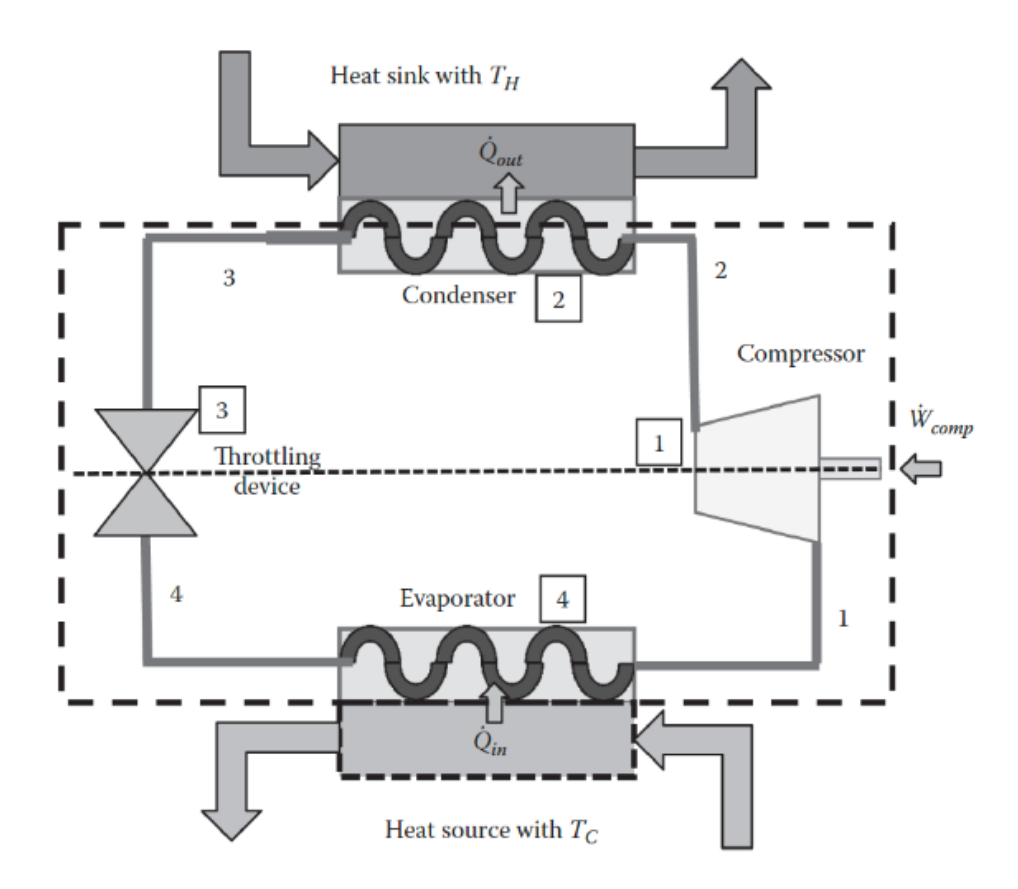


Figure 2.12: Vapor compression cycle used in heat pumps [83]

HP's commonly use refrigerants such as R410A, R134a, R32, R290 (propane) and CO_2 (R744). R410A has been widely used due to its efficiency, but is being phased out because of its high environmental impact. R32 is popular as it offers a lower environmental impact and maintains high efficiency. CO_2 (R744), a natural refrigerant, operates at higher pressures [66]. R290 air-to-water heat pumps have great potential in the near future [22].

By repeating these steps, AWHPs efficiently extract and transfer heat, achieving high coefficients of performance (COP). It is defined as the ratio of useful energy output (heating or cooling) to the energy input required to achieve it. A higher COP indicates a more efficient system [83].

$$COP = \frac{\text{Useful energy output}}{\text{Energy input (work)}}$$
 (2.1)

The COP for heating and cooling differs. For heating systems, the COP is defined as:

$$COP_{\mathsf{heating}} = \frac{Q_h}{W}$$
 (2.2)

2.5. Heat pumps 16

Where:

- Q_h : The amount of heat delivered to the hot side (in joules or kilowatts).
- W: The energy input or work supplied to the system (in joules or kilowatts).

For cooling systems, the COP is defined as:

$$COP_{\mathsf{cooling}} = \frac{Q_c}{W}$$
 (2.3)

Where:

- Q_c : The amount of heat removed from the cold side (in joules or kilowatts).
- W: The energy input or work supplied to the system (in joules or kilowatts).

Under ideal conditions, such as in a reversible Carnot cycle, the COP can also be expressed in terms of the temperatures of the hot and cold sides. All temperatures must be in Kelvin (K) [83].

The COP for heating in terms of temperatures, known as the Carnot efficiency, is defined as:

$$COP_{\text{heating}} = \frac{T_{\text{hot}}}{T_{\text{hot}} - T_{\text{cold}}} \tag{2.4}$$

The COP for cooling in terms of temperatures is defined as:

$$COP_{\text{cooling}} = \frac{T_{\text{cold}}}{T_{\text{hot}} - T_{\text{cold}}}$$
 (2.5)

Where:

- T_{cold} : The temperature of the cold side in Kelvin.
- T_{hot} : The temperature of the hot side in Kelvin.

2.5.3. Market Trends and Policy Implications

Policy support, energy prices, and consumer attitudes heavily influence the demand for heat pumps in the Netherlands. The Nationaal Warmtepomp Trendrapport 2025 presents results and predictions in the domestic heat pump market [68]. After the record year of 2023, with the sale of 168,000 units, excluding air-to-air heat pumps. 2024 saw a dramatic fall to 118,000 due to government policy. 2025 is expected to be at approximately the same level as 2023, see figure 2.13.

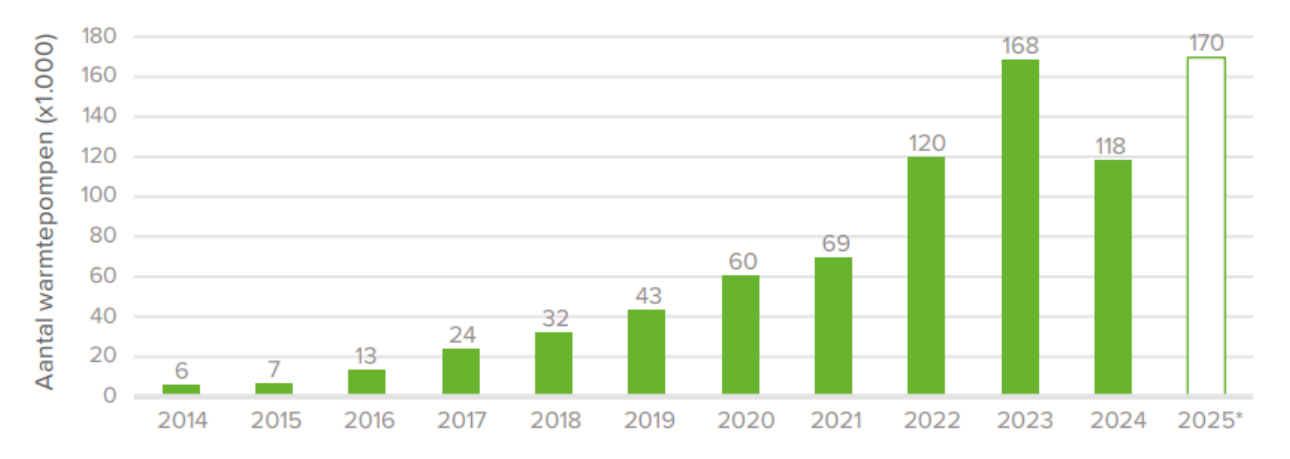


Figure 2.13: Forecast of the number of installed residential HPs (excluding air-to-air HPs) [68]

Concurrently, the increasing use of air conditioners, often used for space heating, creates a new dynamic. In 2024 alone, there will be some 350,000 air conditioner sales, adding nearly 2 GW of thermal capacity. By 2030, an estimated 6.3 million Dutch households are expected to own an air conditioner, consuming approximately 4 petajoules of electricity [67].

2.6. Conventional heat transfer station

Conventional HTSs play a crucial role in transferring thermal energy from primary heat sources, such as geothermal wells, biomass plants, or waste heat from industrial processes, to secondary networks that distribute heat to end-users. These systems are designed to ensure efficient heat delivery by regulating temperature, pressure, and flow rates, making them an essential component of district heating networks. In figure 2.14, an HTS is shown where it connects the heat source with the residential area.

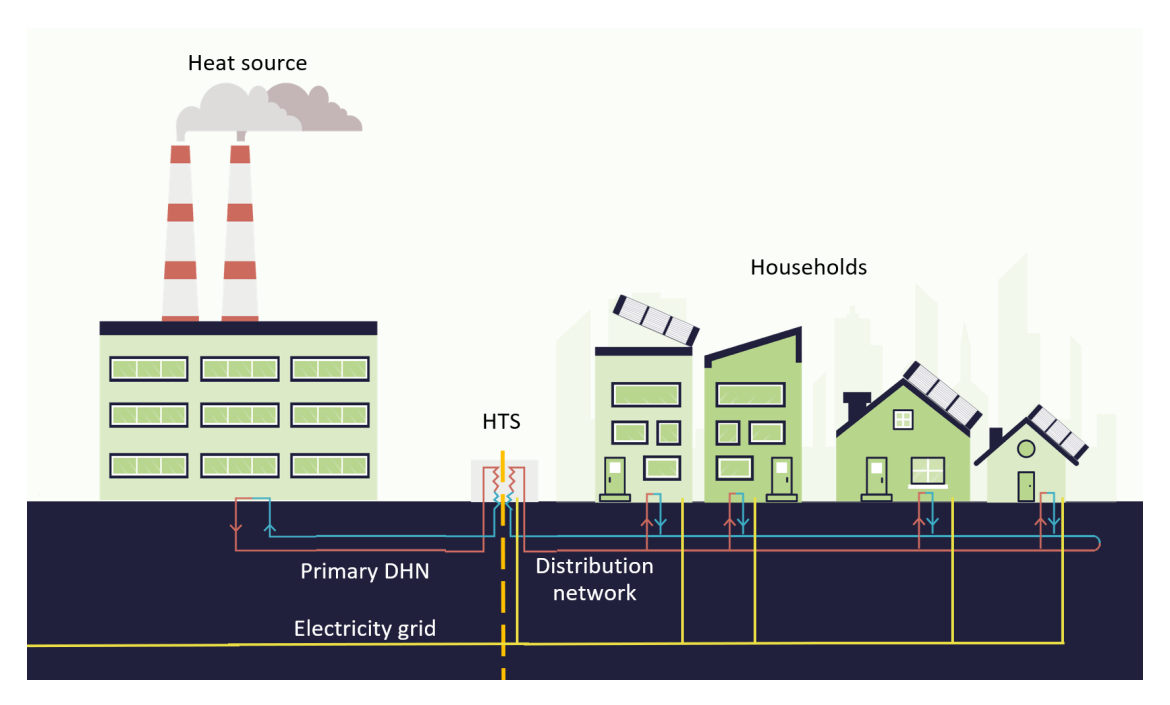


Figure 2.14: Schematic set up Heat Transfer Station

2.6.1. Components

An HTS facilitates the distribution of thermal energy within district heating systems, incorporating essential components such as heat exchangers, circulation pumps, control systems, sensors, and insulated piping. These elements work together to regulate heat flow, optimize efficiency, and ensure reliable operation.

A key feature of HTSs is the heat exchanger, which separates the primary and secondary networks, preventing direct fluid mixing. This separation is necessary when the two networks operate under different pressures, temperatures, or fluid types, allowing the primary network to function independently at higher operating conditions while optimizing the secondary system for end-users. This also enhances safety by protecting the secondary network from pressure surges, contamination, or failures in the primary system affecting the secondary system, and vice versa [7]. Additionally, in the near future, the roles of transport operator (primary) and distribution operator (secondary) may be separated. Making the separation between the responsibilities of the operators clear.

However, in some cases, direct connections between the primary and secondary networks eliminate the need for a heat exchanger. This simpler, more cost-effective setup allows thermal energy to flow directly to end-users when both networks share the same fluid type. Direct connections are standard in localized systems and modern low-temperature district heating networks. A direct connection allows for the use of the lowest possible supply temperature. While reducing installation and maintenance costs, these systems may expose the secondary network to potential operational and performance issues from the primary system. They will only operate at lower pressures [80]. In district heating setups, a delivery set (afleverset in Dutch) with a built-in heat exchanger is standard for connecting consumers. This ensures hydraulic separation and prevents mixing between the district heating water and the residential heating circuit. In low-temperature networks, a heat pump can replace the heat exchanger.

2.6.2. Thermal Demand and Capacity

The capacity of an HTS depends on the size of the network and the heat demand of connected households. In district heating systems, a single household typically requires between 4 and 8 kW of thermal power for space heating and domestic hot water, with variations influenced by insulation levels and household usage patterns. Existing apartments require approximately 6.5 kW for space heating, while larger, less efficient buildings may need between 8.5 and 10 kW. Most heat pumps have a thermal capacity of around 5 kW, underscoring the importance of thermal insulation to ensure a house is HP-ready. For Domestic Hot Water (DHW), a 26 kW connection is required for both types [21]. This high capacity is necessary to quickly heat cold tap water $(12^{\circ}C)$ to over $60^{\circ}C$ to reduce the risk of legionella. The DHW is then mixed with cold water to obtain the required temperature.

For a DHN supplying 400 households, the total thermal capacity required at the heat transfer station (HTS) would be between 1 and 3 MW. When determining the capacity of an HTS, it is crucial to consider the simultaneity factor (also known as the diversity factor). This factor accounts for the fact that not all households require their peak heat demand at the same time, thereby reducing the overall peak load that the system must supply.

The simultaneity factor depends on several factors, including the number of connected households and the type of heat demand. Generally, the larger the network, the lower the simultaneity factor, as peak demands tend to be spread out over time. Furthermore, the type of heat demand also affects the simultaneity factor: DHW typically has a much lower simultaneity factor, sometimes as low as 0.05, calculated using $\frac{1}{\sqrt{n}}$, compared to space heating, which ranges between 1 and 0.55. Hot water usage is more sporadic and spread throughout the day, whereas space heating demand tends to be more continuous, particularly in cold weather [21][17].

By incorporating the simultaneity factor into capacity calculations, the required peak thermal power at the HTS can be significantly reduced, leading to lower infrastructure costs and improved system efficiency. In figure 2.15, a conventional HTS is shown as a visual representation. Appearance of other HTSs can vary widely.



Figure 2.15: A Heat Transfer Station in Amsterdam [56]

2.7. Smart Technologies for Energy Systems

Smart district heating networks

Smart District Heating Networks (SDHNs) are an evolution of traditional heating systems, integrating decentralized energy production, prosumers, and intelligent control technologies to improve overall efficiency and sustainability.

Brand et al. (2014) in Applied Energy examine the impact of prosumers with solar collectors and heat pumps on district heating networks. They find that decentralized heat sources can improve efficiency but require precise control to avoid fluctuations and pressure issues [13]. However, the study gives limited attention to the impacts of large-scale systems, such as grid congestion.

Additionally, flow rate control in smart DH has been extensively studied using deep reinforcement learning. A study by Zhang et al. (2019) demonstrates how Al-based algorithms can optimize flow rate control within SDHNs, resulting in better heat distribution, lower pumping costs, and increased energy efficiency [94]

Future district heating systems will need to integrate more fluctuating renewable heat sources and operate at lower temperatures to improve efficiency. In a study by O'Donovan et al. (2018), a simulation of a district heating network incorporating solar collectors, thermal storage, and prosumers is conducted. Their case study achieved a 93% renewable share and a 12% reduction in heat losses, demonstrating the value of advanced control and simulation tools in smart network design [61].

A study by Min-Hwi et al. (2021) proposed an energy prosumer system using a simultaneous heating and cooling heat pump. Compared to a conventional ASHP, this set-up greatly improved self-consumption, reduced grid feed-in from 60% to 12.5%, and over 30 times more operational profit from July to September. While this is very promising, the study notes that more realistic cost modeling and scalability analysis are needed in the future [45].

Further research by Kroger et al. (2024) also simulates smart grids. A coordinated operation of district-scale flexible heating systems, demonstrating how these systems can provide stability to the grid and enable the use of renewable power sources [48]. The findings show a decrease in RES curtailment, resulting in cost savings. Although it is designed for use at a larger scale, their approach is insightful and offers valuable lessons that can be applied at the local scale.

Smart Energy Management

In the Netherlands, the adoption of smart metering systems in households has been significant. As of 2020, 59% of Dutch households had smart water, gas, or electricity meters installed, enabling remote reading and real-time monitoring of energy consumption [1]. These smart meters facilitate the integration of renewable energy sources and support optimization.

However, there is a lack of measuring equipment in more central parts of our energy networks, such as transformer substations (transformatorhuisjes in Dutch), limiting insights for network operators into the energy throughput at these hubs or nodes [21].

Smart Thermal Energy Storage

Smart charging of thermal energy storage systems is pivotal in enhancing energy efficiency and grid stability. By integrating advanced control strategies and real-time data analytics, TES systems can dynamically manage energy storage and release, aligning with demand fluctuations and the availability of renewable energy.

The integration of the heat and electricity sectors plays a crucial role in optimizing energy systems and enhancing sustainability. Rehman et al. (2021) provide a comprehensive review of enabling technologies for sector coupling, with a focus on the role of heat pumps and thermal energy storage in balancing supply and demand across thermal and electrical grids. [5]. However, this research is more focused on a larger scale, rather than the more local scale on which this thesis is focusing.

EV Integration

Vehicle-to-Grid (V2G) and Vehicle-to-Home (V2H) systems have the potential to redefine electricity demand management by turning EVs into dynamic energy storage units. V2G technology allows EVs to discharge electricity back to the grid during peak demand, acting as decentralized battery storage to improve grid stability [32]. Conversely, during periods of excess renewable energy production, EVs can absorb surplus power, thereby reducing the need for short-term energy storage and enhancing the utilization of renewable energy sources. Similarly, V2H enables EVs to supply power directly to households, offering resilience during power outages or high electricity price periods [95].

Hermans et al. (2024) present a model predictive control approach for optimizing EV charging in grid-connected microgrids. Managing 174 chargers, their system reduced peak grid load by 59% through smart scheduling and power distribution, highlighting the role of intelligent control in V2G/V2H systems for grid balancing and energy autonomy [41].

However, despite its potential, the large-scale implementation of V2G and V2H presents several challenges. Charging stations must be equipped with bidirectional inverters and upgraded grid infrastructure to handle the reverse flow of electricity [95].

2.8. CO_2 emissions

2.8. CO_2 emissions

Emission trading scheme

The European Union Emission Trading System (EU ETS), introduced in 2005, aims to reduce greenhouse gas emissions. It relies on an approach where an equal amount of emission permits is assigned or auctioned to large polluters, primarily power generation stations and industrial installations with a high installed thermal input. By 2023, the EU ETS has helped bring down emissions from European power and industry plants by approximately 47%, compared to 2005 levels [29].

The price of emission allowances under the EU ETS was approximately \in 25 per tonne of CO_2 in 2020. Since then, prices have risen significantly. Figure 2.16 shows the expected development of ETS prices until 2030. Forecasts suggest an increase to \in 70- \in 75 [54]. These rising costs aim to incentivize companies to reduce emissions and shift toward low-carbon technologies.

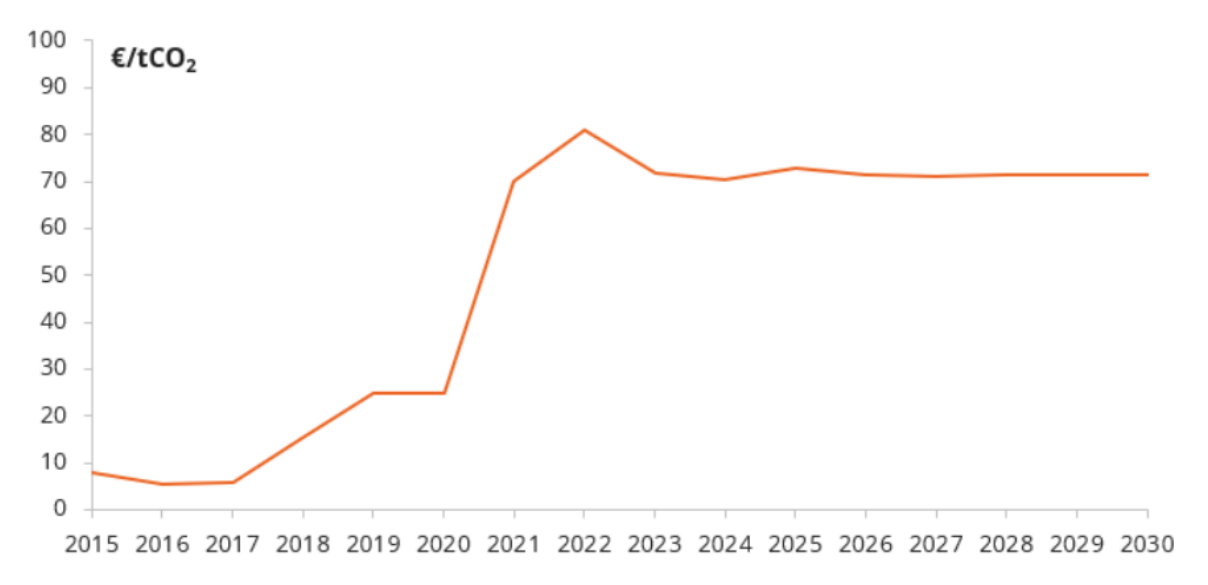


Figure 2.16: The EU ETS carbon price evolution until 2030 [54]

From 2030, emission allowances are expected to decrease, and scarcity is anticipated to drive prices to exponentially high levels. Projections indicate a potential increase to over €500 per tonne in 2044 [54]. Figure 2.17 illustrates the expected long-term evolution of the carbon price in the EU ETS. This increase has important implications for energy markets.

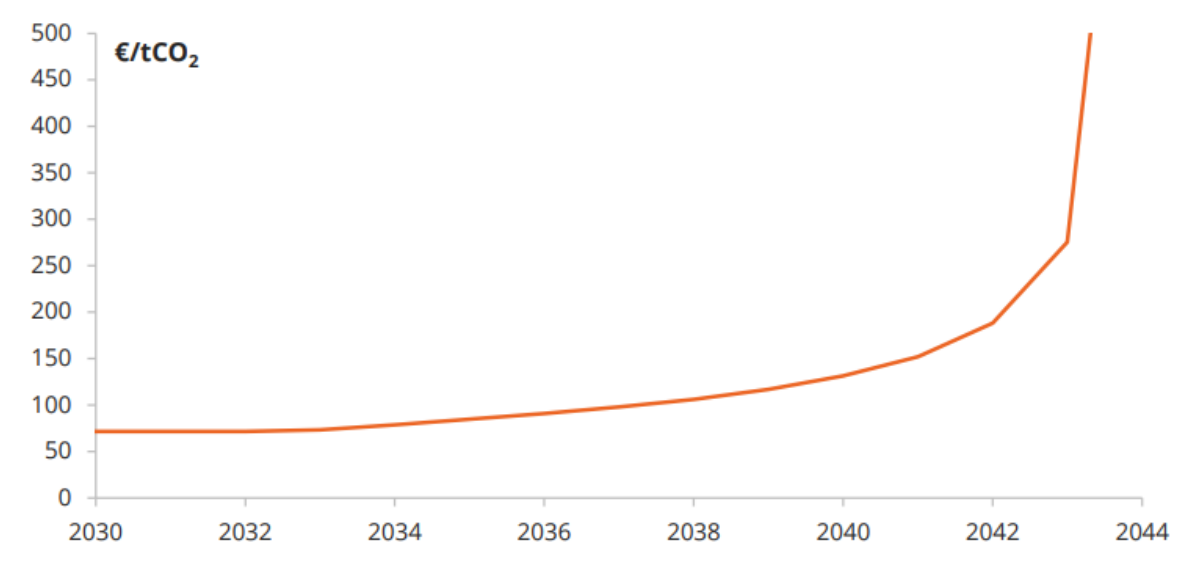


Figure 2.17: The EU ETS carbon price evolution after 2030 [54]

 $2.8. \text{ CO}_2 \text{ emissions}$

CO₂ emissions electricity

The carbon intensity of electricity production varies greatly depending on the primary energy source. Fossil fuels, such as coal, produce the highest emissions, with values of 820 g/kWh due to their low efficiency and high carbon content. Natural gas, while somewhat cleaner, still emits around 490 g/kWh [92]. In contrast, renewable energy sources such as wind, solar, and hydro generate electricity with almost negligible CO_2 emissions, excluding emissions from their production processes. Figure 2.18 shows the average life-cycle CO_2 equivalent emissions per energy source.

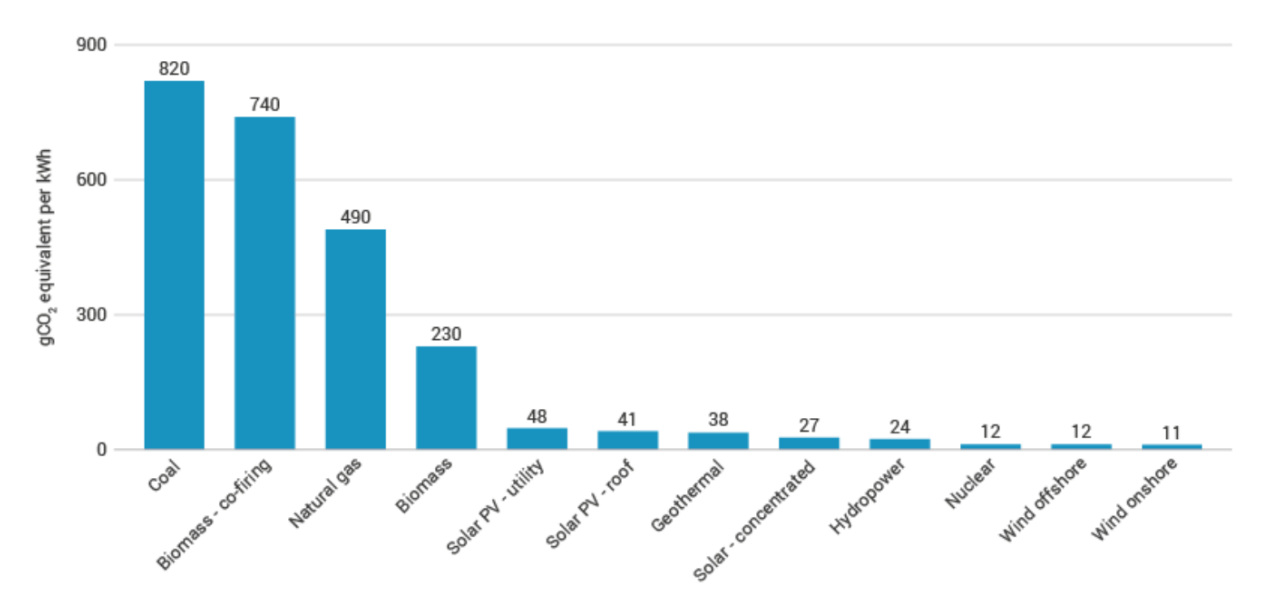


Figure 2.18: Average life-cycle CO_2 equivalent emissions [92]

In the first half of 2024, more than half of all electricity produced in the Netherlands was produced from renewable sources, see figure 2.19, with solar and wind taking the lead [73]. Yet natural gas remained the most significant fossil contributor, providing about 35%, as reliance on fossil fuels during periods of low renewable generation or peak demand persisted.

2.8. CO₂ emissions

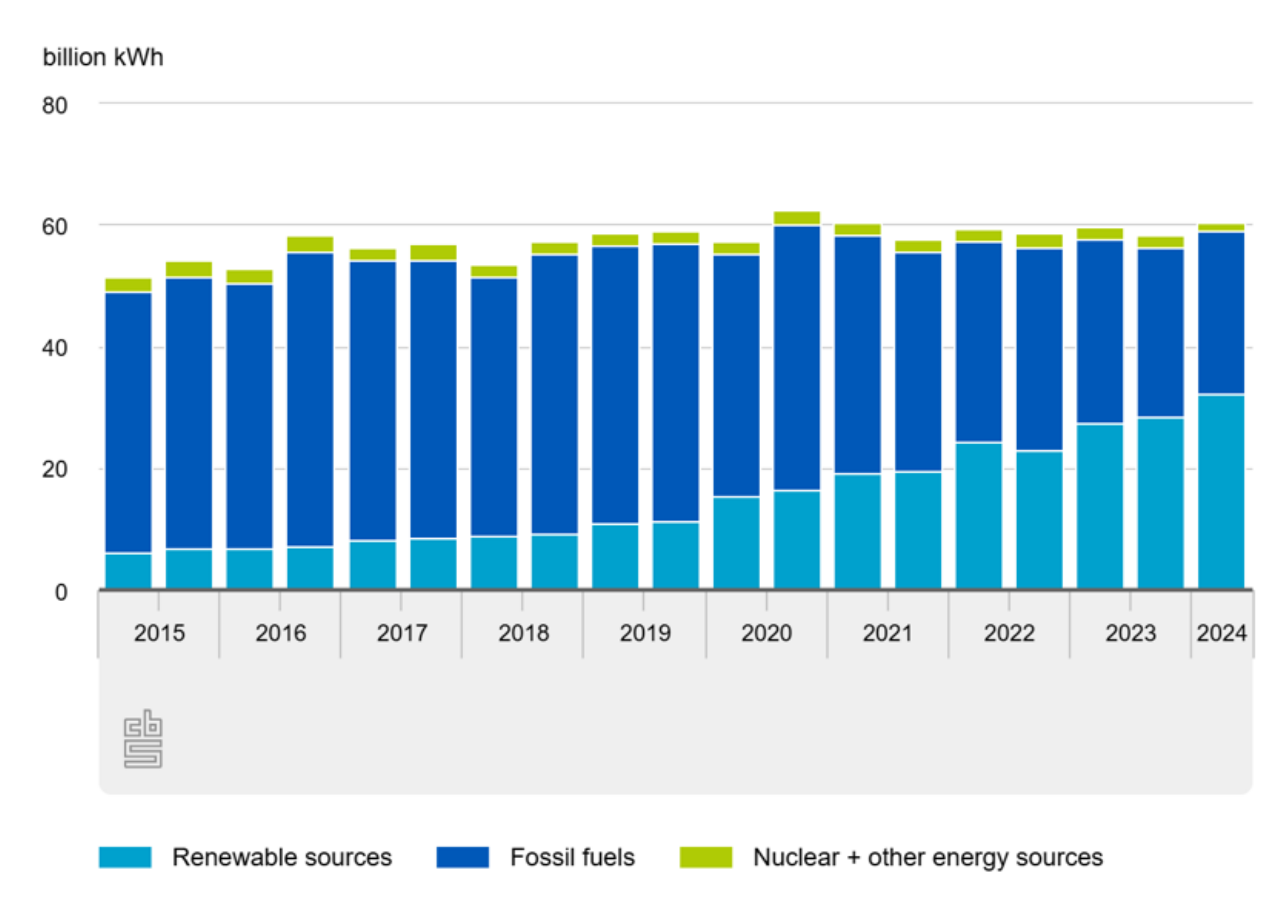


Figure 2.19: Electricity produced by energy source [73]

CO₂ emissions DHN

The carbon intensity of DHNs in the Netherlands varies depending on the heat source. According to "Duurzaamheidsrapportage Warmtenetten 2021" [88], networks rely on average 38% on renewable energy sources, and 10% on waste heat. This can vary a lot per DHN, from 0% to 90% renewable, and from 0% to 21% waste heat. Varying from 7 to 104 kg CO_2 /GJth, the average DHN emits 21.93 kg CO_2 /GJth. This is equivalent to about 80 g/kWh of heat.

2.9. Electricity and heat pricing

Electricity prices in the Netherlands can vary significantly, influenced by numerous factors such as fuel prices, weather, supply-demand mismatches, and the increasing share of renewable energy sources. The day-ahead market prices can range from negative prices when there is surplus, caused by solar or wind generation, to hundreds of euros per megawatt-hour during periods of scarcity or peak demand. Fluctuating electricity prices are the central factor affecting the design of smart energy systems and flexible consumption strategies.

Figure 2.20 shows the average electricity price per hour for each month in 2024. Daily patterns are visible, with prices typically peaking in the early morning and late afternoon. These peaks are higher in winter months. In contrast, midday prices tend to be lower, especially in summer, due to high solar PV generation. These trends highlight opportunities for SHTS. Shifting electricity use, such as heat pump operation, to low-cost hours can reduce energy costs and grid congestion due to electricity feed-in.

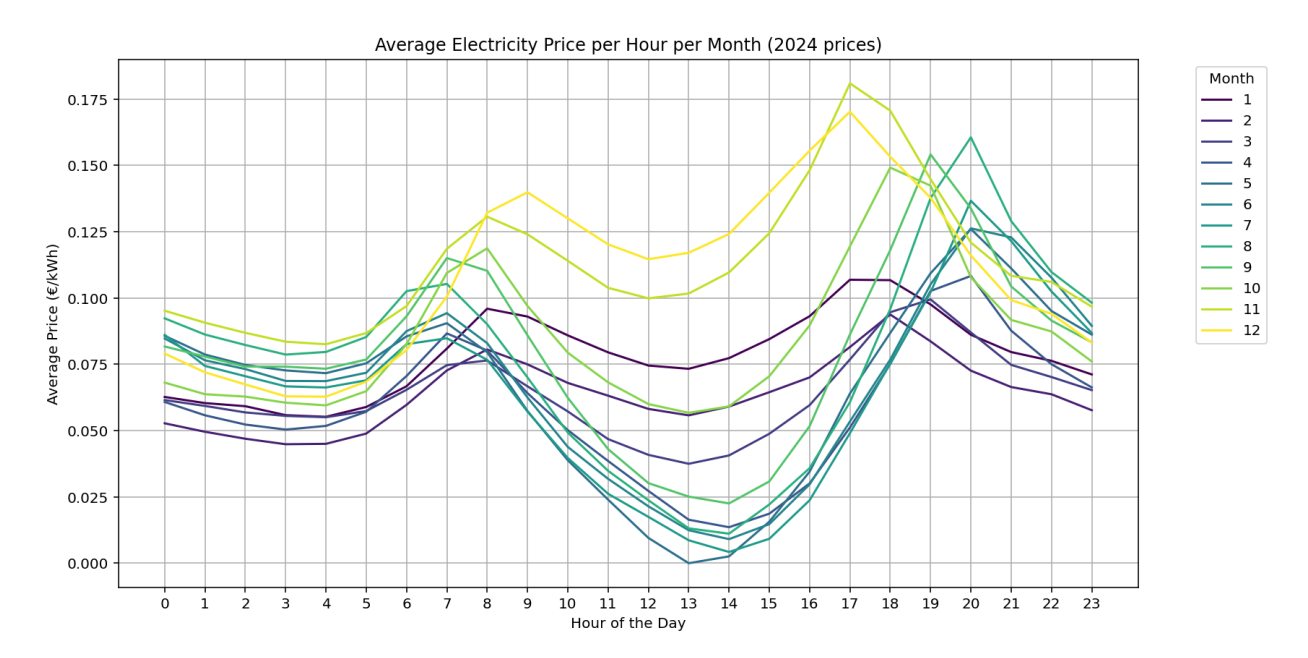


Figure 2.20: Average electricity price per hour per month (2024)

On the other hand, prices paid by DHN customers for heat are fixed and controlled. In recent years, the Dutch "Niet Meer Dan Anders" (NMDA) principle dictates that DHN prices be capped at a rate comparable to the price of single natural gas heating. However, district heating has been significantly more expensive than a regular gas connection. In 2023, the cost of district heating was 22% more expensive, and this difference can increase in 2024 [33]. This can be an incentive to develop an SHTS.

District heating typically involves a fixed connection fee and a variable charge based on heat consumption. While this stability benefits end-users, the upcoming "Wet Collectieve Warmte" (WCW) may further limit pricing flexibility in DHN. The fixed connection fee could increase, and could have negative effects on the costs for end-users.

2.10. Key Components SHTS

This section outlines the technical foundation of the SHTS by comparing it to a conventional HTS configuration.

Sub-question 1: What are the key differences between a conventional HTS and an SHTS?

The conventional HTS was described in section 2.6. The operation, components, and capacity sizing requirements were discussed. Conventional systems feature a heat exchanger that separates the primary and secondary networks, along with circulating pumps, controls, and pipes. Figure 2.21 shows a schematic view of a conventional HTS. Their setup ensures steady system operation and security against system imbalance, explained in more detail in section 2.6.

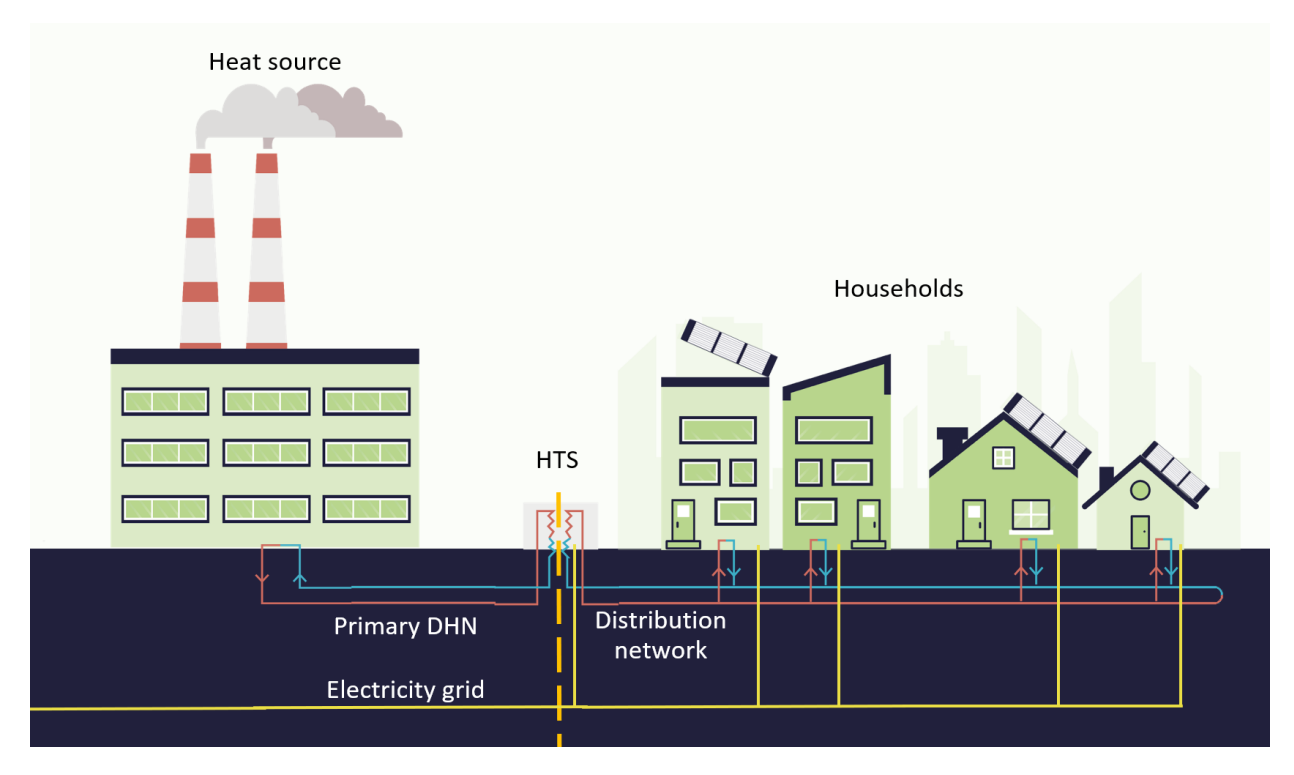


Figure 2.21: Reproduction of the schematic Heat Transfer Station, see figure 2.14, for clarity

The SHTS differs from the conventional configuration by integrating extra components that enable flexible and active control strategies, see figure 2.22. Unlike the conventional HTS, which is based on centralized heat supply, the SHTS integrates an HP, TTES, and an e-boiler into the station. Together with smart control, these components enable the system to dynamically adjust its operation in response to excess solar-generated electricity produced by the households. The addition of components in the SHTS is expected to require significantly more installation space than the conventional HTS. The additional space requirement will primarily be determined by the TTES, which can range in size from several parking spaces to that of a small house. Besides potential operational cost savings, the system reduces electricity grid feed-in and can help relieve part of the stress of the electricity network operator. Without congestion management, the grid may become overloaded, forcing curtailment of renewable energy sources.

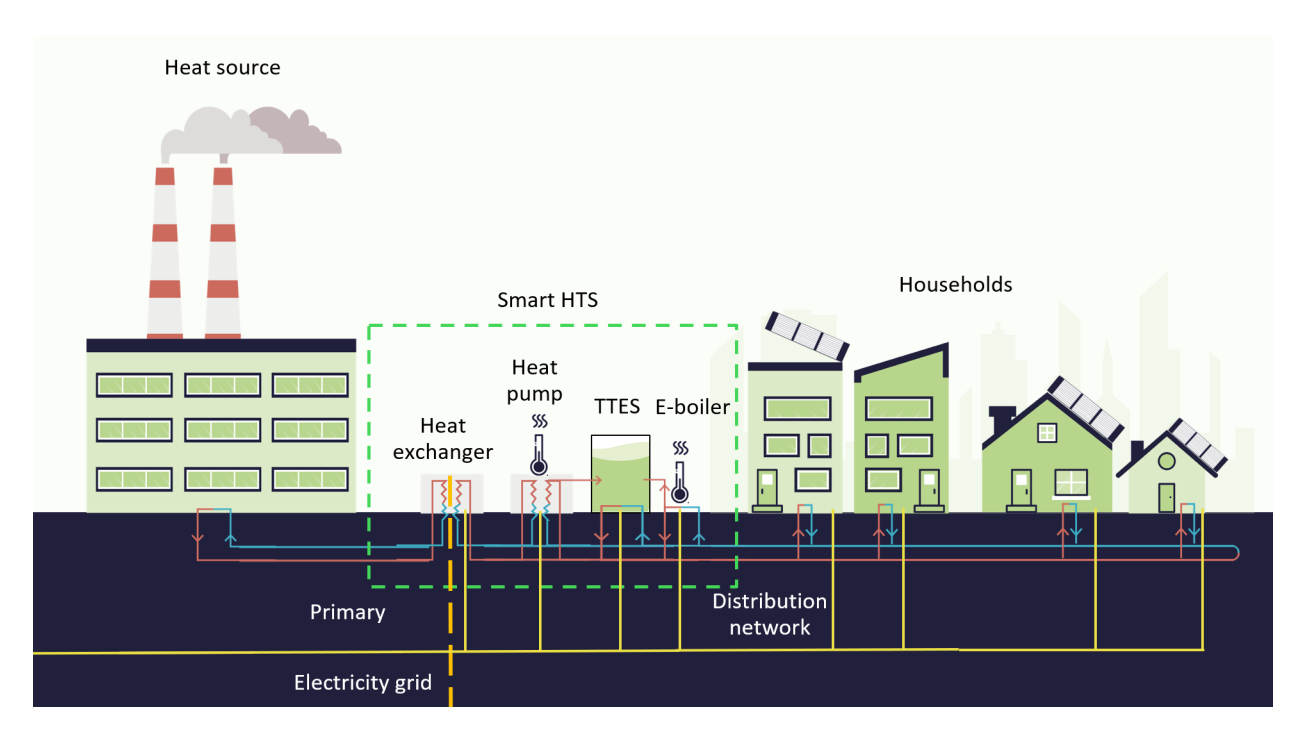


Figure 2.22: A schematic view of an SHTS

The heat pump can charge the TTES during periods of solar surplus or low electricity prices, while the e-boiler can serve as a backup during periods of peak demand or high solar electricity generation due to its flexibility. It also enhances operational flexibility, allowing for the separation of heat production and consumption at the same time, a level of flexibility not possible in conventional HTSs.

The schematic views in figure 2.21 and 2.22 show that the SHTS redefines the role of the heat transfer station at its core. Unlike the conventional HTS, which operates passively based on centralized heat supply, the SHTS integrates components as an HP, e-boiler, and a TTES. This shift enables the system to respond to solar surplus, low electricity prices, and predicted heat demand.

These additional components introduce flexibility. This enables the SHTS to operate as a local smart energy hub, supporting self-consumption, reducing grid feed-in, and enhancing overall efficiency. The smart configuration enhances both operational performance and system efficiency, which are increasingly relevant in future energy systems driven by variable renewable energy sources.

Overall, the SHTS transforms the conventional HTS from a passive heat transfer station into an active energy management node that interacts with local renewable energy sources.

$\frac{1}{3}$

This chapter provides the structure of how the model is set up. The model is applied to an urban area of 300 households and compared to a conventional HTS. The objective of this study is to use a simulation model to highlight the potential of SHTSs to support a more flexible, efficient, and sustainable energy system and contribute meaningfully to the energy transition. To that end, the study assesses the SHTS's ability to reduce peak loads, enhance local energy flows, limit CO_2 emissions, and mitigate grid congestion. To achieve this, a numerical energy model was developed in Python using the Spyder programming environment.

First, in section 3.1, a closer look is given at the modes of operation of the SHTS. The chapter breaks down the different modes of operation and how each piece of equipment, from the heat pump to the buffer tank, is modeled.

Section 3.2 then dives into what fuels the simulations: the data. This includes profiles of energy use in homes, weather information, and the amount of electricity solar panels generate throughout the day.

When it comes to optimization, discussed in 3.3, it consists of two parts: the day-to-day operation of the system was controlled by carefully crafted manual rules, while a broader analysis examined different combinations of equipment sizes and storage capacities to determine the optimum configuration.

In section 3.4, the assessment framework is proposed. It includes a technical analysis of system performance, an evaluation of greenhouse gas (GHG) emissions, and an economic assessment.

This chapter wraps up by verifying the model in section 3.5. This is done to ensure the reliability and credibility of the SHTS model.

3.1. Modes of operation

This section describes the modes of operation in the SHTS. The SHTS is composed of various assets to maximize local energy generation, storage, and utilization. The key assets that are simulated are an air-to-water heat pump, an e-boiler, and a TTES. Each subsequent subsection addresses each asset individually, elaborating on its working principles and citing significant equations, assumptions, and approaches used in its simulation.

Figure 3.1, 3.2 and 3.3 provide an overview of the system's mode of operations. The arrows in the diagrams represent the energy flows within the SHTS. The thickness of each arrow indicate the relative amount of the energy flow. Thicker arrows correspond to a higher energy flow, while thinner arrows indicate smaller contributions. Figure 3.1 illustrates the energy flow during summer months, from the excess electricity is high, and almost no grid electricity is flowing to the HP and e-boiler. During the winter months, shown in figure 3.3, it is the opposite, since there is almost no solar-generated electricity, and thus no excess electricity available for the SHTS. Figure 3.2 is the mode of operation for the spring and autumn months, which is between the modes of operation for summer and winter.

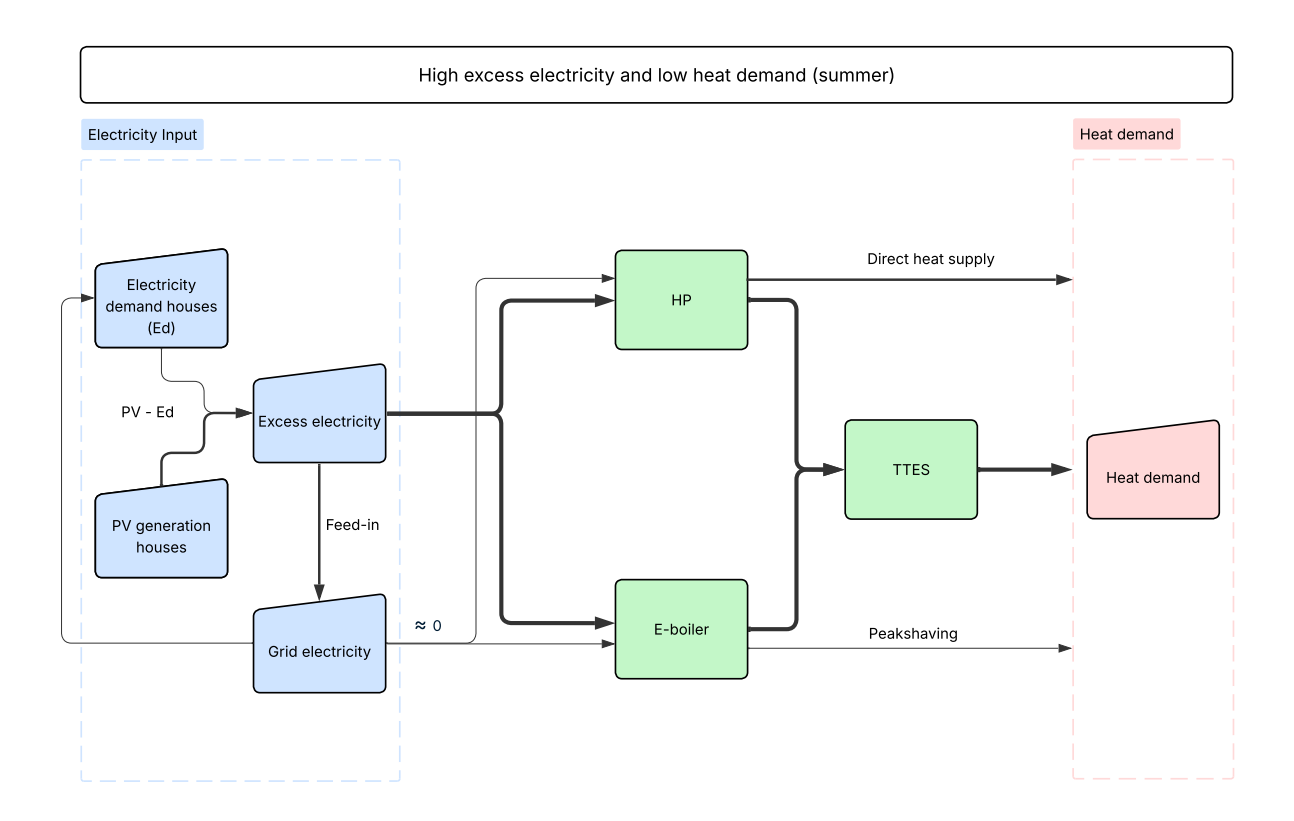


Figure 3.1: Mode of operation during summer months

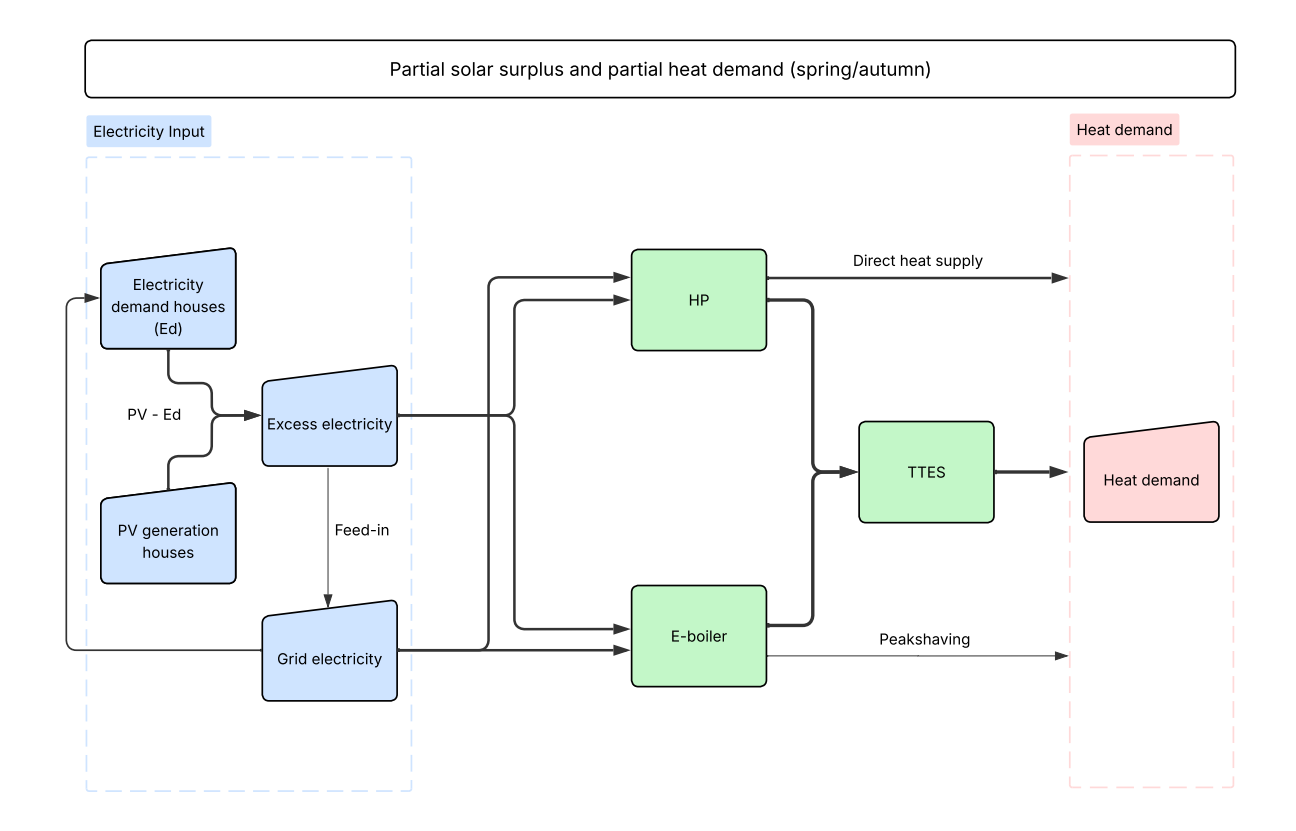


Figure 3.2: Mode of operation during spring and autumn months

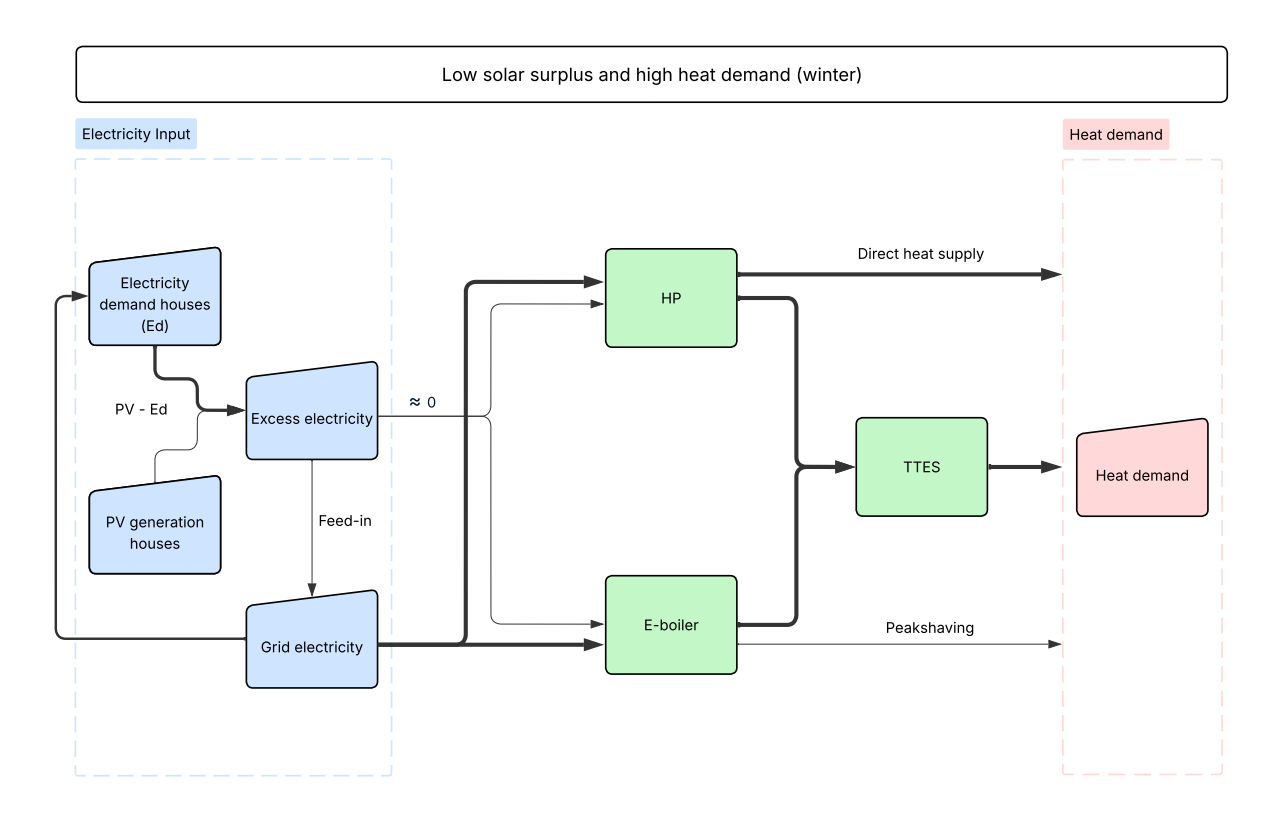


Figure 3.3: Mode of operation during winter months

3.1.1. Heat pump

The heat pump modeled in this study is an air-to-water heat pump, designed to transfer heat from ambient air to the water stored in the TTES. The heat pump is primarily powered by locally produced electricity from solar panels, with supplementary energy drawn from the grid when needed. The heat pump will always prioritize available solar surplus before calling upon the electricity grid.

Outside temperature dependent COP

The efficiency of the heat pump depends on the outside temperature and partial load. As the temperature outside decreases, the heat pump must work harder to extract heat, thereby reducing its COP. Often, a Seasonal COP (SCOP) is taken, but this is not accurate enough. The temperature fluctuates significantly daily; thus, during moments when the HP is active, the COP will vary substantially.

A theoretical upper bound for the COP is defined by the Carnot efficiency, which depends on the temperatures of the heat source (outside air) and heat sink, which is constant in this model:

$$COP_{Carnot} = \frac{T_{\text{sink}}}{T_{\text{sink}} - T_{\text{source}}}$$
 (3.1)

where:

- T_{sink} = temperature of the heated water in Kelvin
- T_{source} = outside air temperature in Kelvin

In practice, real heat pumps operate at a lower COP than the theoretical Carnot efficiency due to thermodynamic and technical losses. To model this more realistically, the actual COP can be expressed as:

$$COP_{\text{real}} = \eta_{\text{HP}} \cdot COP_{\text{Carnot}}$$
 (3.2)

where:

η_{HP} is the Lorentz efficiency factor

A Lorentz efficiency of 0.55 is used to calculate the performance of the HP [72]. This value represents the ratio between the actual COP and the Carnot COP, which is the maximum possible efficiency defined by thermodynamic limits. The Lorentz efficiency accounts for irreversible losses such as heat exchanger losses, compressor inefficiencies, and pressure drops.

This formulation enables the model to account for seasonal and daily effects, where lower outside temperatures lead to a reduced COP while higher temperatures result in more efficient operation.

In figure 3.4, the COP of the heat pump is displayed as a function of outdoor temperature, based on a Carnot efficiency model. The COP increases non-linearly as outdoor temperature rises, reflecting reduced temperature lift required from the heat pump.

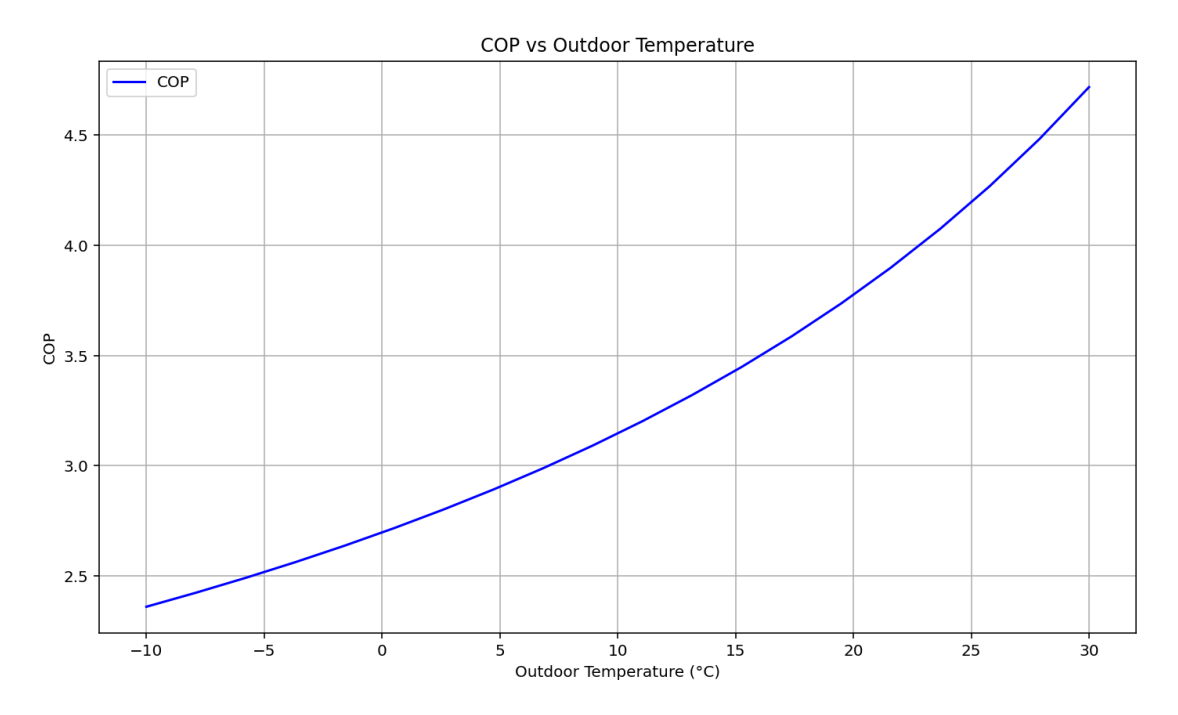


Figure 3.4: COP at different outside temperatures

COP at Partial Load (COPpl)

The Partial Load Ratio (PLR) quantifies the operating capacity of the heat pump relative to its maximum capacity:

$$PLR = \frac{P_{\mathsf{input, actual}}}{P_{\mathsf{input, max}}} \tag{3.3}$$

where:

- *P*_{input, actual} is the actual electrical input [kW]
- $P_{\text{input, max}}$ is the rated maximum input

To account for cycling losses, a cycling coefficient C_c is applied. The Coefficient of Performance at partial load is calculated as [93]:

$$COP_{pl} = COP_{real} \cdot \frac{PLR}{PLR \cdot C_c + (1 - C_c)}$$
(3.4)

where:

- COP_{real} = full-load COP, calculated in equation 3.2
- C_c cycling coefficient

In figure 3.5, the COP is shown at different PLRs. When PLR = 0, the COP is zero. The heat pump must operate at a PLR of a minimum of 0.4. Otherwise, the HP will shut off.

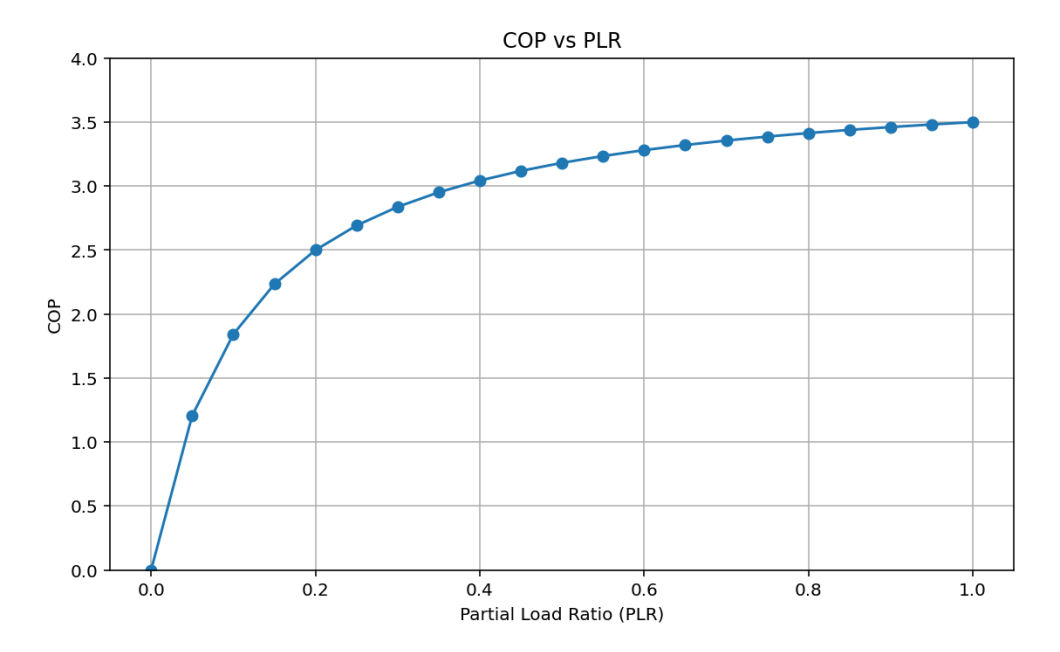


Figure 3.5: COP at different partial load ratios

A cycling coefficient is used to describe the decline in performance under partial loading of the heat pump. It accounts for greater inefficiencies in response to typical on/off cycling and better approximates real-world behavior. The cycling coefficient is assumed to be 0.9 [93].

Cycling losses

Frequent on-off cycling of the heat pump results in efficiency losses. Each cycle introduces transient periods during which the system operates below optimal conditions, thereby increasing wear on components such as the compressor and valves. These inefficiencies are relatively high when the system short-cycles, switching on and off rapidly, resulting in higher energy consumption and reduced component lifespan.

To account for this, startup and cool-down periods are introduced in the model. When the heat pump is switched on, it does not immediately reach full capacity. Instead, it undergoes a 15-minute startup phase, during which the output gradually increases. This delay accounts for the physical behavior of system components such as the compressor and circulation systems, which require time to stabilize internal pressure and temperature [51]. Likewise, when the system shuts down, it may continue to deliver some heat or undergo a thermal ramp-down, which can influence the timing of subsequent heating events and residual losses. These are a few hours and can be easily adjusted.

Heat pump operation conditions

The heat pump operates based on predefined active hours, varying monthly to account for seasonal differences in heating demand and solar availability. Typically, the heat pump is active during nighttime (00:00–06:00), due to relatively low electricity prices, and designated active periods in the afternoon (12:00–17:00), with monthly adjustments made accordingly. During nighttime active hours, the heat pump charges the TTES, ensuring the day begins with a full tank. During other active hours, the heat pump can deliver direct heat to demand, and surplus is stored in the tank. If the direct heat is not enough yet, heat from the tank can also be supplied. The heat pump shuts off once 90% of the tank is filled, to prevent overproduction.

The logic is as follows:

$$Q_{\text{direct}} = \min(Q_{\text{HP,out}}, Q_{\text{demand}}) \tag{3.5}$$

$$Q_{\text{storage}} = Q_{\text{HP,out}} - Q_{\text{direct}}, \tag{3.6}$$

$$\begin{cases} > 0 & \text{heat to storage (charging)} \\ = 0 & \text{no storage activity} \\ < 0 & \text{heat from storage (discharging)} \end{cases} \tag{3.7}$$

where:

- $Q_{\mathrm{HP,out}}$ is the heat output from the heat pump in kWh per 15 min
- Q_{demand} is the heat demand during peak hours in kWh per 15 min

To prevent excessive wear and inefficient cycling, the heat pump is subject to a minimum running time of 2 hours. It will only activate if sufficient storage capacity is available to sustain operation for this duration. When the HP is shut off, there is a cooldown period of 4 hours.

Heat demand forecasting

To further optimize operation, a forecasting strategy is used. Historical heat demand data from the same weekday in the previous week is combined with weather forecasts to predict upcoming solar availability and heating needs. The e-boiler generates the expected heat, as the HP is shut off for the day. Based on this information, the system can decide whether the heat pump should charge the thermal storage tank during the night or rely on expected solar power during the day. This approach enables more informed scheduling decisions, enhancing efficiency. During the springtime, these are compared one-to-one. During autumn, a factor of 1.1 is added to the demand forecast, since demand will probably increase compared to the week before.

3.1.2. E-boiler

The e-boiler in this model serves as a flexible heat source, supporting regular thermal storage and capable of peak shaving. Unlike the heat pump, the e-boiler is not limited by active hours and can operate at any time, given that storage capacity is available or immediate heat demand must be covered.

The E-boiler can use both solar and grid electricity with the same priority as the heat pump. However, the e-boiler is used with only solar electricity and does not use grid electricity, unless during peak shaving.

COP and Efficiency

E-boilers are highly effective in converting electrical energy to heat. Since the process is not dependent on ambient temperature or partial load ratios, the COP is independent of these latter conditions and is constant [65]. The COP of the electric boiler is assumed constant at 0.99 [21], which is a representation of the direct conversion of electricity to heat.

Operational Logic

At moments when there is a surplus of solar-generated electricity and available capacity in the thermal storage tank, the E-boiler becomes active. If the tank reaches 95% of its maximum capacity, the E-boiler is automatically turned off to prevent overcharging. This percentage is higher than the 90% of the HP, since the e-boiler is able to run with the same efficiency at lower capacity, whereas the HP preferably runs at full capacity. Furthermore, the e-boiler is more flexible in varying the energy output, and it is easily turned on or off.

The heat output of the e-boiler is defined as:

$$Q_{\text{e-boiler, out}} = P_{\text{e-boiler, input}} \cdot COP_{\text{e-boiler}} \cdot \Delta t$$
 (3.8)

where $\Delta t = 0.25$ hours (15-minute interval).

Peak Shaving Strategy

The E-boiler plays a critical role in peak shaving by supplying heat when the output from the TTES and the HP is insufficient to meet demand. This typically occurs during peak hours (17:00–20:00), when heat can be supplied directly from the e-boiler. It is important to keep in mind that activating the e-boiler for heat demand peak shaving during peak electricity hours can exacerbate net congestion. Therefore, excessive peak shaving should be avoided.

Excess demand during these moments is defined as:

$$Q_{\text{excess}} = Q_{\text{demand}} - Q_{\text{TTES,discharged}} - Q_{\text{HP,direct}} - Q_{\text{peak threshold}}$$
 (3.9)

The actual grid usage is calculated as:

$$P_{\text{grid,e-boiler}} = \max(0, P_{\text{e-boiler,input}} - P_{\text{solar available}})$$
 (3.10)

where:

• $P_{e-boiler,input}$ = the needed power input for the e-boiler, calculated with equation 3.8

The E-boiler delivers this excess heat to ensure that the total heat supplied does not exceed the peak heat demand threshold, which can be configured based on system constraints or grid limitations. It uses available solar electricity preferentially, and draws from the grid when needed. However, heat peak shaving moments are almost always at moments where solar-generated electricity is unavailable.

3.1.3. Tank thermal energy storage

The thermal buffer tank, also referred to as the TTES, plays a key role in balancing heat production and demand within the smart HTS. It stores excess heat from both the heat pump and the e-boiler and supplies it during periods of demand.

The thermal storage tank is modeled in terms of energy content, expressed in kWh. This allows for a simulation of energy flows during charging and discharging in combination with the heat pump and e-boiler.

To verify whether the required storage capacity is feasible in practice, a calculation is made to estimate the tank volume needed, and vice versa for the maximum TTES size. It is assumed that the tank is perfectly mixed, and no stratification occurs. A more detailed calculation of a stratified TTES is provided in appendix A.

The total water volume V (in m³) required to store a certain amount of heat Q (in kWh), given a temperature difference ΔT and specific heat capacity of water C_w , can be estimated as:

$$V = \frac{Q \cdot 3.6 \cdot 10^6}{C_w \cdot \Delta T \cdot \rho} \tag{3.11}$$

Where:

- Q is the thermal energy in kWh,
- $C_w = 4190 \text{ J/(kg·K)},$
- $\Delta T = 30^{\circ}$ C,
- the factor $3.6\cdot 10^6$ converts kWh to joules,
- water density $\rho \approx 1000 \text{ kg/m}^3$.

This formula offers a quick way to verify whether the calculated thermal storage capacity translates to a physically acceptable tank size in practice. Assuming a maximum tank size of $100m^3$, this results in a maximum of 3500kWh, see table 3.1. The calculated TTES volume per household ranges from 0.096 to $0.334m^3$ depending on the total storage capacity. Minimizing the outer layer, and thus the heat losses, the height needs to be twice the radius [20]. Dimensions of the tank can be calculated accordingly. This step provides realistic design parameters for the tank's physical dimensions.

TTES capacity (kWh)	TTES volume (m ³)	Volume per household (m ³)
1000	28.7	0.096
1250	35.8	0.119
1500	43.0	0.143
1750	50.2	0.167
2000	57.3	0.191
2250	64.5	0.215
2500	71.7	0.239
2750	78.8	0.263
3000	86.0	0.287
3250	93.2	0.311
3500	100.3	0.334

Table 3.1: TTES volume corresponding to capacity at $\Delta T = 30$ °C (based on 300 households)

Energy flows: charging and discharging

During defined discharge periods, the maximum thermal discharge capacity is limited to 240 kW, which is equivalent to 60 kWh per 15-minute interval. This comes down to 6.3% of the maximal heat demand. This is adjustable when it is desirable to discharge the tank at a greater speed during peak demand. These constraints ensure controlled release of heat and efficient use of storage resources throughout the day.

Flow rate and heat capacity design

The design of the heat delivery system starts with a commonly used pipe size, DN50, with an internal diameter of 50mm. To limit pressure losses and avoid mechanical stress, a maximum flow velocity of 1.5m/s is assumed, as recommended in practice [21].

To determine the required pipe diameter, the cross-sectional area is related to the diameter:

$$A = \frac{\pi D^2}{4} \quad \Rightarrow \tag{3.12}$$

We use the relationship between mass flow rate, fluid density, cross-sectional area, and velocity:

$$\dot{m} = \rho \cdot A \cdot v \quad \Rightarrow \tag{3.13}$$

where:

- $\rho = 1000 kg/m^-3$ is the density of water,
- v = 1.5m/s is the assumed maximum flow velocity,
- D = 0.05m is the internal pipe diameter,
- A is the cross-sectional area in m^2 ,
- \dot{m} is the mass flow rate in kg/s.

Using these assumptions, the resulting cross-sectional area is:

$$A = \frac{\pi (0.05)^2}{4} \approx 0.00196 \text{ m}^2$$

$$\dot{m} = \rho \cdot A \cdot v = 1000 \cdot 0.00196 \cdot 1.5 \approx 2.95 \,\mathrm{kg}\,\mathrm{s}^{-1}$$

A maximum design mass flow rate of 3kg/s is therefore adopted.

Based on this mass flow and a maximum temperature difference of $30\,^{\circ}\mathrm{C}$, the maximum thermal power that can be transferred is calculated using:

$$P = \dot{m} \cdot c_n \cdot \Delta T \tag{3.14}$$

where:

- P is the thermal power in W,
- $\dot{m} = 3\,\mathrm{kg}\,\mathrm{s}^{-1}$ is the design flow rate,
- $c_p = 4190\,\mathrm{J\,kg^{-1}\,K^{-1}}$ is the specific heat capacity of water,
- $\Delta T = 30\,\mathrm{K}$ is the temperature difference.

Substituting the values:

$$P = 3 \cdot 4190 \cdot 30 \approx 377 \,\text{kW} \tag{3.15}$$

This calculated capacity sets the design limit for both the heat pump and the e-boiler. Since this is the thermal output, the electrical input must be corrected for the COP. Assuming a COP of approximately 1 for the e-boiler, its electrical demand equals the thermal power. For the heat pump, with typical COP values between 3.1 and 3.6, the electrical input would range between 105kW and 115kW, depending on outside conditions.

For the simulations, slightly higher maximum design capacities were selected. A maximum capacity of 120kW was chosen for the heat pump, and 400kW for the e-boiler.

3.2. Input Variables 36

3.2. Input Variables

The simulation draws on five datasets: solar radiation, ambient temperature, heat demand, electricity demand, and electricity prices. All data were provided initially as hourly time series. To improve temporal resolution, the time series for solar radiation, temperature, and both demand profiles were linearly interpolated to 15-minute intervals. Linear interpolation was chosen for its simplicity, computational efficiency, and ability to capture gradual transitions typical of these variables, especially when modeling aggregated behavior across hundreds of households. For electricity prices, however, step-wise interpolation was applied, assuming the price remains constant within each hour and updates only at the start of the next. After interpolation, each dataset was normalized and scaled to reflect the combined activity of 300 households, representing a heat transfer station scale.

Yearly heat and electricity demand

The yearly heat demand is assumed to be 12,000 kWh per house for space heating and the use of domestic hot water [21]. This is then scaled to the overall demand of the total HTS. The heat demand is made up of domestic hot water and space heating loads. It has a seasonal profile with high winter-month demands and much smaller summer values, where hot tap water is almost the only heat demand.

Annual electricity consumption per household is assumed to be 3,000 kWh, based on national averages [21]. This includes lighting, appliances, and other electrical home equipment. The total sum demand is used to simulate the aggregate electricity consumption of the system.

Solar panels

The solar radiation levels are used in the calculation of solar panel electricity generation. A constant panel efficiency of 24% [21], and an average area of solar panels per house is assumed. This allows calculation of electricity generation, with a peak at noon and a decline to zero at nighttime. While actual efficiency may vary with temperature and angle of incidence, a constant efficiency represents the typical efficiency of modern panels.

The net positive electricity generation profile is calculated by subtracting household electricity demand from the generation. The pattern of electricity demand is a profile of a residential area, obtained by DWTM, with higher consumption during the early morning and evening, and lower consumption during the night.

Data Type	Unit	Original Resolution	Interpolation Method	New Resolution
Heat demand	kW	Hourly	Linear	15-minute
Electricity demand	kW	Hourly	Linear	15-minute
Solar radiation	W/m ²	Hourly	Linear	15-minute
Ambient temperature	°C	Hourly	Linear	15-minute
Electricity prices	€/kWh	Hourly	Step-wise (forward fill)	15-minute

Table 3.2: Model Input Data

Heat Exchanger Efficiency

In the system, the heat exchangers play a key role in transferring heat between the assets and the DHN. An efficiency of 0.90 has been assumed [49]. There are three heat exchangers in the system. The heat pump, e-boiler, and TTES all have a connection with the DHN with a heat exchanger. The e-boiler and HP have a heat exchanger with the DHN, because they can deliver direct heat to the DHN and bypass the TTES, elaborated in section 3.1.1 and 3.1.2.

Table 3.3 summarizes the input values used in the model.

3.2. Input Variables 37

Table 3.3: Overview of Key Model Assumptions

Parameter	Value	Unit
Number of households in the SHTS	300	Houses
Yearly heat demand per household	12000	kWh
Peak heat demand at SHTS level	947	kW
Yearly electricity demand per household	3000	kWh
Peak electricity demand at SHTS level	203	kW
Solar panel efficiency	24	%
Lorentz efficiency	0.55	_
COP of the e-boiler	0.99	_
Cycling coefficient (partial load)	0.9	_
Temperature delta in TTES	30	$^{\circ}C$
Tank mass inflow/outflow	3	kg/s
Heat exchanger efficiency	0.90	_
Maximum capacity HP	120	kW
Maximum capacity e-boiler	400	kW
Maximum capacity TTES	3500	kWh

3.3. Asset Optimization

Optimization of the SHTS is essential to ensure efficient operation in a residential setting. Two main aspects are subject to optimization: the control strategy and the dimensioning of assets. As the SHTS is embedded in a neighborhood, it is essential that both control decisions and component sizes align with local energy demand and supply conditions, and that these are handled efficiently. The control strategy is suboptimal, as it relies on a rule-based approach rather than a formal optimization process. Using heat demand forecasts, prioritizing solar power, and enforcing minimum running times, which offers a practical yet suboptimal approach to system control.

Asset optimization

Asset sizing was conducted from iterative simulations. The following were set to obtain efficient system performance:

TTES capacity

The storage tank was sized to mitigate most day-night cycles of demand-supply imbalances and remain within acceptable dimensions. This is achieved by setting a capacity in kWh for the tank and subsequently translating it into real dimensions.

HP capacity

The power of the heat pump should be chosen such that it can deliver sufficient heat when needed while also ensuring that it operates at full capacity as often as possible, since it achieves its highest efficiency at full load.

· E-boiler capacity

The maximum capacity of the e-boiler is selected to ensure it can use most of the solar-generated electricity, minimizing the amount of feed-in electricity.

PV area

The system's performance is closely tied to the surface area of the solar panels, requiring tight coordination with the other assets. At the same time, the number of solar panels per household can not be chosen, since it is the choice of the inhabitants. Varying this amount shows the effect and could serve as advice to households.

Table 3.4 shows the definitions for the solar panel area (m^2) , TTES (kWh), HP size (kW), and e-boiler size (kW). These ranges result in a total of 2.156 unique combinations tested in the simulation model. These combinations are simulated with the same number of houses, heat demand and electricity profile.

Parameter	Unit	Range	Step Size
TTES capacity	kWh	1000-3500	250
Heat pump capacity	kW	60-120	10
E-boiler capacity	kW	100-400	50
Solar panel area per house	m^2	11–17	2

Table 3.4: Parameter Ranges for Asset Optimization

3.4. Assessment Framework

This section evaluates the technical, spatial, greenhouse gas (GHG), and economic performance of the smart HTS, considering how each of the critical elements supports the overall heat supply and grid interaction of the system.

3.4.1. Technical metrics

COP system

The COP of the system represents the overall system efficiency and is defined as the ratio of the total useful thermal energy output to the total electrical energy input from the grid:

$$\mathsf{COP}_{\mathsf{system}} = \frac{Q_{\mathsf{useful}}}{E_{\mathsf{input},\mathsf{grid}} + E_{\mathsf{input},\mathsf{solar}}} \tag{3.16}$$

where:

- Q_{useful} is the total useful thermal energy delivered by the system over the year in kWh,
- $E_{\text{input,qrid}}$ is the total electricity consumed from the grid, in kWh.
- $E_{\text{input,solar}}$ is the total solar-generated electricity consumed, in kWh.

This metric quantifies the energy efficiency of the system in converting electrical energy into useful heat.

Grid feed-in

Grid feed-in quantifies the fraction of generated solar electricity that is not utilized within the system and is instead exported to the grid, potentially contributing to feed-in net congestion:

$$\mathsf{Feed-in}(\%) = \frac{E_{\mathsf{feed-in}}}{E_{\mathsf{total.solar}}} \tag{3.17}$$

where:

- $E_{\text{feed-in}}$ is the total solar energy that is generated but not consumed locally (fed into the grid), in kWh,
- $E_{\text{total,solar}}$ is the total solar electricity generated over the year, in kWh.

This provides an indication of how efficiently the system is able to self-consume its own renewable energy.

Tank contribution

The contribution of the tank to the overall system heat supply is calculated. The total number of full load cycles is used as a performance indicator. The number of tank cycles over the year is defined as:

$$N_{
m cycles} = rac{Q_{
m extracted}}{Q_{
m TTES}}$$
 (3.18)

where:

- $Q_{\text{extracted}}$ is the total heat extracted from the TTES throughout the year in kWh,
- Q_{TTES} is the energy capacity of the tank in kWh.

This gives an intuitive measure of how actively the tank is utilized within the system, independent of its instantaneous storage efficiency.

Heat supply coverage

This metric indicates the part of the total annual heat demand that is met by the total system. It is calculated as:

$$\mathsf{Coverage(\%)} = \frac{Q_{\mathsf{system}}}{Q_{\mathsf{total},\mathsf{demand}}} \tag{3.19}$$

where:

- Q_{system} is the sum of all heat delivered from the SHTS to meet demand over the year in kWh,
- $Q_{\text{total,demand}}$ is the total annual heat demand in kWh.

A high coverage rate suggests that the system can substantially reduce heat supply from external heat sources.

DHN load

The DHN grid relief metric measures the extent to which the energy system alleviates stress on the DHN. It is expressed as the percentage reduction in heat drawn from the grid compared to a conventional HTS. The focus is on identifying the reduction during peak moments:

Grid Relief(%) =
$$\frac{\text{Conventional HTS peak load} - \text{SHTS peak load}}{\text{Conventional HTS peak load}}$$
(3.20)

where:

- Common HTS peak load is the highest heat delivery in the reference scenario in kW,
- SHTS peak load is the highest heat delivery in the simulated SHTS in kW.

This metric helps assess the system's potential for relieving DHN during peak moments.

Heat pump Full Load Hours (FLH)

The annual FLH of the HP indicates how intensively the HP is used throughout the year. This is calculated by dividing the total thermal energy delivered by the HP by its nominal thermal capacity:

$$\mathsf{FLH}_{\mathsf{HP}} = \frac{Q_{\mathsf{HP}}}{P_{\mathsf{HP}}} \tag{3.21}$$

where:

- Q_{HP} is the total annual heat output provided by the HP in kWh,
- P_{HP} is capacity of the HP kW.

This metric gives insight into the annual utilization of the HP. A very low number of full load hours may indicate underutilization, or an HP with too much power. While excessively high values could indicate a too small HP, and can lead to accelerated wear.

3.4.2. Greenhouse Gas Emissions

This section calculates the GHG savings of the SHTS by approximating the avoided CO_2 emissions thanks to reduced reliance on electricity and heat from the grid.

Avoided emissions

To calculate the avoided CO₂ emissions, two key components are considered:

- $\Delta Q_{\text{DHN, saved}}$ Reduction in heat demand from the district heating network
- $\Delta E_{
 m HP/E-boiler,\ used}$ Additional electricity consumed by the heat pump, supplied by the grid

Each component is multiplied by its respective emission factor:

- $\epsilon_{\rm el,arid}$ for grid electricity in kg ${\rm CO_2}/kWh$
- $\epsilon_{\text{heat},\text{DHN}}$ for heat from the district heating network in kg CO $_2/kWh$

The emission factors of grid electricity and heat from DHN are assumed to be $0.328~{\rm kg~CO_2}/kWh$ and $0.079~{\rm kg~CO_2}/kWh$, respectively [9] [21]. The extra electricity used by the heat pump is assigned the same emission factor as the grid and is subtracted from the total savings. The resulting net avoided emissions are calculated as:

Added Emissions_{electricity,kg} =
$$\Delta E_{\text{HP/E-boiler, used}} \cdot \epsilon_{\text{el,grid}}$$
 (3.22)

Avoided Emissions_{DHN,kg} =
$$\Delta Q_{\text{DHN, saved}} \cdot \epsilon_{\text{heat,DHN}}$$
 (3.23)

The total avoided emissions are the sum of the two:

This formulation ensures that both environmental savings and additional emissions from system operation are properly accounted for in the analysis.

CO_2 cost evaluation

In order to translate these benefits into the economy, avoided carbon emissions are assigned a dollar value. Valuation provides feedback on the economic effect of avoided greenhouse gas emissions and allows this to taken into account in the economic analysis.

The cost benefit from avoided emissions is calculated using:

$$CO_2 \text{ Value}_{\text{total}} = \text{Avoided Emissions}_{\text{total}} \cdot CO_2 \text{ Price}_{\text{per ton}}$$
 (3.25)

where:

- Avoided Emissions: The estimated yearly reduction in carbon emissions due to lower reliance on grid electricity heating, expressed in tonnes/year.
- CO₂ Price: The market or policy-driven price per ton (€/ton CO₂)

The CO_2 price per ton is assumed as 87,90 euros, according to [58].

3.4.3. Economic Evaluation

This section describes the methodology used to assess the economic performance of the smart heat reception system. The input parameters for financial analysis, such as Capital Expenditures (CapEx), annual savings, and Operational Expenditures (OpEx), were directly obtained from DWTM. DWTM provided reference data from completed projects, market data, and technical specifications.

Electricity price integration

Electricity price data exclude VAT, energy tax (which varies depending on total annual energy consumption), and a small supplier's purchasing fee. Since the simulation operates on a 15-minute resolution, the hourly price data was step-wise interpolated to match the simulation result resolution. Electricity consumed directly from the solar panels is excluded from energy taxes [10], and the supplier's fee is accordingly factored into the electricity cost calculations. The energy tax, based on total annual energy consumption, is added to the electricity consumed from the grid.

Cost calculation approach

The following equation was used to determine the cost of electricity consumed from the grid at each time step:

$$Cost () = P \cdot \Delta t \cdot p \tag{3.26}$$

where:

- P is electricity use in kW (from grid or solar)
- Δt is the duration of each timestep (0.25 hour)
- *p* is the electricity price in €/kWh, where the solar-generated electricity price is excluded from energy tax.

Payback time

The payback time is the time in years necessary for the initial investment to be returned from savings over a year, displayed in equation 3.27. This involves savings from lower electricity costs resulting from the self-consumption of solar-generated electricity, as well as saved heating costs due to the use of TTES.

Payback Time =
$$\frac{\text{Total initial investment}}{\text{Annual cost savings}}$$
 (3.27)

Net Present Value (NPV)

The NPV is calculated using equation 3.28, the current value of future cost savings that would be incurred as a result of investment in the SHTS. It also reflects the time value of money by discounting future cash flows. An NPV greater than zero indicates that the investment is expected to generate positive returns over its 15-year lifetime, as assumed in this thesis.

$$NPV = \sum_{t=0}^{n} \frac{CF}{(1+r)^t}$$
 (3.28)

where:

• *CF*: Cashflow (revenues - expenses)

r: Discount rate

• t: System lifetime in years

A higher discount rate puts less value on future savings, and this will have a considerable effect on the NPV outcome. Revenues in the analysis include electricity use reductions and avoided heating costs. The expenses are the OpEx to keep the SHTS running. While a comprehensive financial analysis would typically account for subsidies and tax effects such as depreciation-related tax shields, these are excluded to keep focus on net operational benefits. Moreover, no explicit subsidies for SHTS systems are currently known.

Levelized Cost Of Heat (LCOH)

The LCOH is the cost per unit of useful heat produced over the system's life, calculated with equation 3.29, in kWh. It makes a comparison possible among different heat production technologies since it includes both CapEx and OpEx.

$$LCOH = \frac{\sum_{t=1}^{n} \frac{CapEx_{t} + OpEx_{t}}{(1+r)^{t}}}{\sum_{t=1}^{n} \frac{Energy}{(1+r)^{t}}}$$
(3.29)

where:

CapEx: Capital expenditures

OpEx: Operational expenditures

Energy: Generated energy by the SHTS

• r: Discount rate

• t: System lifetime in years

A lower LCOH indicates a less expensive heating solution. In this research, the LCOH is used to compare the economic performance of the smart heat reception system in providing heat with other traditional solutions.

Internal Rate of Return (IRR)

The IRR is the discount rate at which the NPV of all future cash flows equals zero. It is important to note that the IRR must be compared to the discount rate to assess profitability. Specifically,

• when IRR > discount rate, the NPV is positive,

• when IRR = discount rate, the NPV is zero,

when IRR < discount rate, the NPV is negative.

Therefore, an IRR above 0% does not necessarily imply a profitable investment, as it must exceed the chosen discount rate.

IRR is calculated by solving the equation below for r:

$$0 = \sum_{t=0}^{n} \frac{CF_t}{(1+r)^t} \tag{3.30}$$

3.5. Model Verification 43

where:

- CF_t: Net cashflow in year t (revenues minus costs)
- r: Internal Rate of Return (to be determined)
- t: System lifetime in years

A higher IRR suggests that an investment is financially more appealing. In this research, the IRR is used to assess whether the SHTS can be considered financially viable. This is not only relevant for internal evaluation, but also because a sufficiently high IRR is often essential to secure external funding, such as from a bank.

3.5. Model Verification

To ensure the reliability and credibility of the SHTS model, a verification step was conducted. This process aimed to confirm that the model operates realistically under the defined conditions.

The verification focuses on key system outputs:

- HP SCOP: The simulated seasonal COP is compared to specifications for similar collective air-towater heat pumps, from data from DWTM.
- HP COP (-10 °C:) The simulated COP is compared to the COP for comparable HP at -10 °C, according
 to DWTM data.
- **HP FLH:** The amount of FLH of the simulated HP is compared to the FLH from the SDE++ 2025 (Stimulering Duurzame Energieproductie en Klimaattransitie [65]).
- PV generation: The annual electricity generation of the installed PV panels is compared with estimates from PVGIS for the same location and surface area.
- TTES cycles: The number of full thermal cycles of the TTES per year is compared to values of other daily TES systems. The World Business Council [91] states that most current daily TES systems are designed for at least one cycle per day.

Each comparison is quantified using the relative deviation percentage. This is done for three different output configurations of the model.

Metric	Simulated Value	Reference Value	Relative Deviation
SCOP (HP)	2.92	2.80 [21]	4.3%
COP (HP at -10 °C)	2.36	2.30 [21]	2.6%
Full load hours HP (hour/year)	2548	3500 [65]	-27.2%
Annual PV yield [kWh/m²/year]	249.7	246.3 [44]	1.4%
TTES cycle (cycles/year)	289	365 [91]	-20.8%

Table 3.5: Validation of model outputs against reference data

While the verification indicates that the model shows generally plausible behavior, there are notable deviations in the FLH of the heat pump and the number of TTES full load cycles.

The relatively large deviations in FLH and TTES cycles occur because the reference values are not based on a comparable smart system, but rather serve as indicative benchmarks. Since this system is new, no comparable system exists. The reference values are therefore used to demonstrate that the results are within the correct order of magnitude.

The SDE++ 2025 subsidy scheme plays an important role in evaluating cost-effectiveness and financial feasibility [65]. For heat pump systems, the SDE++ assumes a maximum of 3,500 full-load hours per year when calculating subsidy levels. This standard value enables comparison, despite actual performance variations that may depend on the system intelligence, weather, and demand patterns. The deviations in FLH in this study are therefore not problematic.

4

Results

This chapter presents the results of the study. It begins with a sensitivity analysis aimed at investigating the impact of key parameters on the model's performance. After these general checks, each subsection is dedicated to one of the sub-questions formulated in section 1.5.

To answer sub-questions 2, 3, and 4, a base scenario is applied. This base configuration serves as the reference point for all scenario variations and sensitivity analyses. The specific asset values of the base scenario are shown in Table 4.1.

Asset	Value (Base Scenario)
PV area (m^2)	13
Heat pump input capacity (kWe)	100
E-boiler capacity (kW)	350
TTES size (kWh)	3000

Table 4.1: Base configuration of the SHTS

Before presenting the performance outcomes of the SHTS, a sensitivity analysis is conducted to assess the model's sensitivity to variations in input parameters.

4.1. Sensitivity Analysis

To assess the robustness of the SHTS, a sensitivity analysis is conducted. The goal is to determine how variations in key design parameters affect system performance.

In this analysis, one parameter is varied at a time, while all other parameters are held constant at the base scenario shown in table 4.1.

For each scenario, the following key performance indicators (KPIs) are evaluated:

- Heat supply coverage (%)
- Grid feed-in (%)
- NPV (€)

For each parameter, discussed in more detail in section 3.4.1, the system performance is compared against a baseline configuration. Table 4.2 presents the change in KPIs relative to the baseline for a lower and a higher value of each asset input parameter. The different tints of orange are different sensitivity levels [50].

The sensitivity is determined by comparing the relative change in the output to the relative change in a specific input, expressed as:

Sensitivity =
$$\frac{\% \text{ change in output}}{\% \text{ change in input}}$$
 (4.1)

 Δ (kWh) Sens. $\mathsf{NPV}\ \Delta$ Parameter Input Heat Cov. Δ Sens. Grid feed-in Δ Sens. TTES -250 -8.3% -0.5% +0.059 +1.2% -0.143-1.8% +0.220 **TTES** +250 +8.3% +0.5% +0.055 -0.4% -0.047 +1.8% +0.219 HP -10 -10.0% -4.4% +0.440 +0.5% -0.053-0.7% +0.069 HP +10 +10.0% +4.0% +0.404 +1.2% +0.122-0.5% -0.049-0.274 E-boiler -50 -14.3% -1.2% +0.084 +34.2% -2.394 +3.9% E-boiler +50 +14.3% +0.4% +0.028 -16.1% -1.124 -7.2% -0.503PV -2 -15.4% -1.6% +0.103 -48.9% +3.176 +3.8% -0.248 PV +2 +15.4% +1.1% +0.073 +55.0% +3.572 -5.0% -0.326

Table 4.2: Sensitivity analysis for the SHTS components

The TTES shows relatively stable behavior in response to size variation. Increasing or decreasing the size of the thermal buffer results in relatively small changes in the KPIs. This indicates that the system's performance is relatively robust to variations in TTES sizing.

The HP demonstrates a more substantial impact. Variations in its capacity lead to notable changes in heat coverage, reflecting the role that the heat pump plays in meeting heat demand and charging the TTES. The effect on the grid feed-in and NPV is limited. This implies that the heat pump primarily influences the heat delivery of the system, with less influence on how solar energy is utilized or on the economic outcome.

E-boiler capacity has a markedly different profile. Changes in e-boiler sizing result in substantial shifts in the amount of PV electricity fed into the grid. The e-boiler acts as a key asset in the system: an undersized e-boiler restricts the system's ability to use solar-generated electricity, while increasing e-boiler capacity allows for significantly more use of this electricity, since it is relatively inefficient compared to the HP. However, this has a financial downside, as increasing the e-boiler capacity harms the NPV.

The PV panel area is a sensitive parameter in the analysis. Small changes in the PV surface area result in significant changes in grid feed-in behavior. This highlights the system's strong dependence on the amount of solar energy being produced and how much of it can be utilized or stored within the SHTS. However, the effect on the heat coverage and NPV is not as sensitive as the grid feed-in indicator.

4.2. Assessment Parameters

To evaluate the SHTS in a structured way, it is important to define how the performance and impact will be measured.

Sub-question 2: What assessment parameters objectively describe the performance and impact of the SHTS?

To objectively evaluate and quantify the impact of the smart HTS, a dedicated assessment framework has been developed, as outlined in section 3.4. This framework introduces a comprehensive set of performance metrics that together assess the smart HTS.

This section presents the base scenario results for each of these metrics, before asset optimization. These results serve as a reference point for assessing how effectively the system currently performs. The base scenario is shown in table 4.1 in section 4.1.

The defined metrics used to assess the performance of the smart HTS are:

- COP_{system}: Ratio of total useful heat output to total electricity input (grid + solar-generated), reflecting system efficiency.
- **Tank cycles**: Number of complete equivalent full charge-discharge cycles per year, indicating thermal storage utilization.
- Heat supply coverage: Percentage of total annual heat demand met by the SHTS.
- HP FLH: Total thermal energy delivered by the heat pump divided by its capacity, reflecting utilization intensity.

Metric	Result
COP _{system} (-)	1.59
Tank cycles (cycles/year)	289
Heat supply coverage (%)	30.4
HP FLH (hours/year)	2548

Table 4.3: Performance metrics of the SHTS for the base scenario

The base scenario, with a seasonal coefficient of performance (SCOP) of the SHTS of 1.59, reflects an acceptable level of system efficiency when combining both grid-sourced and PV-sourced electricity. The 2,548 full-load hours indicate substantial usage of the heat pump throughout the year, while 289 tank cycles demonstrate active utilization of thermal storage, with almost a full cycle every day. The heat supply coverage of 30.4% suggests that a significant share of demand can be delivered by the SHTS, and 70% by the district heating network, leaving room for further optimization.

The defined metrics used to assess the impact of the smart HTS are:

- **Reduced primary energy use**: Energy savings achieved through reduced district heating demand and efficient use of grid electricity. This is excluding the solar-generated electricity usage.
- Heat demand relief: Relative reduction in peak heat demand compared to conventional systems.
- **Grid feed-in**: Fraction of solar PV production that is not self-consumed and is instead exported to the grid.
- Avoided CO₂ emissions: Emissions saved due to reduced heat import from the district heating network, corrected for additional grid electricity used by the smart HTS.

Table 4.4: Impact metrics of the SHTS

Metric	Result
Reduced primary energy use (MWh/year)	892 *
Heat demand relief (%)	6.33
Grid feed-in (%)	14.2 **
Avoided CO ₂ emissions (kg/year)	19,679

^{*} equal to the annual heat demand of 74 houses, which is almost 25% of the 300 houses.

** 85.8% of PV production is self-consumed.

On the impact side, the SHTS contributes to both energy system efficiency and climate goals. The reduction in primary energy use (892 MWh/year) and the avoidance of CO_2 emissions (19.7 tonnes/year) reflect environmental benefits associated with the internal heat supply. These reductions include the correction of extra electricity and CO_2 consumed by the SHTS. The observed DH grid relief (6.33%) indicates that the system's peak reduction of heat demand is not substantial. Nevertheless, for the electricity grid, the feed-in rate of 14.2% shows that a predominant fraction of solar-generated electricity is self-consumed (85.8%).

The results highlight that the performance of the SHTS can be captured through a set of multiple indicators covering system performance and impact. This demonstrates the value of the evaluation framework and enables a transparent assessment of technical performance and lays the base for optimization and comparison across different configurations.

4.3. Operational Behavior

In addition to overall performance indicators, it is essential to understand how the system operates under changing heat demand and solar-generated electricity.

Sub-question 3: How does the SHTS operate under varying heat demand and solar energy conditions?

While the annual performance and impact indicators provide a high-level overview of the SHTS, they do not capture how the system dynamically responds to 15-minute time-step variations in energy supply and demand.

The results show the SHTS operation during the first two weeks of June. This is a period with significant solar availability and varied heat demand. This time frame effectively illustrates how the system responds and performs. The same base scenario is used as in section 4.2, shown in table 4.1.

Tank State of Charge (SoC) and Tank Cycling Behavior

Figure 4.1 shows the SoC of the TTES. The SoC reflects the dynamic balance between charging and discharging. The fluctuations in SoC indicate how the storage tank responds to varying solar availability and heat demand.

During periods of high solar production, the tank charges rapidly as excess solar electricity is converted to heat by the heat pump and the e-boiler. Conversely, when heat demand is high and solar input is insufficient, the tank discharges. This pattern of filling and emptying results in measurable tank cycles. The number of annual full cycles, from 0% to 100%, is also used as a performance metric to evaluate how effectively the tank is utilized throughout the year.

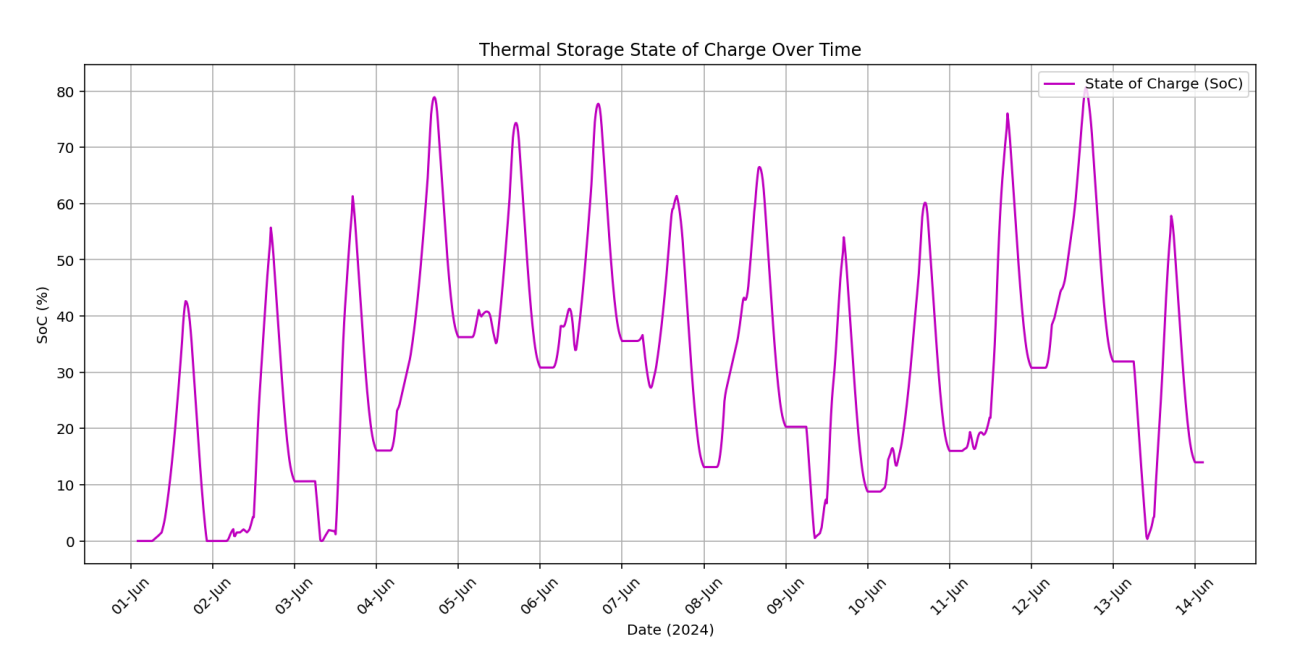


Figure 4.1: Thermal energy in the TTES during the first two weeks of June

Figure 4.2 illustrates the SoC of the thermal storage tank during the first two weeks of February. The regular charging and discharging patterns show that the tank undergoes almost the same cycle each day, consistently charging at night and discharging at the beginning of the day. The SoC is constantly below 65%, since the HP does not have enough time and power to charge the TTES higher during the night. Although there are HP active hours in the afternoon, this heat is needed for direct heat supply instead of charging the TTES.

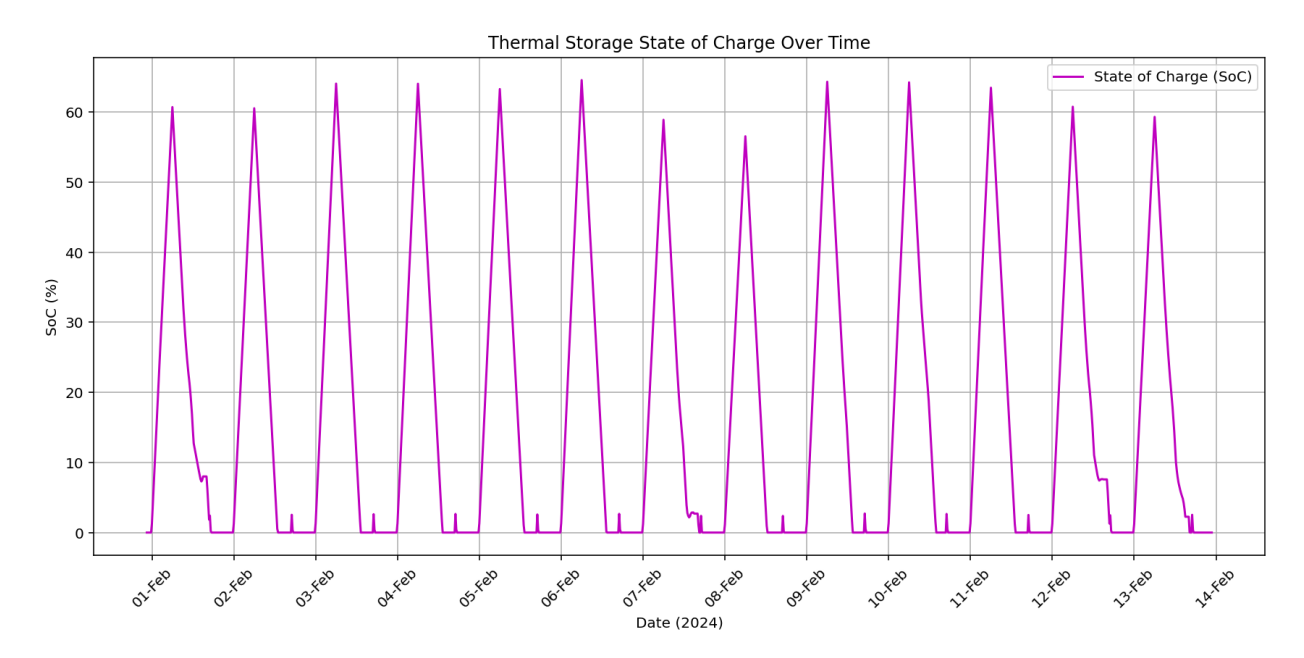


Figure 4.2: Thermal energy in the TTES during the first two weeks of February

Figure 4.3 illustrates the SoC of the thermal storage tank during the first two weeks of March. In contrast to February, the charging and discharging behavior becomes more dynamic. A pattern of two distinct charging moments per day emerges: one during the night and another in the afternoon, when solar-generated electricity is available. The SoC graph shows that the tank regularly reaches high states of charge and subsequently discharges in response to heat demand. This demonstrates that the thermal storage is effectively used in this period of the year when heat demand is higher than in the summer months, and solar-generated electricity is increasing.

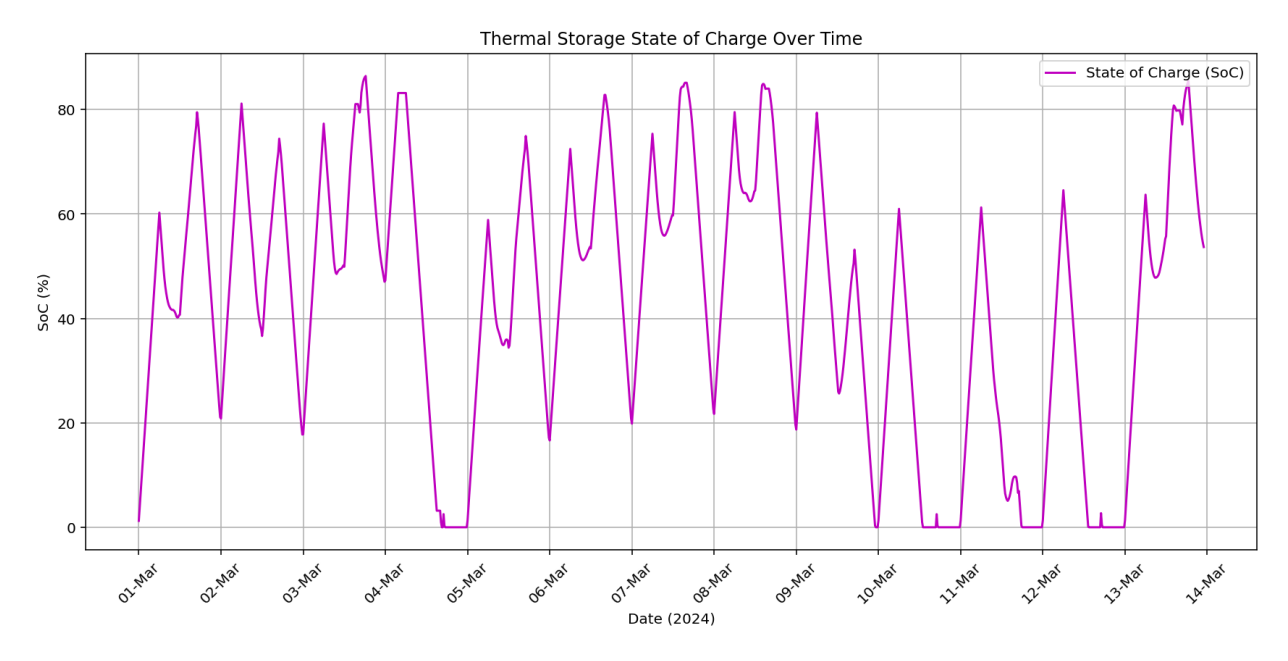


Figure 4.3: Thermal energy in the TTES during the first two weeks of March

Figure 4.4 shows the cumulative number of full-load discharge cycles of the thermal storage tank over the entire year. The curve increases steadily throughout the year, with some minor seasonal variation visible in the slope, reflecting variations in system activity across different months. The final value of 289 cycles aligns with the result reported in table 4.3.

The trend in figure 4.4 appears more linear than you might expect, which is due to differences in the electricity source and which component, HP or e-boiler, is producing heat. During the winter months, the HP typically operates on grid electricity, with a COP of around 3. In the summer months, the system uses more solar-generated electricity, primarily used by the e-boiler with a COP of 1. As a result, the variation in the TTES is flattened by changes in electricity to heat efficiency. Seasonal variation in electricity input is more clearly visible in Figures 4.6 and 4.7.

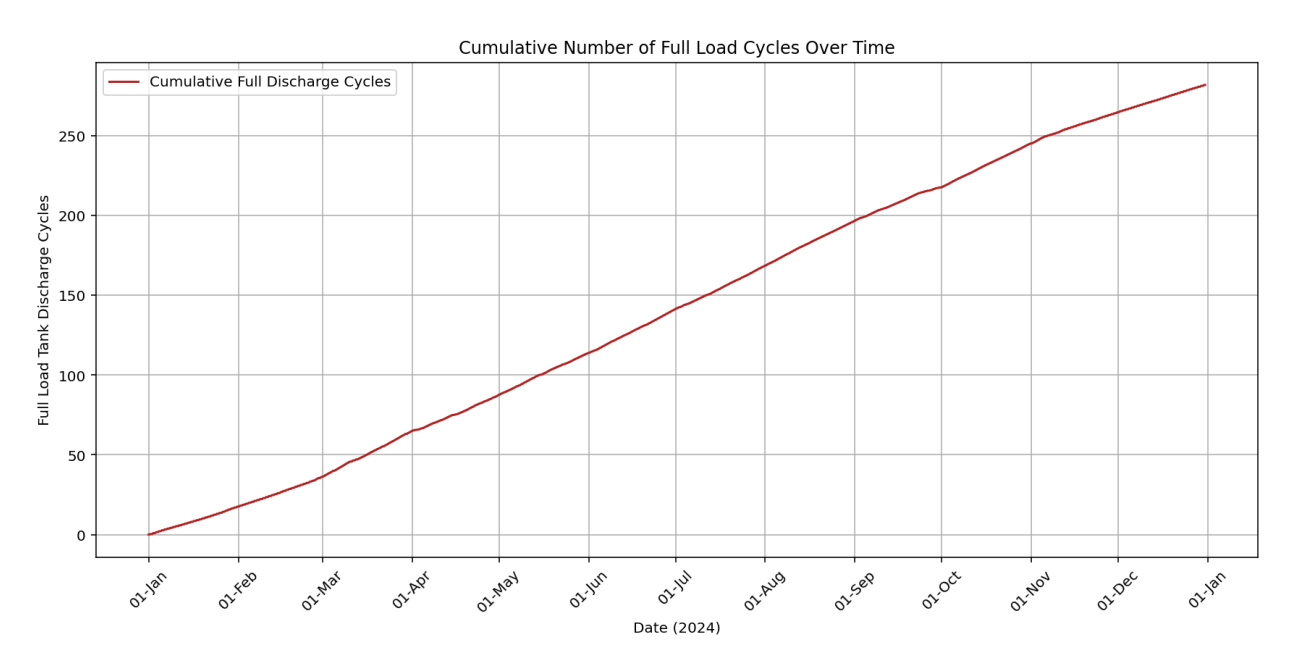


Figure 4.4: Cumulative number of full load cycles over the whole year, corresponding to the 289 cycles in table 4.3

Electricity source allocation:

Figures 4.5, 4.6, and 4.7 provide insight into the electricity supply of the SHTS, focusing on the contribution of solar and grid electricity at different time scales. Figure 4.5 zooms in on two representative weeks to analyze the detailed operational behavior of the HP and e-boiler, while figures 4.6 and 4.7 illustrate the seasonal variation and cumulative trend in electricity input throughout the year. Together, these figures show how the system prioritizes solar energy and uses grid electricity when necessary.

Figure 4.5 presents a breakdown of the electricity consumption by the HP and e-boiler, clearly distinguishing between PV-generated electricity in the neighborhood and grid electricity. When solar-generated electricity is available, it is first prioritized for the HP during its active hours. This means the HP always draws from solar power up to its full capacity before the e-boiler receives solar-generated electricity. This prioritization is due to the HP's higher efficiency. In moments when solar power is insufficient, but the HP is scheduled to operate (during nighttime or periods of low irradiance), the HP uses grid electricity. These periods are visible as the dark blue line complementing the light blue line, adding up to the maximum power the HP is asking for.

In this configuration, the e-boiler does not use grid electricity. However, the system is designed to support peak shaving. During peak-shaving, the e-boiler can temporarily rely on grid power to prevent high heat demand from the DHN. This mechanism is configurable, allowing precise control over the maximum allowable DHN load.

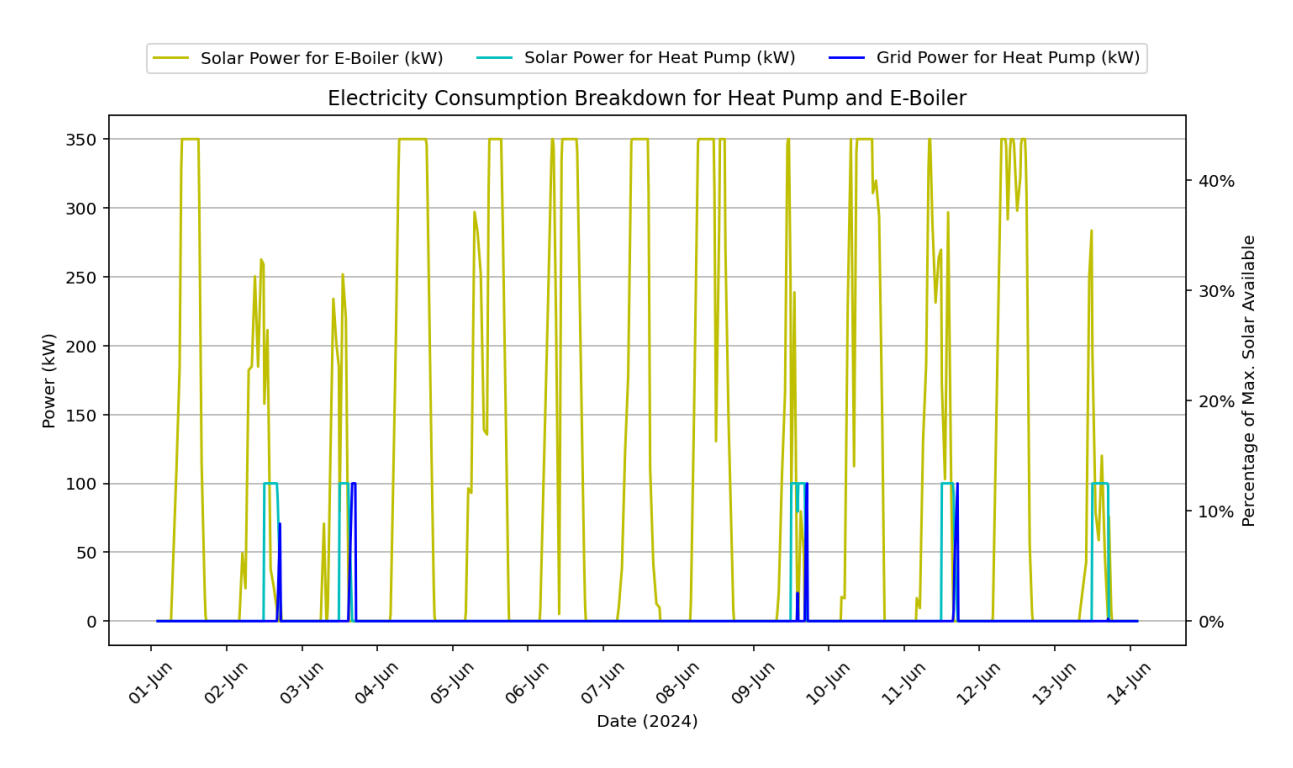


Figure 4.5: Solar and grid consumption of the HP and e-boiler

Figure 4.6 shows the smoothed daily electricity input into the SHTS for one year, broken down by solargenerated electricity and grid electricity. A clear seasonal trend is visible, with solar input increasing during the spring and summer months (roughly from March to October).

In these months, most of the electricity is covered by solar energy. During winter months, the blue-shaded area (grid electricity) increases, supplying the HP with electricity when there is no solar-generated electricity available.

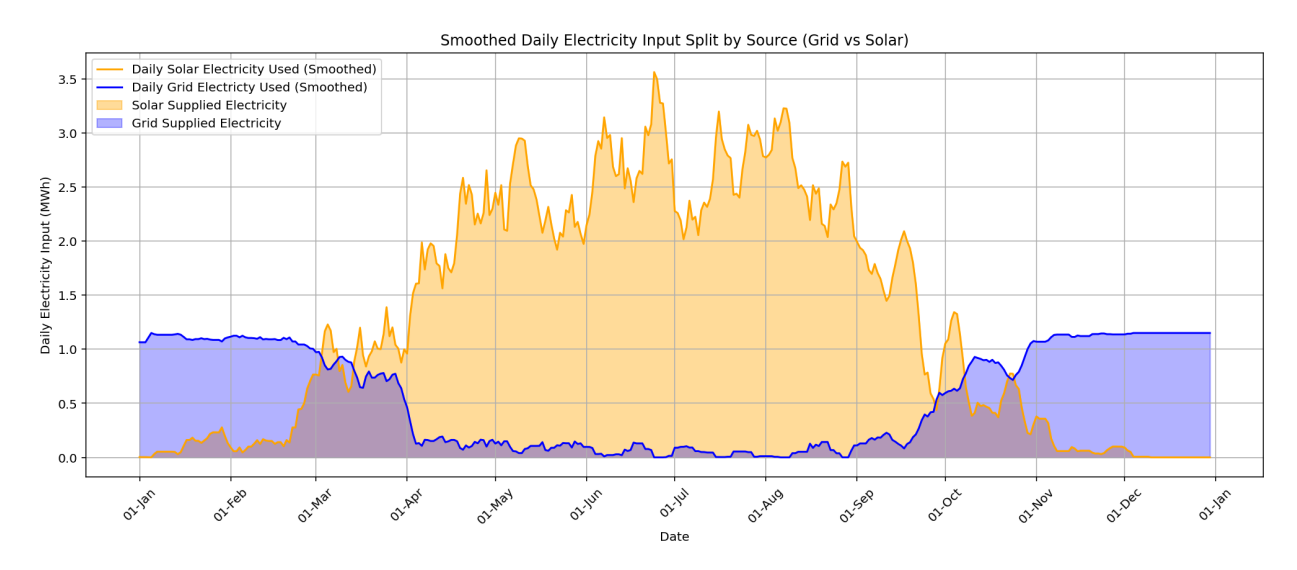


Figure 4.6: Smoothed daily electricity input into the SHTS, split by grid and solar

Figure 4.7 presents the cumulative electricity input into the SHTS, split by grid and solar-generated electricity. It provides an overview of how grid and solar-generated electricity contribute throughout the year. The orange area shows the cumulative contribution from solar electricity, while the blue area represents grid-supplied electricity. The green line indicates the total input.

A seasonal effect is visible between March and October, where solar electricity grows at a higher rate than

grid electricity, reflecting the high availability of solar power during spring and summer. After September, the slope of the solar contribution flattens significantly, while the grid input starts to increase more rapidly, especially in November and December. Between April and October, the grid electricity curve remains nearly flat, indicating low input from the grid during this period.

This illustrates that over the entire year, solar energy accounts for a substantial portion of the total electricity input. However, grid electricity remains essential, especially in the colder months.

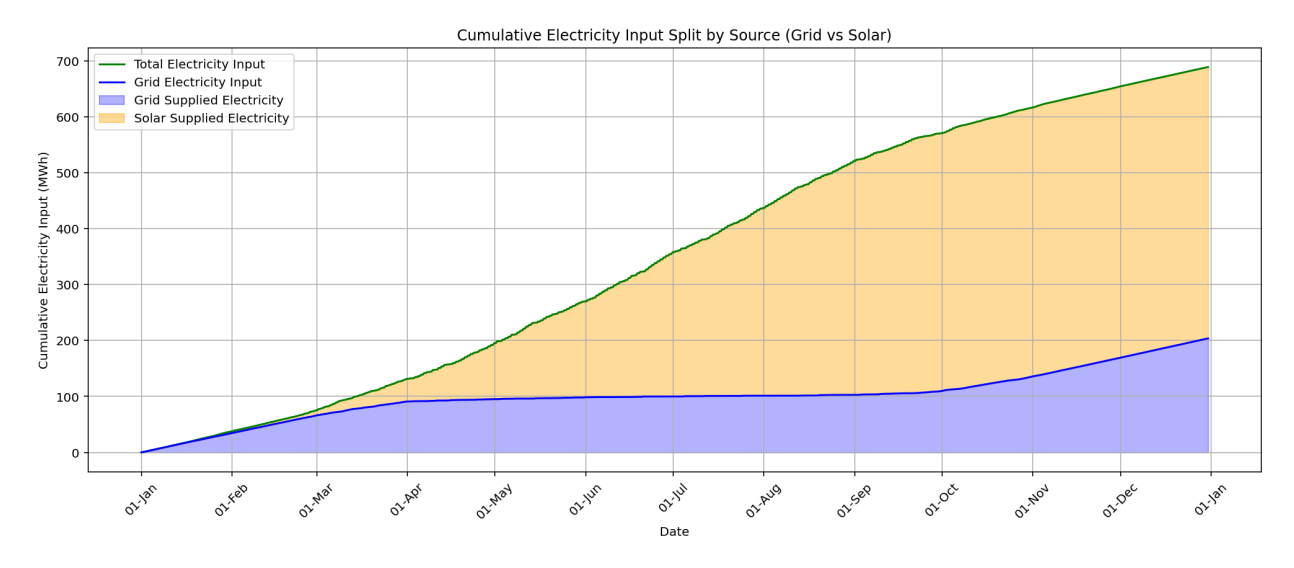


Figure 4.7: Cumulative electricity input into the SHTS, split by grid and solar

PV generation vs utilization

Figures 4.8 and 4.9 illustrate the system's ability to utilize the available solar electricity. The orange line shows the total available solar-generated electricity. This is after subtracting the electricity demand of the households.

In Figure 4.8, we observe clear daily radiation patterns. During several midday hours, the system reaches its operational limits, causing surplus solar electricity to be fed into the grid. The red area highlights this portion that remains unused.

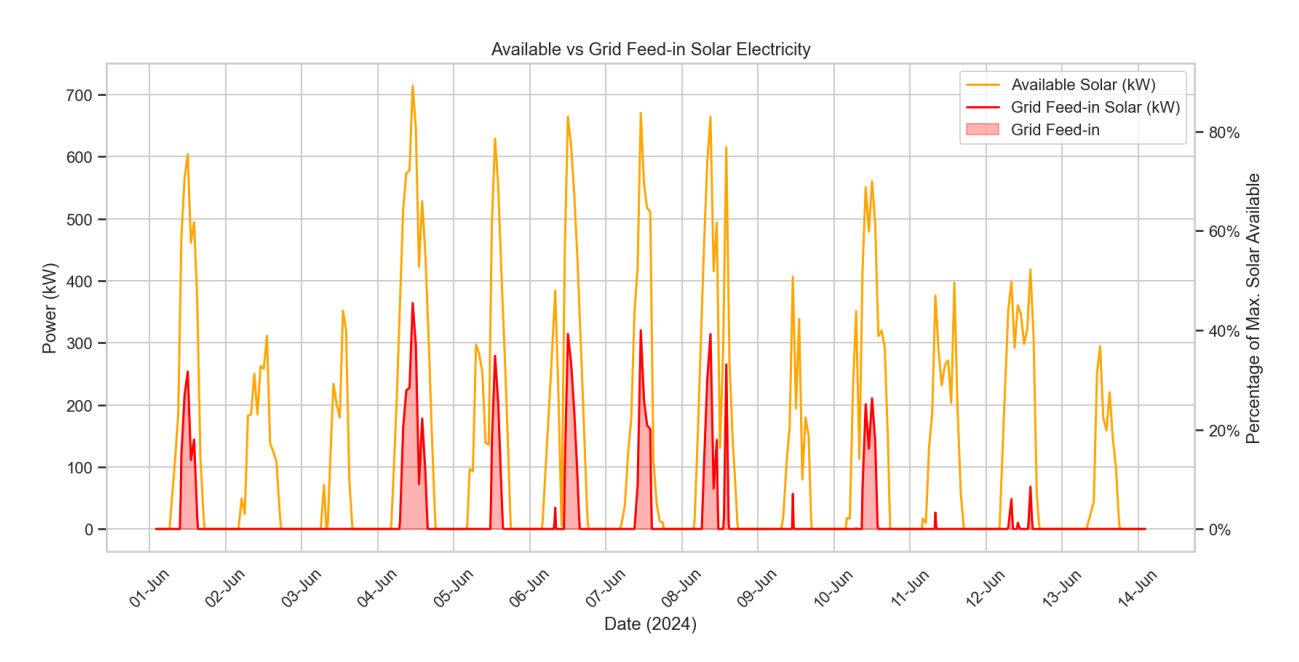


Figure 4.8: Total and feed-in solar electricity in the first two weeks of June

Figure 4.9 shows this dynamic across the whole year. The bulk of solar generation and feed-in occurs in the summer months, when solar potential is high, but heat demand is relatively low. Despite the prioritization of solar-generated electricity, there are still frequent periods when not all solar energy can be utilized. The feed-in percentage over the year is 14% of the total available solar-generated electricity.

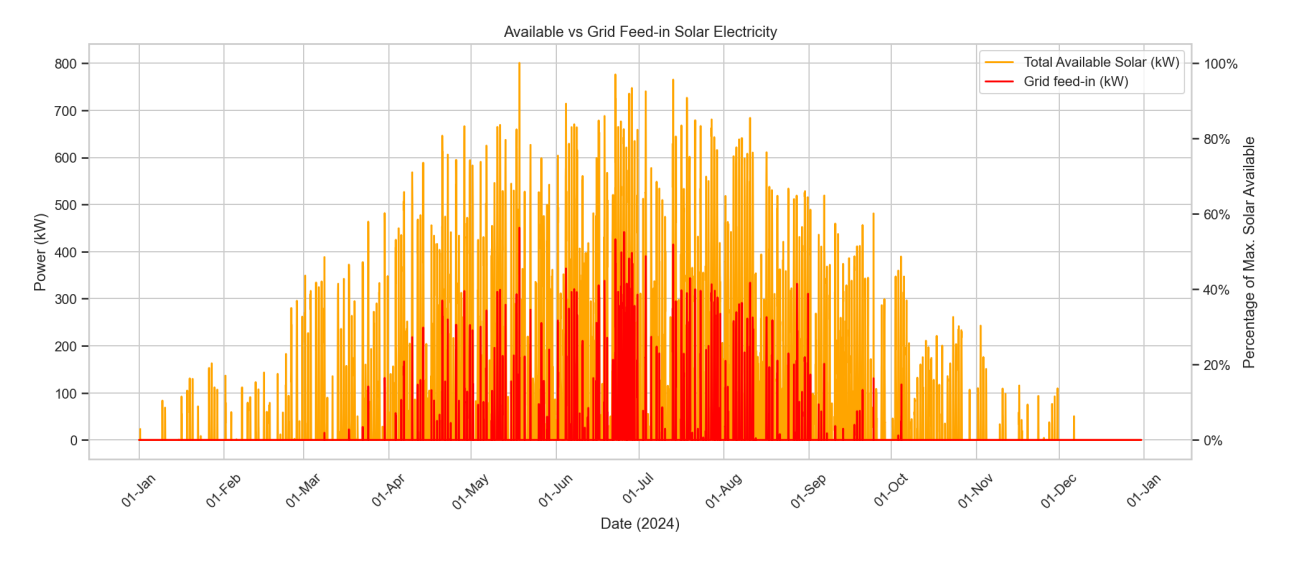


Figure 4.9: Total and feed-in solar electricity in the whole year 2024

Heat supply coverage

Figures 4.10 and 4.12 below visualize to what extent the SHTS can meet the total heat demand over time. Figure 4.10 shows the situation during the first two weeks of June, while figure 4.12 aggregates this across the whole year.

In both figures, the dashed red line represents the total thermal demand. The solid red line and area beneath show the unmet heat demand, while the yellow-filled area between the two lines represents the heat successfully supplied by the system. This includes contributions from TTES, HP, and the e-boiler.

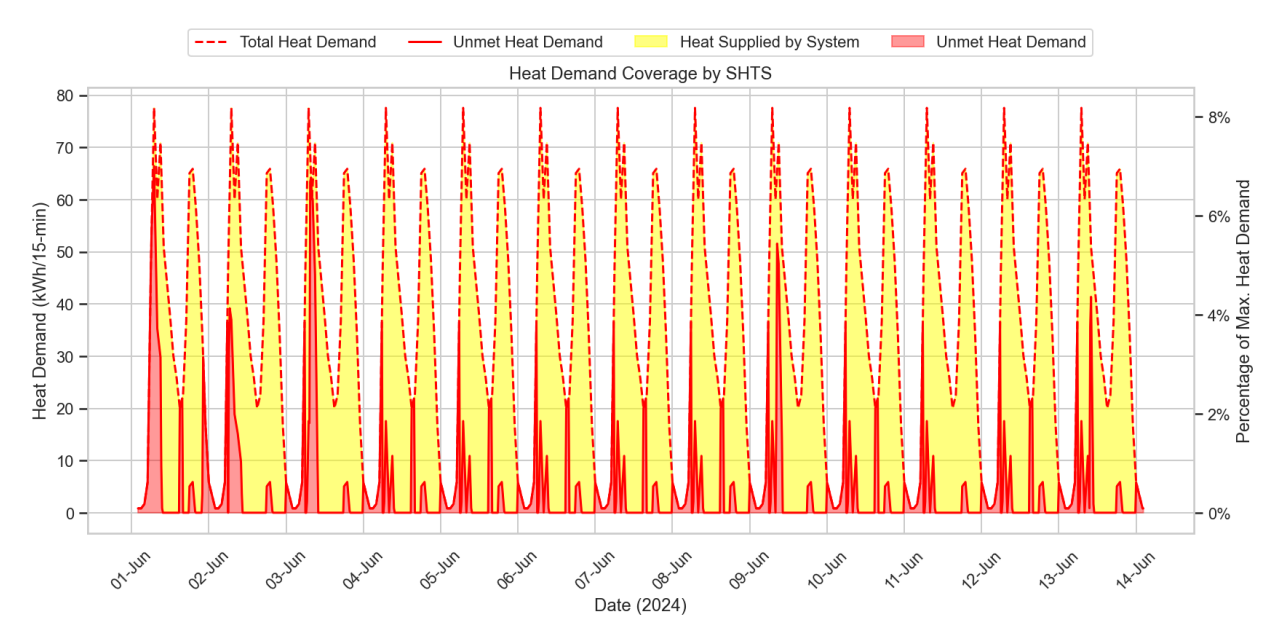


Figure 4.10: Heat covered during the first two weeks of June

The direct heat supply provided by the heat pump, plotted in figure 4.11, represents the heat demand that is directly covered during the defined hours. During these hours, not all generated heat may be needed directly. The remaining heat output from the heat pump is therefore stored in the TTES for later use. These direct supply moments correspond with the activity of the HP in figure 4.13.

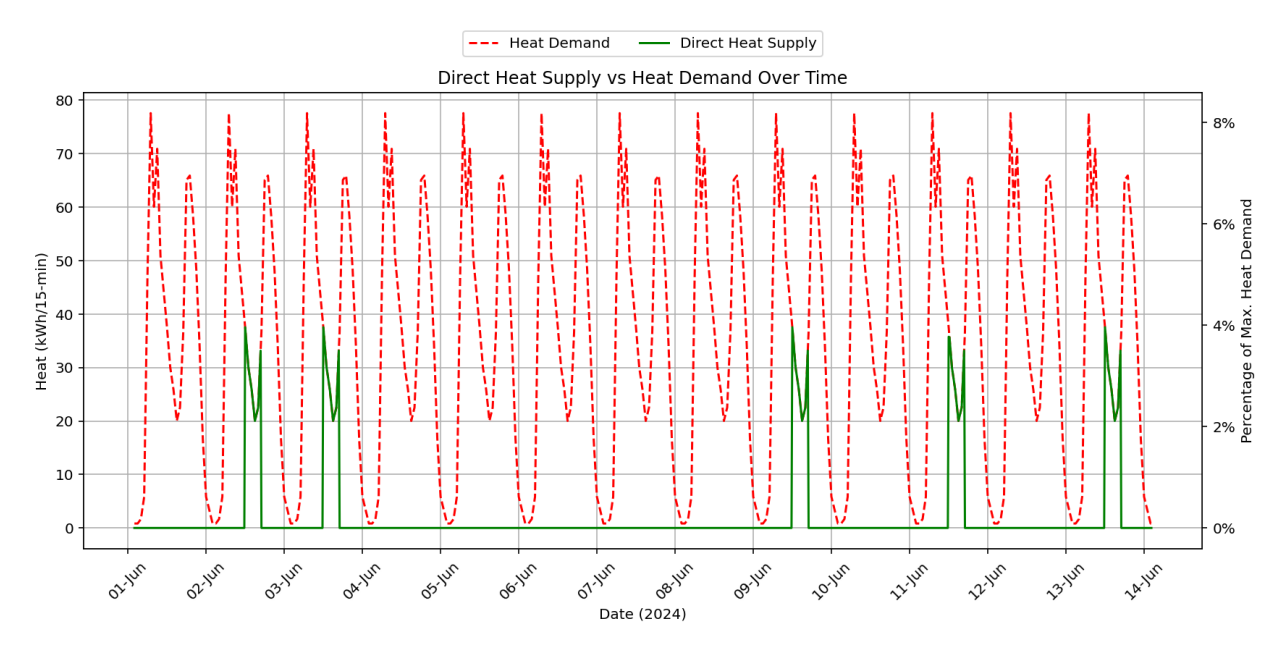


Figure 4.11: Direct heat supply during the first two weeks of June

From the annual view, figure 4.12 shows that the SHTS performs best in the summer months, when most of the heat demand is covered. During this period, the system performs well with the solar availability and has a relatively low heat demand. In contrast, during the winter months, the system is less capable of covering heat demand. This is primarily due to high demands and limited radiation. Overall, the whole system ensures, in this configuration, that 30.4% of the annual heat demand is met by the SHTS.

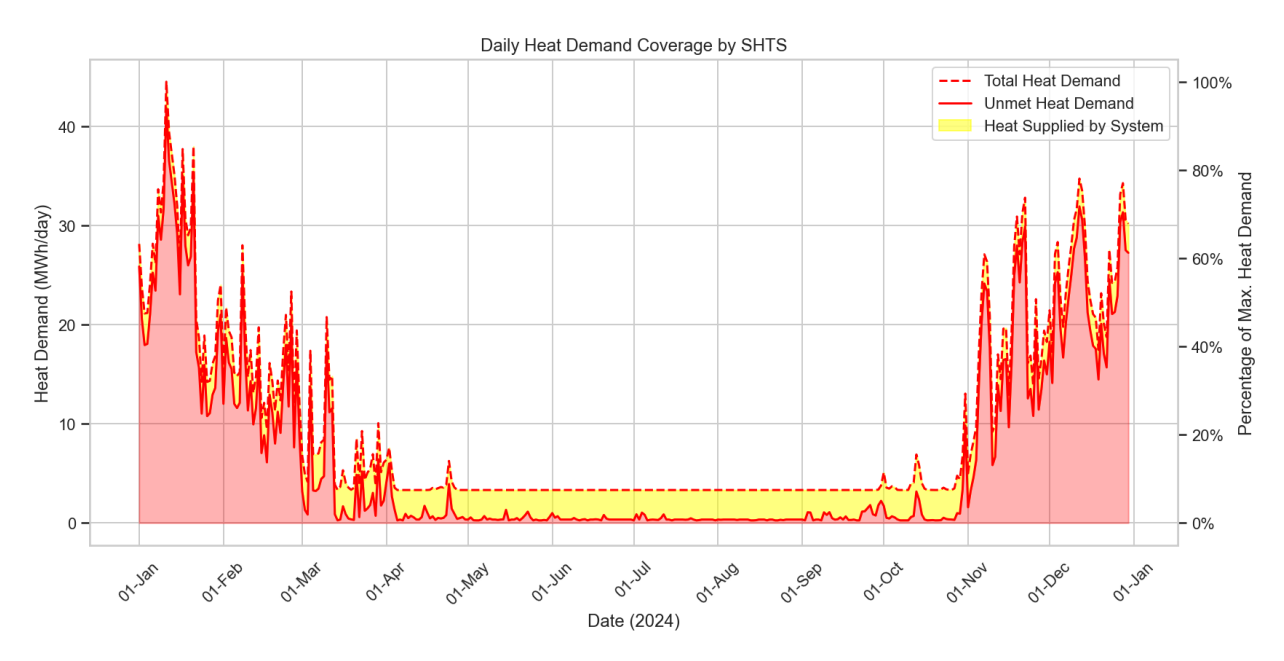


Figure 4.12: Heat covered during the whole year (2024)

Heat pump full-load hours/COP:

In this system, the COP is both temperature-dependent and partial-load adjusted, capturing realistic variations in performance. Figure 4.13 shows the COP behavior during the first two weeks of June. The distinct peaks reflect periods when the heat pump is operating, typically with a COP between 3 and 4. These values result from relatively high outdoor temperatures. The rest of the time indicates when the heat pump is off. Either because the heat demand is already met, the tank is fully charged, or the system logic has disabled the pump due to heat demand forecasting, elaborated in section 3.1.1. The latter is the case in the figure 4.13

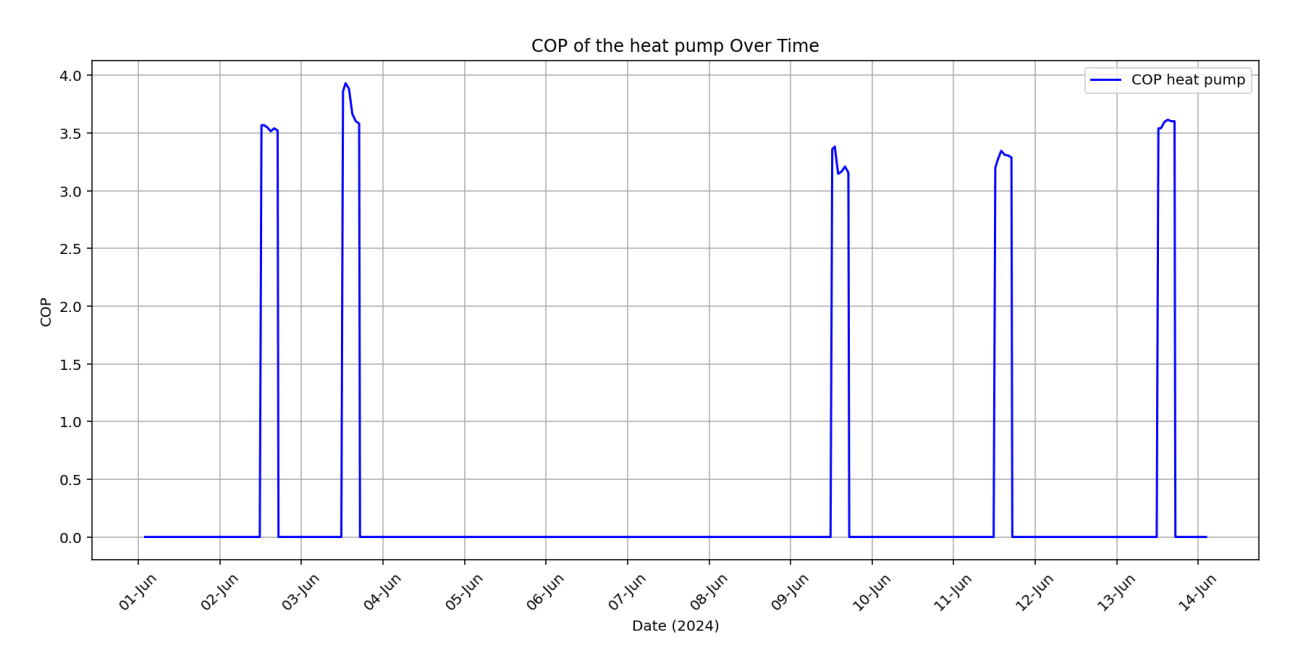


Figure 4.13: COP of the heat pump during the first two weeks of June

Figure 4.14 displays the COP over the whole year. It clearly shows seasonal variation. In winter months, the COP tends to be lower due to colder ambient temperatures, which increase the temperature lift and reduce the Carnot efficiency. In summer months, the COP improves significantly as outdoor conditions are higher. Over the whole year, there are 2548 FLH.

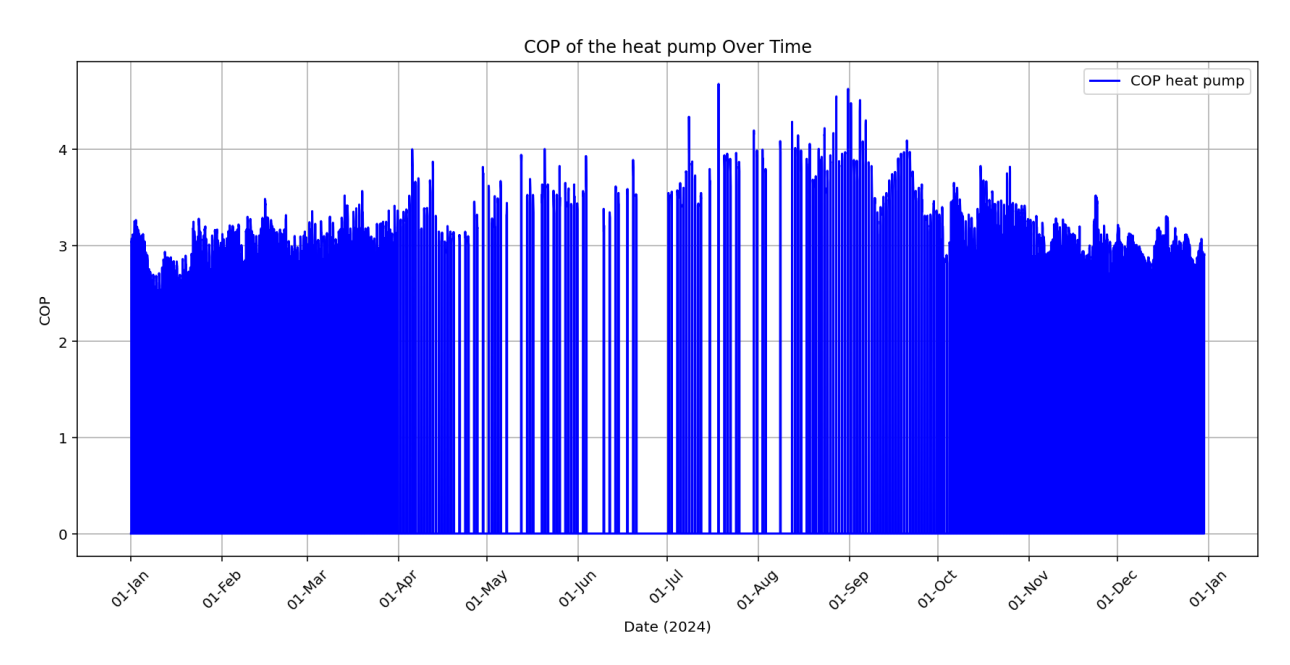


Figure 4.14: COP of the heat pump during the whole year (2024)

The simulation results offer detailed insight into how the SHTS dynamically responds to fluctuating heat demand and solar energy supply. Through 15-minute resolution data, the operational behavior of the system reveals the critical role of coordinating the different assets.

The TTES plays a key role in buffering supply and demand. Figure 4.1 shows significant fluctuations in the tank's state of charge, confirming its function as an active balancing element. With 289 complete charge-discharge cycles per year, the tank is effectively utilized, indicating that the SHTS frequently charges and discharges the thermal storage to absorb excess solar generation and release heat during periods of high heat demand.

A priority hierarchy guides the allocation of electricity sources. Solar power is first allocated to the HP. The e-boiler acts as a secondary device, only activating when excess solar-generated electricity is available. Most of the solar-generated electricity is used by the e-boiler, since the e-boiler can vary in power input, and still have a constant COP. The HP has a varying COP according to the partial load, and it will only activate when there is room for a minimum running time of 2 hours. This logic ensures that high-efficiency components are prioritized. Nonetheless, excess solar power is occasionally exported to the grid when storage is full or the HP and e-boiler are already running at full capacity.

Feed-in electricity remains a persistent challenge, particularly in summer months when solar generation is high, but heat demand is low. Despite intelligent prioritization strategies, in the base scenario, 14.2% of the available PV electricity is fed into the grid annually. This indicates a need for either increased assets or a reduced number of solar panels. Both options have their downsides, increasing the size of assets, resulting in fewer hours of using the full capacity, and resulting in an expensive configuration. A reduction in solar panel capacity limits sustainable energy availability and contradicts long-term sustainability goals.

The SHTS's ability to meet heat demand is dependent on the season. During summer, a high share of heat demand is met by the SHTS, while in winter, the SHTS struggles due to increased demand and limited solar-generated electricity.

The heat pump's COP further confirms seasonal behavior. COP values are higher in summer, most of the time ranging between 3 and 4, and lower in winter, often below 3. This is due to the temperature-dependent nature of heat pump efficiency, as colder conditions require a higher temperature lift and reduce performance.

In summary, the SHTS demonstrates flexible, responsive behavior under varying conditions. However, its effectiveness is highly dependent on the alignment between solar availability and heat demand.

4.4. Economic Benefit 57

4.4. Economic Benefit

This section shifts focus to the economic benefits of the smart HTS.

Sub-question 4: How can the potential economic benefits for the system operators of the SHTS be quantified?

To objectively assess the economic viability of the smart SHTS, a dedicated financial evaluation has been defined. This framework captures the key economic performance indicators that reflect both the costs and the long-term savings associated with the system. These indicators enable operators to evaluate profitability, investment feasibility, and cost-effectiveness throughout the system's 15-year lifetime.

The defined metrics used to assess the economic benefits of the SHTS are:

- CO₂ cost evaluation: Economic value of avoided CO₂ emissions, calculated using a CO₂ price per tonne. This translates environmental effects into monetary value.
- CapEx: Refers to the upfront investment cost of the SHTS components, including the HP, TTES, e-boiler, circulation pumps, piping, building, and heat exchangers.
- OpEx: Includes recurring costs such as electricity costs based on dynamic market pricing, maintenance, and operational overhead. It accounts for both imported grid electricity and self-consumed solar energy. Electricity consumed directly from PV panels is excluded from energy taxation, explained section 3.4.3.
- **Annual savings**: Annual savings, resulting from a decreased heat demand from the DHN, corrected for the extra electricity costs.
- Payback time: Number of years required to recover the initial investment through annual operational savings.
- **Net Present Value (NPV)**: The present value of future cash flows, discounted over the system's lifetime. A positive NPV indicates long-term profitability.
- Levelized Cost of Heat (LCOH): The average cost per unit of delivered useful heat (€/kWh), providing
 a benchmark to compare with alternative heating systems.
- Internal Rate of Return (IRR): The annualized return rate at which the net present value of future cash flows equals zero. A higher IRR reflects a more attractive investment.

Table 4.5 summarizes the key financial metrics of the SHTS.

 Table 4.5:
 Economic performance metrics of the SHTS for the base scenario

Metric	Result
CO ₂ cost savings (€/year)	1.730
CAPEX (€)	678.126
OPEX (€/year)	75.698
Annual savings (€/year)	96.968
Payback time (years)	7
NPV (€)	399.997
LCOH (€/kWh)	0.125
IRR (%)	11.51

These results indicate that the SHTS provides a positive financial return over time. With a payback period of 7 years and an NPV of almost €400,000, the system proves economically feasible. The LCOH (€0.125/kWh) remains competitive with the variable cost of district heating, being €0.158/kWh in 2025 [23]. Besides the measurable economic value, the SHTS also contributes positively to society by addressing the net congestion challenge, proving that its impact extends beyond financial metrics alone.

To complement table 4.5, figure 4.15 illustrates how the NPV evolves as the system continues to operate. Note that the payback time shown in table 4.5 does not account for the discount rate, and is therefore shorter than the actual payback period. As reflected in figure 4.15, the actual payback time is just over 8 years.

4.4. Economic Benefit 58

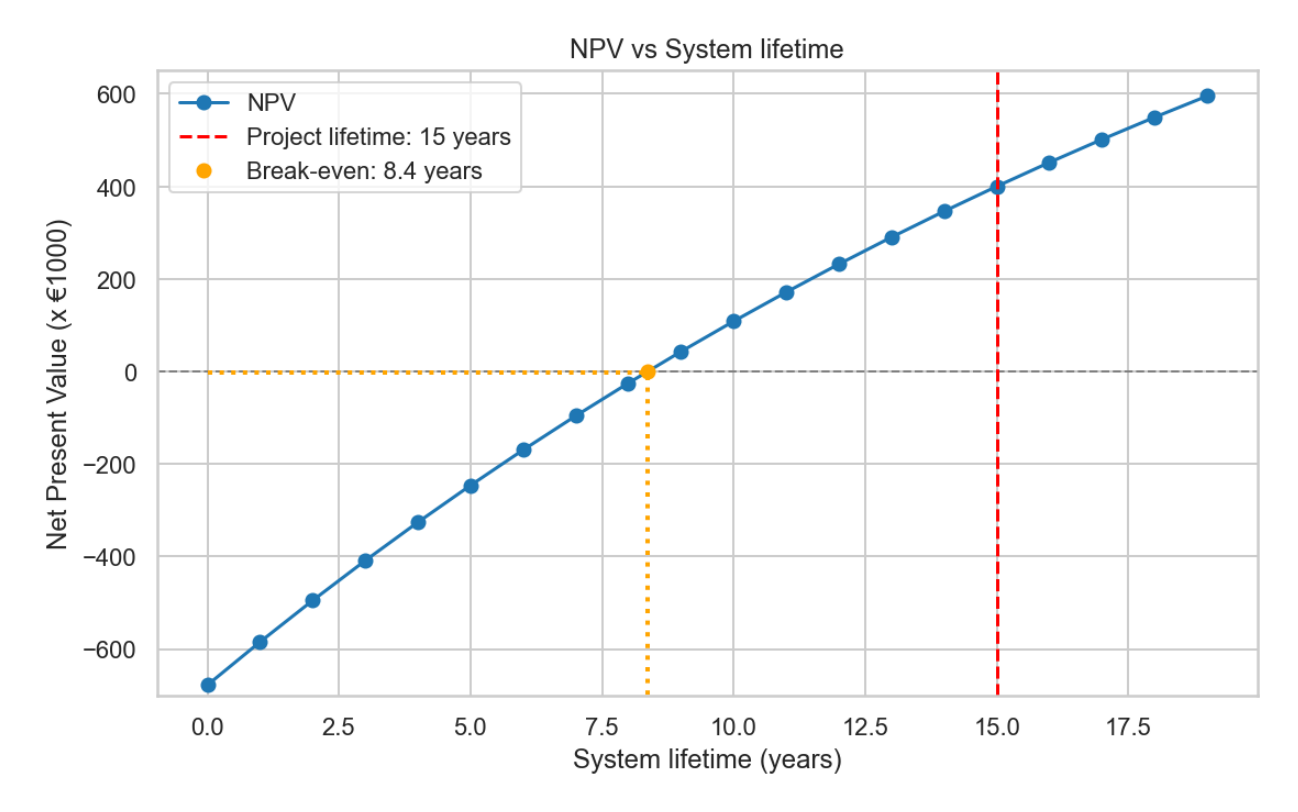


Figure 4.15: NPV of the SHTS as a function of the system lifetime

The simulation results confirm that the SHTS offers promising economic value over its operational lifetime. Key financial indicators demonstrate that the system is economically viable from an operator's perspective.

With an annual energy cost savings of just under €97,000, already offset by the annual operational expenses (€75,698), the system achieves a return on investment within half of the system's lifetime. The actual breakeven point is well within the assumed 15-year project horizon, indicating long-term profitability. The NPV reflects substantial cumulative savings over the system's lifetime.

In terms of upfront investment, the CAPEX for the SHTS is estimated at €678,126. Although it is a high investment, when compared to the low LCOH of €0.125/kWh, this investment is favorable to alternative decentralized heat systems. Additionally, the CapEx per household comes down to €2260/house, which is comparable to the connection costs of a house to a DHN.

The calculated IRR of 11.5% underlines the investment potential of the system. The IRR is relatively high for long-term infrastructure investments. Nevertheless, the return remains sensitive to energy price volatility, policy changes, and unforeseen implementation costs.

Within the economic gains above, the monetized value of avoided CO_2 emissions is estimated at \in 1,730 per year. Although modest in comparison to other savings, the emission taxes may rise exponentially, potentially increasing significantly in the future, as elaborated in section 2.8.

Overall, the SHTS demonstrates a favorable balance between cost and benefit. These economic insights underscore the system's relevance not just as a technical solution, but as a financially justifiable investment for system operators.

4.5. Optimal Configurations

After evaluating the system's performance and impact at the technological and economic level, the next step is to explore how its components can be optimally configured.

Sub-question 5: What is the optimal configuration of the SHTS components to maximize performance under a consistent and suboptimal control strategy?

This section explores the optimal configuration of the SHTS components under a fixed, suboptimal control strategy. Given the inherent trade-offs between performance parameters, no single configuration is universally superior.

While the solar panel area (PV area) per household is explored as a variable parameter to assess its influence on technical system performance, a fixed value of $13m^2$ per household is adopted as the baseline for further evaluations. The PV area is a decision made at the household level, making it less controllable from a system design perspective. As such, the variation in PV sizing primarily serves as a design advisory tool, illustrating whether more PV area would have a positive or negative effect on the different indicators.

The optimal configuration depends on the balance between technical performance and economic feasibility.

- **Technical**: SCOP, grid feed-in and CO_2 emissions
- · Economic: LCOH and NPV

The percentages shown in the figures and tables indicate the relative sizing of the system components:

- TTES capacities are expressed as a percentage of the average daily heat demand before the implementation of the SHTS.
- HP and e-boiler capacities are expressed as a percentage of the maximum grid feed-in capacity, with a conventional HTS.

These normalizations allow for a clearer comparison of asset sizes across configurations of the system.

Parameter	Unit	Range	Step Size
TTES capacity	kWh	1000–3500	250
HP capacity	kW	60–120	10
E-boiler capacity	kW	100-400	50
PV area per house	m^2	11–17 (base = 13)	2

Table 4.6: Parameter Ranges for Asset Optimization

Based on the parameter ranges and step sizes in table 4.6, a total of 2.156 unique system configurations were simulated. Each configuration was simulated under consistent external conditions and suboptimal control logic to ensure comparability across technical and economic metrics.

4.5.1. Technical Performance Evaluation

This section evaluates the performance of the SHTS from a technical perspective, independent of financial effects. The focus lies on three indicators: the system's seasonal COP (SCOP), grid feed-in from solar-generated electricity, and the avoided CO_2 emissions. Each figure presents the same set of data points for the given performance indicator. The color variation highlights the effect of changing the size of an asset.

SCOP

The SCOP provides insight into the overall efficiency of the SHTS across a full operational year. A clear trend is visible in the plots: higher heat coverage generally leads to higher system efficiency. Figure 4.16 shows that increasing E-boiler capacity tends to reduce SCOP. In contrast, the figure 4.17 and 4.18 demonstrate that a higher heat pump capacity and increased TTES improve SCOP performance.

Preferred place to be in the figures: in the upper right region, where system SCOP is high and a large share of the heat demand is covered.

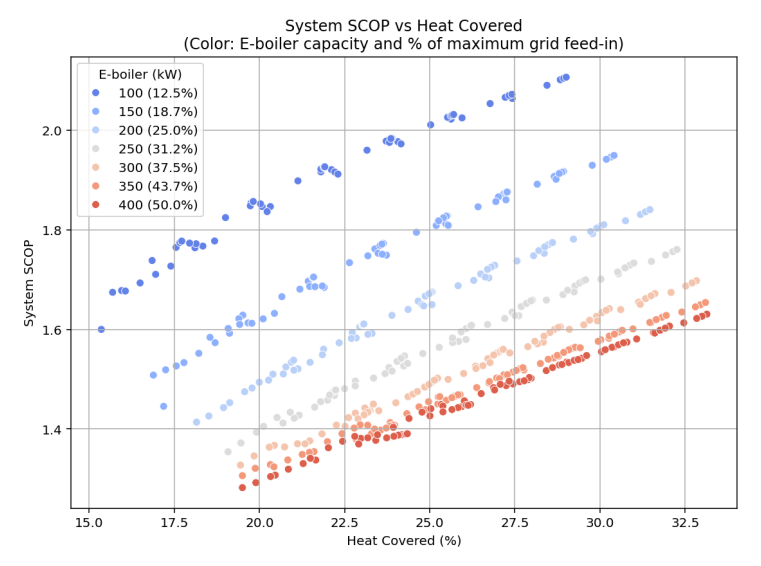


Figure 4.16: SCOP vs. heat coverage, colored by E-boiler capacity

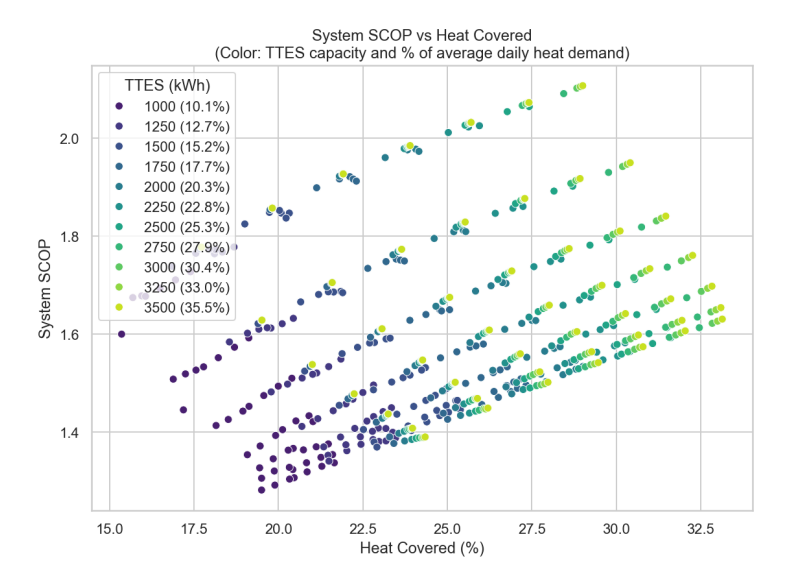


Figure 4.18: SCOP vs. heat coverage, colored by TTES capacity

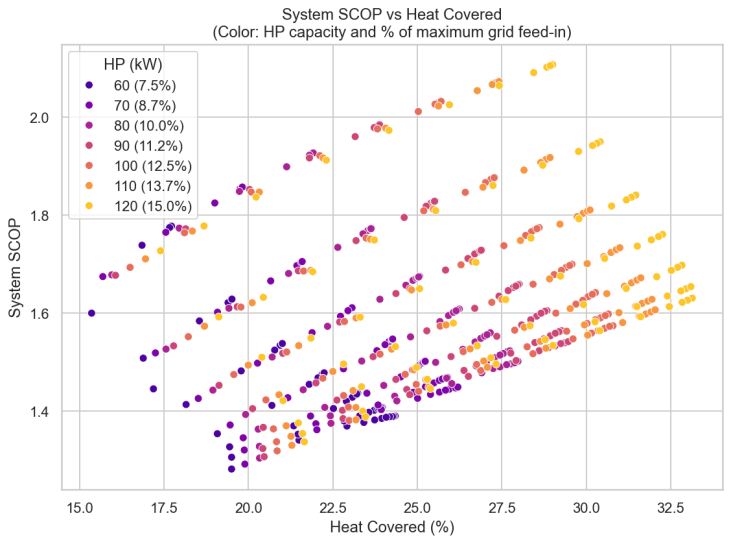


Figure 4.17: SCOP vs. heat coverage, colored by HP capacity

Table 4.7: Optimal SCOP parameters

* Percentages indicate relative sizing of the components. See section 4.5 on page 59 for more details.

	Unit	Value *
TTES capacity	kWh	3500 (35.5%)
HP capacity	kW	120 (15%)
E-boiler capacity	kW	100 (12.5%)
SCOP	-	2.11
Effect of PV increase	m^2	negative

Grid feed-in

Figure 4.19, 4.20, and 4.21 show the relationship between grid feed-in and heat coverage under varying E-boiler, HP, and TTES capacities. A lower e-boiler capacity results in a significantly higher feed-in percentage. Larger TTES sizes help slightly reduce grid feed-in across all e-boiler levels. Varying the HP capacity does not have a significant effect.

Preferred place to be in the figures: as low as possible, and toward the right side, where grid feed-in is low while heat coverage remains high. While several configurations have comparable low grid feed-in percentages, they vary in the amount of heat coverage.

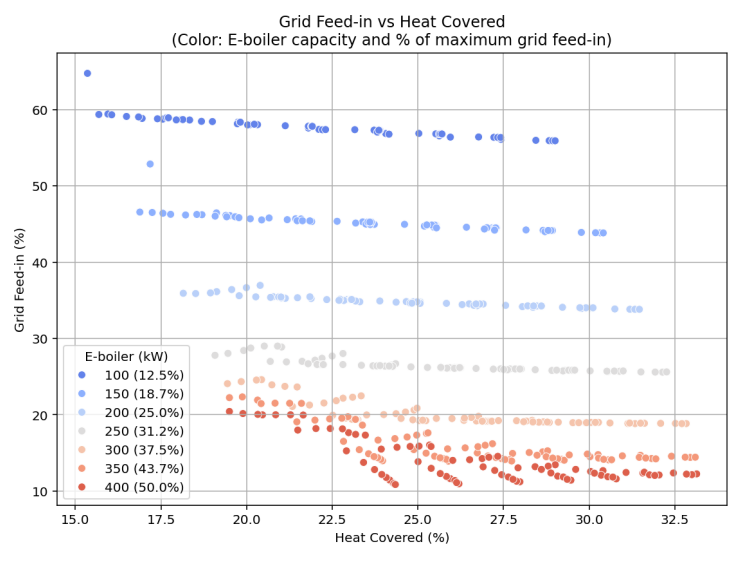


Figure 4.19: Grid feed-in vs. heat coverage, colored by E-boiler capacity

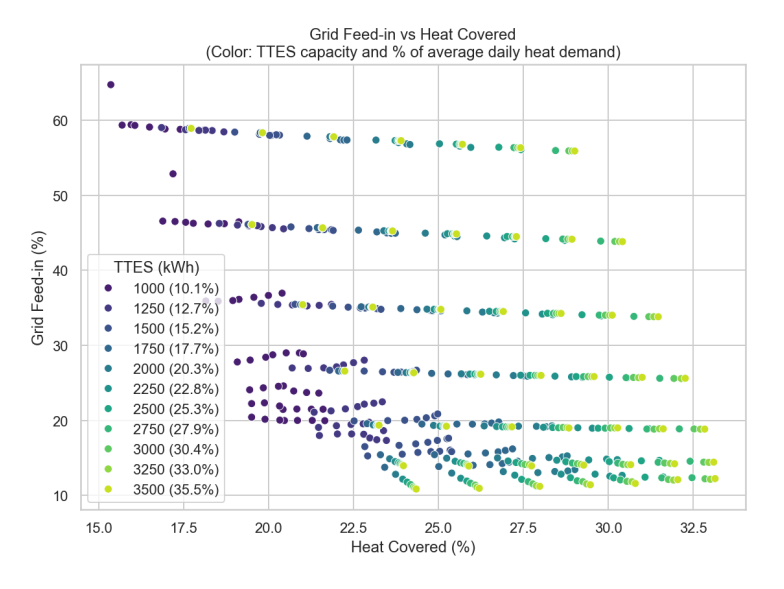


Figure 4.21: Grid feed-in vs. heat coverage, colored by TTES capacity

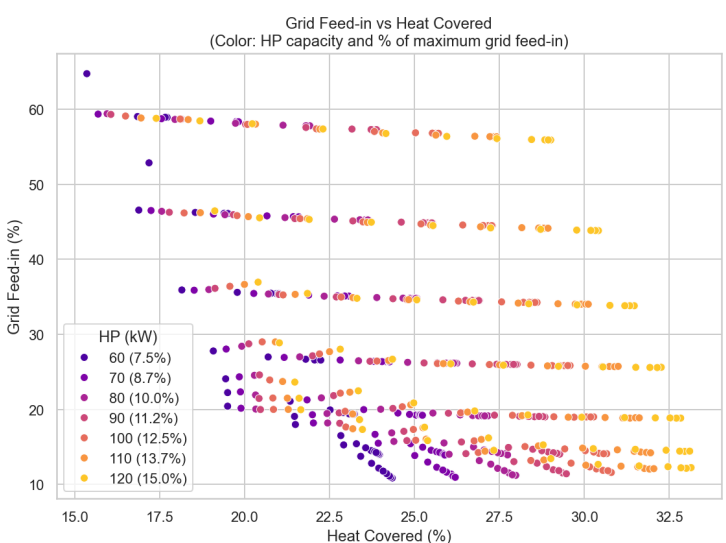


Figure 4.20: Grid feed-in vs. heat coverage, colored by HP capacity

Table 4.8: Optimal grid feed-in parameters

* Percentages indicate relative sizing of the components. See section 4.5 on page 59 for more details.

-		
	Unit	Value *
TTES capacity	kWh	3500 (35.5%)
HP capacity	kW	60-80 (7.5-10%)
E-boiler capacity	kW	400 (50%)
Grid feed-in	%	11
Effect of PV increase	m^2	negative

CO_2 Emissions

Figure 4.22, 4.23, and 4.24 display the annual CO_2 emission savings as a function of heat coverage. Figure 4.22 shows that larger E-boiler capacities are associated with higher CO_2 savings. Figure 4.23 shows that increasing heat pump capacity generally leads to reduced CO_2 savings. This is due to the heat pump's control system operating at night when solar energy is unavailable, resulting in higher grid electricity usage and associated emissions. Increasing the TTES has a slight positive effect on the emissions saved.

Preferred place to be in the figures: in the upper middle area, where CO_2 savings are relatively high while maintaining a moderate level of heat coverage.

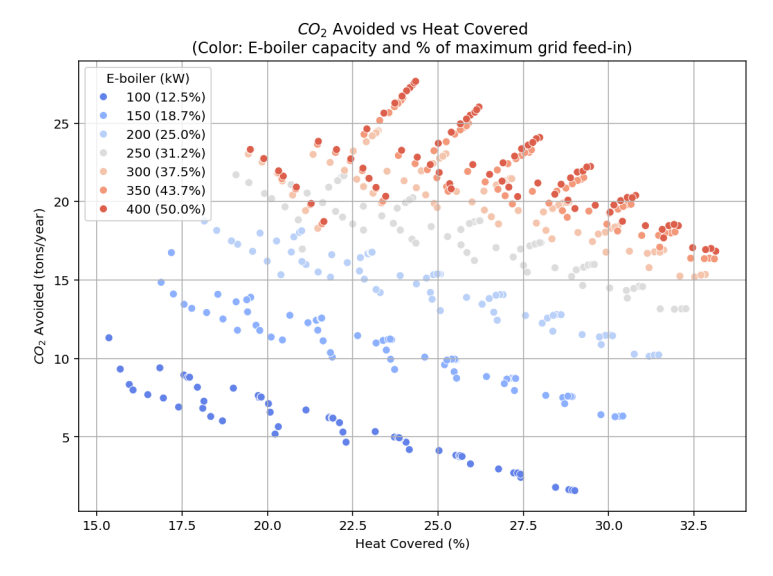
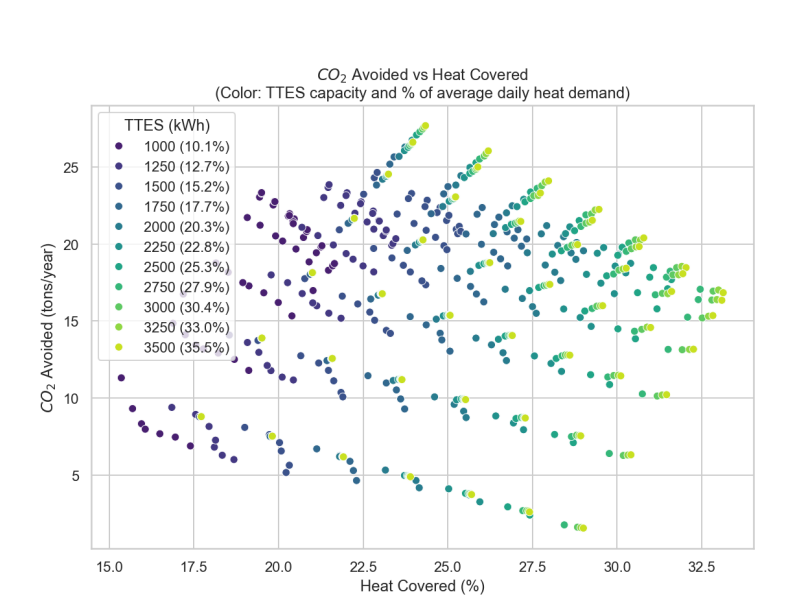


Figure 4.22: CO_2 emission savings vs. heat coverage, colored by E-boiler capacity



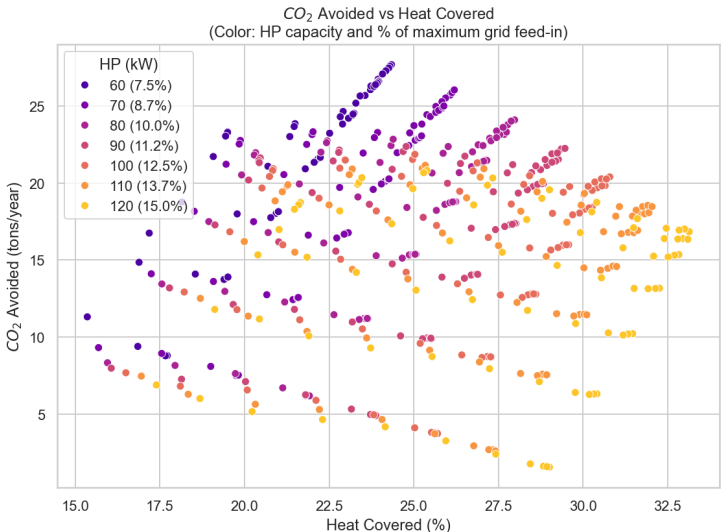


Figure 4.23: CO_2 emission savings vs. heat coverage, colored by heat pump capacity

Table 4.9: Optimal CO_2 emission saving parameters

* Percentages indicate relative sizing of the components. See section 4.5 on page 59 for more details.

	Unit	Value *
TTES capacity	kWh	3500 (35.5%)
HP capacity	kW	60 (7.5%)
E-boiler capacity	kW	400 (50%)
CO_2 savings	ton/year	27.7
Effect of PV increase	m^2	positive

4.5.2. Economic Performance Analysis

This section evaluates the performance of the SHTS from an economic perspective. The focus lies on two indicators: the LCOH and NPV.

LCOH

Figure 4.25, 4.26, and 4.27 show the LCOH of the system. Figure 4.25 shows that increasing the heat pump capacity is generally associated with an increase in CapEx. Figure 4.26 highlights that larger thermal storage units contribute to lower LCOH values across varying levels of heat coverage. Figure 4.27 shows that the mid-range of the e-boiler size is associated with the lowest LCOH.

Preferred place to be in the figures: in the lower part of the plots, where the LCOH is lowest. This corresponds with moderate CAPEX and heat coverage levels.

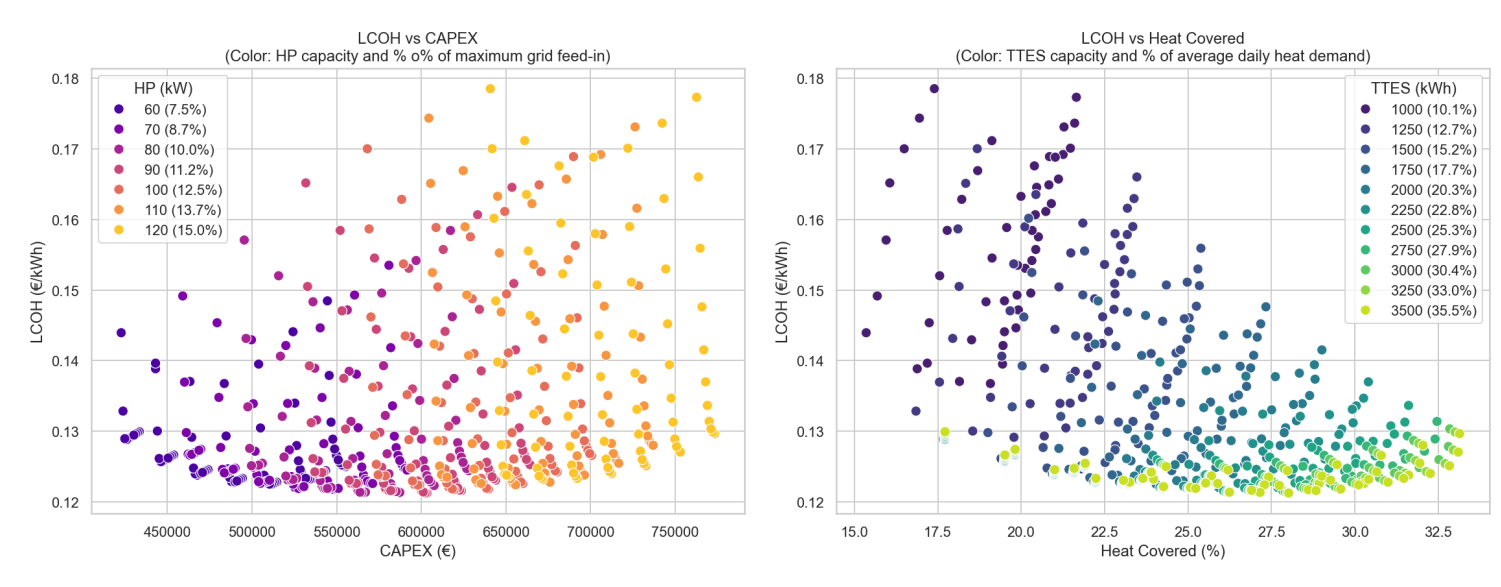


Figure 4.25: LCOH vs. CapEx, colored by heat pump capacity

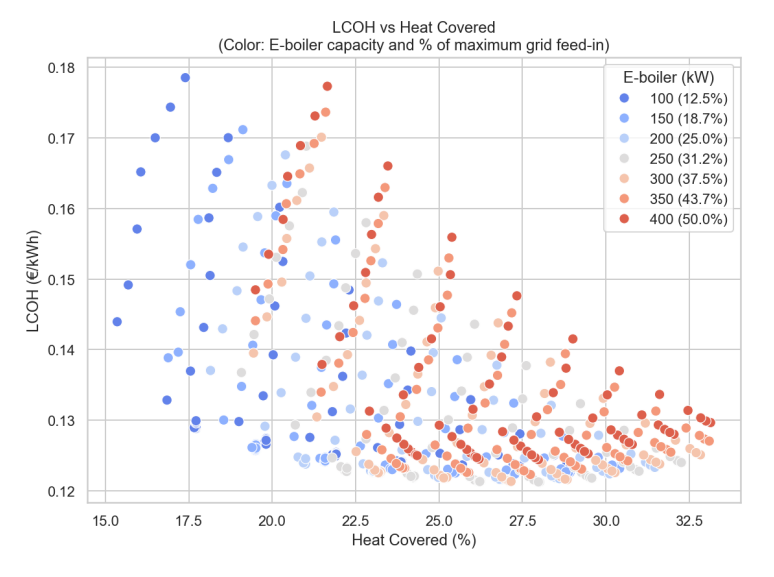


Figure 4.27: LCOH vs. heat coverage, colored by e-boiler capacity

Figure 4.26: LCOH vs. heat coverage, colored by TTES capacity

Table 4.10: Optimal LCOH parameters

* Percentages indicate relative sizing of the components. See section 4.5 on page 59 for more details.

	Unit	Value *
TTES capacity	kWh	3500 (35.5%)
HP capacity	kW	80-100 (10-12.5%)
E-boiler capacity	kW	250 (31.2%)
LCOH	€/kWh	0.12
Effect of PV increase	m^2	neutral

NPV

Figure 4.28, 4.29, and 4.30 illustrate the NPV of the system under different configurations. Figure 4.28 demonstrates that a higher CapEx is associated with higher NPV values across a broad range of e-boiler capacities. However, the highest NPVs are obtained with moderate e-boiler capacities. Figures 4.29 and 4.30 show that larger TTES capacities lead to higher NPV values and increased levels of heat coverage.

Preferred place to be in the figures: in the upper part of the plots, where NPV is the highest. These correspond to moderate to high CAPEX and heat coverage levels.

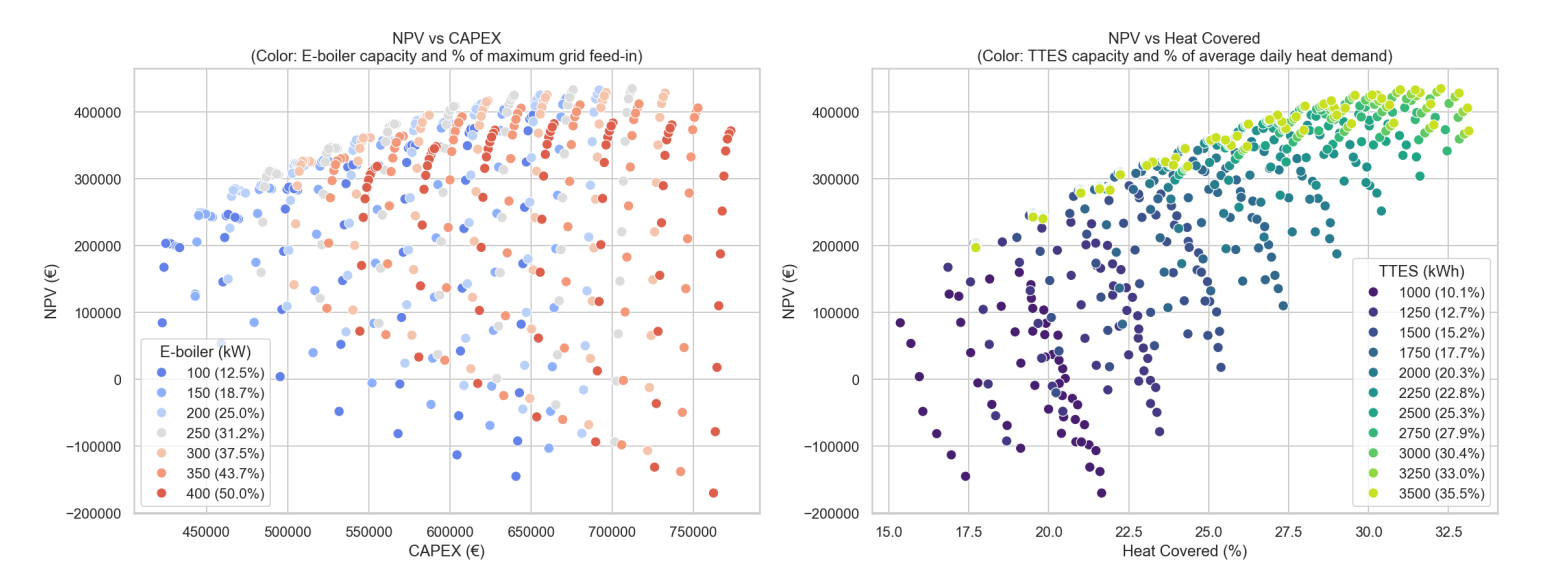


Figure 4.28: NPV vs. CAPEX, colored by e-boiler capacity

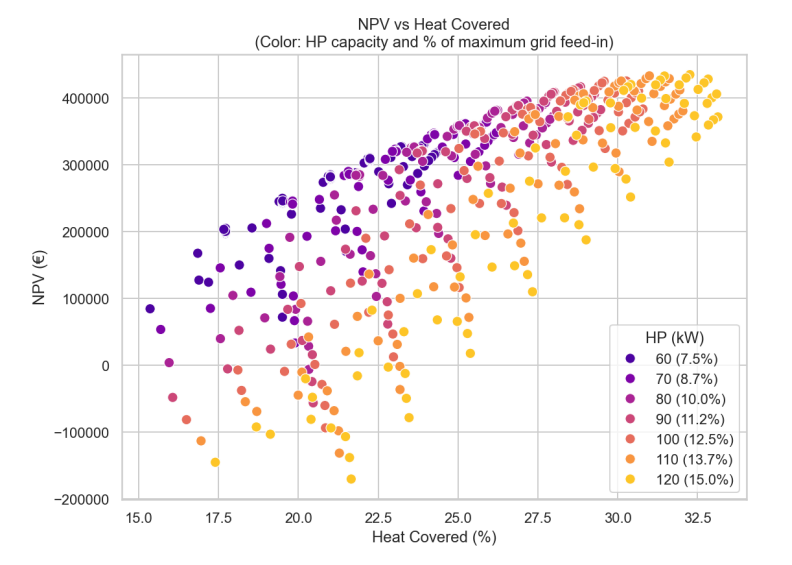


Figure 4.30: NPV vs. heat coverage, colored by HP capacity

Figure 4.29: NPV vs. heat coverage, colored by TTES capacity

Table 4.11: Optimal NPV parameters

* Percentages indicate relative sizing of the components. See section 4.5 on page 59 for more details.

	Unit	Value *		
TTES capacity	kWh	3500 (35.5%)		
HP capacity	kW	120 (15%)		
E-boiler capacity	kW	250 (31.2%)		
NPV	€	435.000		
Effect of PV increase	m^2	negative		

The simulation results reveal that there is no single configuration of the SHTS that performs best across all evaluation indicators. Instead, the "optimal" design depends on the trade-offs between technical indicators (SCOP, grid feed-in, CO_2 emissions) and economic indicators (NPV and LCOH).

Technical performance

The SCOP offers a broad indicator of the whole system's efficiency over the year. The highest SCOP value (2.11) was achieved with a configuration combining a large TTES (3,500 kWh), a high heat pump capacity (120 kW), and a minimal E-boiler capacity (100 kW). These results align with expectations: increased reliance on the heat pump, with its COP of around 3, boosts the SCOP instead of the e-boiler with a COP of nearly 1. Higher e-boiler capacities consistently led to lower SCOP values (Figure 4.12), highlighting the lower efficiency of direct electrical heating. However, a high SCOP can lead to a higher feed-in percentage. Since the e-boiler will use less solar-generated electricity due to its low capacity, this is not favorable.

Grid feed-in analysis reveals that the size of the e-boiler mainly drives this, see figure 4.19. Smaller E-boiler capacities are associated with higher feed-in percentages, due to limited ability to absorb excess solar generation. Increasing TTES capacity reduces feed-in moderately by allowing more flexible temporal storage, while heat pump size has a limited effect on feed-in. The lowest grid feed-in configuration (11%) included a large TTES, moderate HP size, and a large E-boiler (400 kW), suggesting a technically resilient configuration.

 CO_2 emission savings follow a different optimization path. Emissions are minimized when the e-boiler is large enough to absorb excess solar-generated electricity that would otherwise be fed into the grid, while keeping reliance on grid electricity low. This balance was achieved with a configuration of TTES at 3,500 kWh, e-boiler at 400 kW, and HP at only 60 kW, resulting in the highest annual savings (27.7 tonnes CO_2 /year). Notably, the heat pump's contribution to CO_2 savings decreases when its capacity grows, which is due to more frequent nighttime operation on grid electricity.

Economic performance

From a financial perspective, the system performs most efficiently when asset sizing achieves a balance between capital cost and operational savings. The lowest LCOH of €0.12/kWh was achieved with a large TTES (3,500 kWh), a moderate heat pump capacity (80–100 kW), and an E-boiler of 250 kW. These sizes ensure sufficient internal coverage while avoiding excessive investment costs. Notably, mid-range E-boiler and heat pump sizes consistently yielded the most favorable LCOH outcomes. This can be linked to their ability to operate efficiently throughout the year while avoiding the disproportionately high capital costs and the few maximum capacity running hours associated with larger units.

The highest NPV of €435,000 was associated with a configuration with a large TTES, maximum HP size, and a mid-range e-boiler (250 kW). While this configuration has the highest NPV, it also has one of the highest CAPEX. Keeping in mind that this is an absolute value, it does not have the highest IRR.

Solar panel area influence

The impact of increasing solar panel area was not uniformly positive. For SCOP and grid feed-in, expanding the solar panel area had a negative effect, as it resulted in higher feed-in when additional solar energy exceeded system absorption limits. However, for CO_2 reduction, an increase in PV area had a positive effect, as the additional renewable input reduced reliance on grid electricity, thereby lowering emissions. The LCOH is not significantly affected, and the overall heat production costs remain largely stable despite variations in PV area. Although solar-generated electricity is relatively inexpensive and lowers electricity costs per kWh, much of it is converted to heat with the e-boiler, which operates with a lower COP than the HP. As a result, the LCOH does not decrease as much as expected. These results highlight the trade-offs between different performance indicators.

No one-size-fits-all

Overall, the results confirm that optimal SHTS configuration is highly context-dependent. The best setup for reducing emissions is not the same as the one that maximizes NPV or minimizes LCOH. For instance, prioritizing emission reductions tends to push the design toward larger E-boilers, whereas economic optimality favors smaller or moderate E-boiler capacities. Similarly, technical efficiency (SCOP) benefits from maximizing assets, whereas financial performance requires more nuanced balancing to avoid overinvestment. These findings underscore the importance of aligning design with stakeholder objectives.

4.6. SHTS Design Trade-offs

Each system configuration performs differently depending on specific performance indicators. By comparing optimal outcomes across the indicators, the trade-offs in SHTS design become clear.

Main research question: Under what conditions does the implementation of a smart heat transfer station (SHTS) improve the performance of energy supply systems in neighborhoods?

Table 4.12 summarizes the optimal system configurations for each performance indicator, as derived from the simulation results.

Metric	TTES (kWh)	HP (kW)	E-boiler (kW)	Value	Effect of PV Increase
SCOP	3500 (35.5%)	120 (15%)	100 (12.5%)	2.11	Negative
Grid feed-in	3500 (35.5%)	70 (8.7%)	400 (50%)	11%	Negative
CO_2 saved	3500 (35.5%)	60 (7.5%)	400 (50%)	27.7 ton/year	Positive
LCOH	3500 (35.5%)	80 (10%)	250 (31.2%)	€0.12 /kWh	Neutral
NPV	3500 (35.5%)	120 (15%)	250 (31.2%)	€435,000	Negative

Table 4.12: Summary of optimal configurations per performance indicator

High capacity Medium capacity Low capacity Positive effect Negative effect

In all cases, a large TTES appears favorable. This highlights the importance of buffering in SHTS design. The size of the heat pump and E-boiler varies depending on the indicator. A large HP favors SCOP and NPV, while a large e-boiler is more effective for reducing grid feed-in and CO_2 emissions.

Figure 4.31, 4.32, 4.33, 4.34, and 4.35 show a comparison of the optimal configurations per performance indicator, plotted against heat coverage, for each configuration. The color and shape of each data point indicate which metric the configuration was optimized for, enabling visual cross-comparison across tradeoffs.

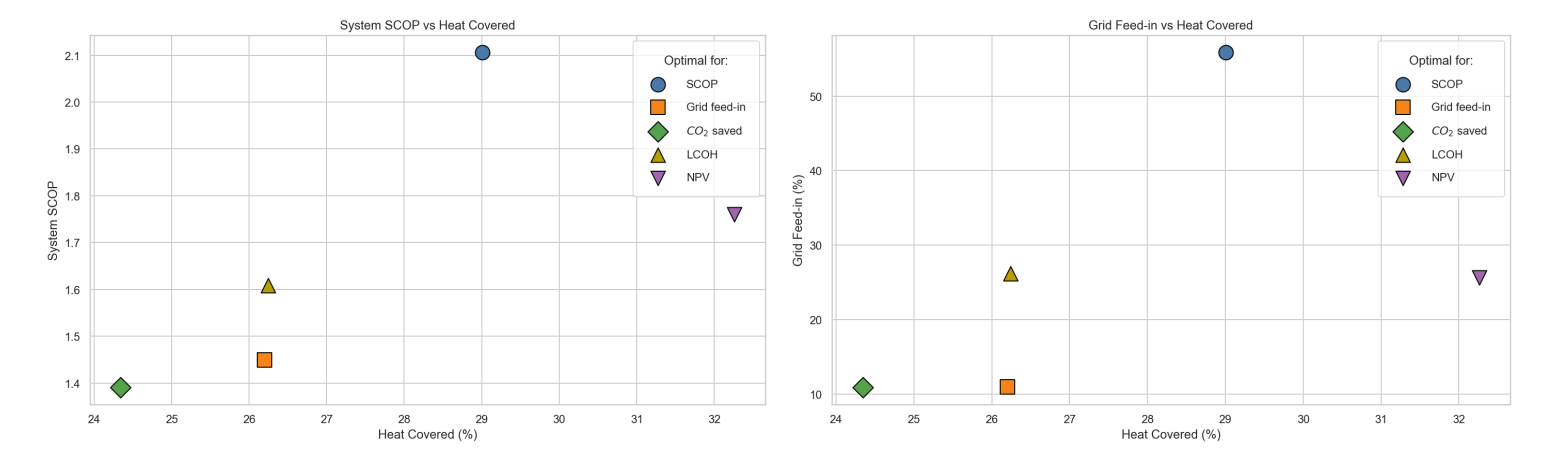


Figure 4.31: Optimal configurations per performance indicator, plotted by system SCOP and heat coverage

Figure 4.32: Optimal configurations per performance indicator, plotted by grid feed-in and heat coverage

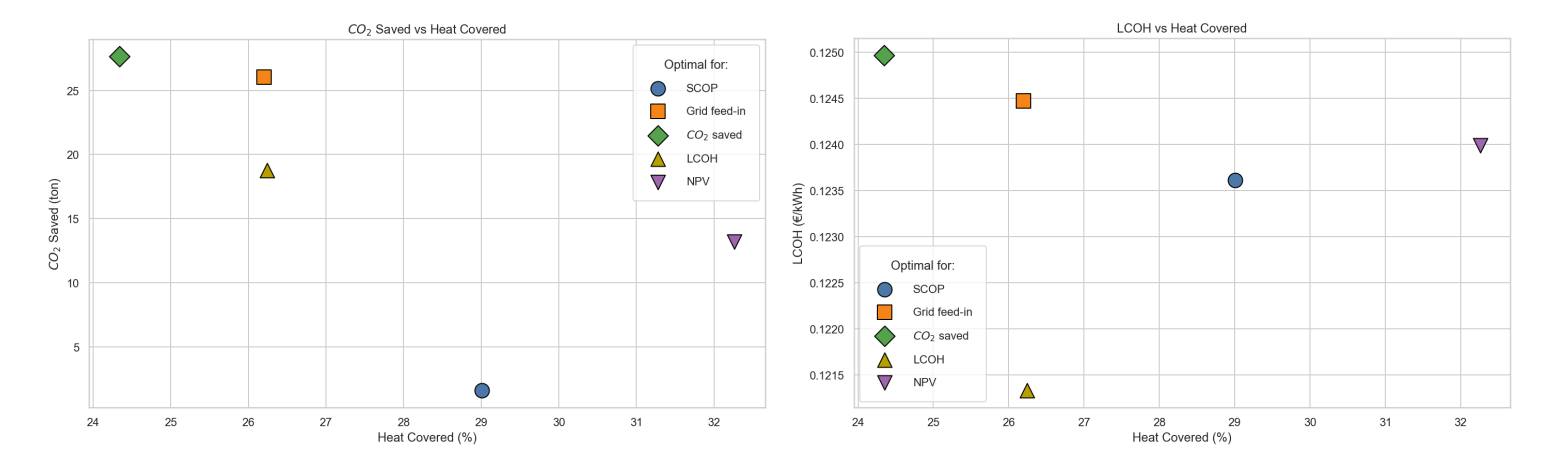


Figure 4.33: Optimal configurations per performance indicator, plotted by saved CO_2 and heat coverage

Figure 4.34: Optimal configurations per performance indicator, plotted by LCOH and heat coverage

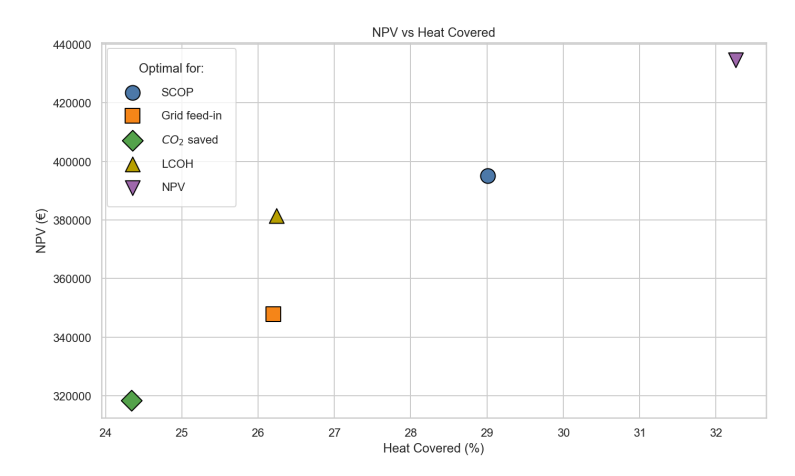


Figure 4.35: Optimal configurations per performance indicator plotted by NPV and heat coverage

The impact of component sizing is indicator-specific. A high HP capacity is particularly beneficial for maximizing the SCOP and NPV. In contrast, the configurations that minimize grid feed-in and maximize CO_2 savings rely more heavily on a large e-boiler and a smaller HP. This is because the e-boiler can absorb excess solar electricity, reducing curtailment and saving CO_2 , while the HP often runs on grid electricity. Interestingly, the lowest LCOH is achieved with a medium-sized HP and E-boiler. This suggests that beyond a certain point, increasing component size does result in lower-priced heat production, but may also introduce unnecessarily high CAPEX. Another key insight is the heat coverage associated with each optimal configuration. Higher heat coverage (\geq 30%) aligns with the best NPV and SCOP results, while lower coverage values are associated with minimized feed-in, LCOH, and CO_2 emissions.

While there is no single optimal configuration across all objectives, the consistent presence of large TTES units indicates that buffering is a non-negotiable feature of well-performing SHTS designs. The LCOH may serve as the most robust guiding metric for system design. As a comprehensive measure, it balances technical efficiency with economic feasibility. The configuration optimized for LCOH also performs acceptably on other indicators, without extremes in component sizing. Increasing and decreasing the e-boiler or HP could be an option when preferring a specific trade-off. Increasing the e-boiler has the most significant impact on the feed-in, while increasing the HP has the most significant effect on the heat coverage.

5 Discussion

This discussion reflects on how the SHTS performs technically, economically, and in terms of societal relevance, and what this implies for the practical relevance and applicability in urban settings. The analysis shows that the SHTS distinguishes itself from conventional HTS by actively managing local heat and electricity flows through a heat pump, e-boiler, and thermal storage. This enables flexible and efficient operation in response to local solar-generated electricity supply and heat demand.

An evaluation framework based on SCOP, grid feed-in, and CO_2 savings effectively captures the SHTS's technical and environmental performance. Simulations reveal that the system performs most effectively during periods when solar generation is sufficiently high to meet heat demand, which primarily occurs in the summer months. This alignment enables efficient internal use of renewable electricity for heat production.

Economically, the SHTS offers strong returns, with a favorable LCOH and a competitive NPV, despite its relatively high initial investment. The system remains sensitive to energy prices and policy changes. Optimization results confirm that the ideal configuration depends on strategic trade-offs: maximizing financial return, minimizing emissions, or maximizing heat coverage. Each trade-off requires a different combination of asset sizes.

5.1. Model Limitations

While the model offers valuable insights into the operation and potential of an SHTS, it is based on several simplifying assumptions that may affect the accuracy of the results. The following limitations should be considered when interpreting the results.

Control logic and technical assumptions

First, no optimization algorithm was applied to the control strategy of the SHTS. Instead, the system relied on rule-based logic. For example, prioritizing PV electricity, enforcing a minimum runtime for the heat pump, and enabling nighttime pre-charging based on heat demand forecasting. While sufficient for exploring relative performance between configurations, this approach is inherently suboptimal and underestimates the system's potential. Applying optimization techniques could optimize HP's operational hours, TTES charging and discharging, and e-boiler activity.

Secondly, technical assumptions, such as constant PV efficiency (24%), fixed tax rules, and linear interpolation of weather and demand data, were necessary to maintain traceability. While this enabled efficient simulation and comparison across configurations, it may not accurately capture yearly performance variations, prices, or policy dynamics. For example, PV efficiency drops under high temperatures or partial shading. This leads to lower annual yields than modeled, since the majority of the solar-generated electricity is produced when temperatures are higher.

Demand profiles and economic assumptions

The model input depends on a generic, scaled heat and electricity demand profile representative of a typical neighborhood. While this approach captures the overall magnitude and structure of demand for 300 households, it does not reflect household-level diversity in behavior, comfort preferences, or responsiveness to dynamic pricing. For example, if 10–20% of households have higher evening heat demand, this could require larger storage or extra backup capacities. As a result, the system design and costs may shift significantly.

While SHTSs support decarbonization by reducing the heat demand from district heating and increasing self-consumption of renewable electricity, the model assumes constant CO_2 emission factors for both grid electricity and district heat per kWh. As the electricity grid continues to decarbonize, the benefits of the SHTS may increase over time, since it will rely on increasingly cleaner electricity to produce heat. This means that the results are likely a lower bound of the potential emission reductions. As the electricity grid decarbonizes further, the actual CO_2 reduction of the SHTS will likely be greater.

Finally, the economic analysis in this study is based on 2024–2025 market estimates provided by De WarmteTransitieMakers. While these values reflect current pricing for capital and operational expenditures, they may not capture future developments in the rapidly evolving energy sector. In particular, electricity prices were modeled using historical 2024 market data, assuming fixed hourly profiles. However, electricity markets are inherently volatile, and future price predictions, driven by increasing electrification, renewable integration, or policy interventions, could substantially affect the cost-effectiveness of SHTS. Similarly, current feed-in rules and net metering incentives are expected to be phased out. As electricity prices are expected to become more volatile, particularly due to the growing share of solar and wind energy, the SHTS may become even more effective. Since the system is capable of responding quickly, it can be activated during periods of very low electricity prices, allowing it to optimize heat production even when there is no self-generation, but cheap grid electricity is available. This operational flexibility enhances its potential to reduce costs, thereby increasing the financial attractiveness of the SHTS.

5.2. System Design Considerations and Sensitivity

Seasonal storage vs. daily storage

Replacing daily thermal storage, which is used in the SHTS, with seasonal thermal storage could address the mismatch between high summer production and high winter heat demand. In the base case, 14% of solar-generated electricity is fed back into the grid, see section 4.2. If seasonal heat storage were available, this 14% could be converted into heat and be stored for later use. Additionally, both the HP and e-boiler could operate more frequently during hours with low electricity prices. As a result, a significantly larger share of the total yearly heat demand could be supplied by the SHTS, resulting in higher heat coverage and potentially lower costs.

However, the required storage capacity increases drastically, making above-ground storage infeasible in urban settings. Subsurface solutions, like ATES or BTES systems, may offer a viable alternative. However, their applicability depends heavily on local soil and groundwater conditions. Aligning the available space in the built environment with the specific ground conditions needed will be a major challenge. Moreover, seasonal storage systems respond more slowly than daily buffers, making them unsuitable for real-time flexibility or rapid adjustments to fluctuations in solar generation or heat demand, and will therefore be unable to match the smart and dynamic behavior of the SHTS.

A combined daily—seasonal storage setup could theoretically support the SHTS by combining short-term flexibility with long-term storage capacity. However, it would introduce additional complexity and investment costs. Moreover, in practice, the spatial and technical requirements of seasonal storage make such a hybrid solution largely unfeasible in most built environments.

Heat pump control logic

The operational logic of the HP has a significant influence on the overall system performance of the SHTS. In the current model, HP behavior is pre-defined by a set of rule-based controls, including minimum runtime and cool-down periods. These assumptions directly affect the timing and frequency of heat production.

Shortening such constraints by reducing the minimum runtime from two hours to one, or shortening the cooldown duration, allows the system to respond more flexibly to intermittent solar generation. However, this may also lead to more frequent cycling of the HP, potentially reducing its efficiency and lifespan. Extending the minimum running time reduces the amount of HP running hours, since it will only turn on when it can stay on for the minimum running time.

Not predefining HP operation would increase adaptability and lead to higher heat production, and improve the performance of the SHTS. However, such behavior does not align well with the characteristics of an HP, which is not designed for frequent start-stop cycles or highly variable loads.

District heating integration

In the base scenario, the SHTS is capable of supplying approximately 30% of the total annual heat demand, see section 4.2. This share is relatively higher during summer, particularly in periods with low heat demand. As shown in figure 4.10, the system covers most of the heat demand during summer. In contrast, the contribution of the system in the winter months is limited, as shown in figure 4.12. However, from a system-wide perspective, this can be problematic as this high percentage may conflict with the operation of a DHN. DHNs rely on maintaining a base level of flow and temperature to ensure stability and efficiency. If SHTS replaces most of the DHN-supplied heat during several months of the year, this could negatively affect the network's efficiency.

A potential strategy is to enforce a base load connection to the DHN, even when the SHTS could supply all heat demand. This would help maintain stable operating conditions in the network. To evaluate this, a scenario was tested in which the DHN was continuously delivering a minimum amount of heat. This minimum amount of heat often exceeded the heat demand during summer, allowing the TTES to be charged with this base load. Results showed that this reduced the system's overall efficiency and limited the use of solar-generated electricity. Despite these drawbacks, such a constraint may be necessary in practice to support broader system integration.

Additionally, a possible approach to improve summer integration is to completely disconnect the DHN during the summer months, allowing it to cool down. In this case, the neighborhood would rely entirely on the SHTS for heat supply during this period. One clear advantage of this approach is the reduction of distribution-related heat losses, which are relatively high in low-demand conditions. However, this approach comes with implications. First, yearly temperature fluctuations in the DHN infrastructure, due to the full cooldown and reheating, may lead to material stress or operational issues. Second, if the SHTS has a failure, there is no immediate backup available. To cover this risk, each SHTS would probably need to be equipped with an additional backup gas boiler, increasing the investment costs. An additional challenge lies in the decision-making process itself, particularly in determining when it is safe for the DHN operator to allow the entire network to cool down. This is likely to remain a highly complex and situation-specific question that requires careful consideration in each specific context.

Impact of weather and demand profiles

To assess the robustness of the SHTS, the model was tested using alternative input profiles for heat demand, solar radiation, and electricity prices. This represents variations in household behavior, weather conditions, and economic factors. Results indicate that while the overall system behavior remains consistent, the amount of heat that can be produced and delivered fluctuates depending on the solar radiation and the alignment between heat demand and solar-generated electricity availability. This assessment is based on an aggregated demand profile at the level of an SHTS and does not represent simulations with unique demand profiles per household.

Variations in the input profiles resulted in periods of solar-generated electricity that could not be fully utilized or stored, while under low-generation or high-demand conditions, the system increasingly depended on DHN supply, and vice versa. Changes in electricity prices influenced system behavior; higher prices during low-solar periods made grid-based heat production less attractive, while low or negative prices occasionally had a positive effect, even when solar generation was limited. This affects the business case of the SHTS. These findings suggest that the effectiveness is sensitive to the input variables and underscore the importance of using representative and up-to-date data when running the model.

5.3. Strategic, Social, and Policy Implications

Uncertainty forecasting and supply

The efficiency of the SHTS relies on the ability to anticipate future heat demand and solar-generated electricity. In the current model, control strategies are based on forecasting assumptions, such as daily solar predictions and weekly demand patterns. However, in practice, both sustainable electricity generation and heat demand are subject to uncertainty. Factors such as changing weather patterns and user behavior can introduce substantial deviations from expected values.

When forecasting is inaccurate or unavailable, the system's ability to charge the TTES at night or shift production to a later moment can be disturbed. This may lead to inefficient operation or missed opportunities for self-consumption.

In addition to uncertainty in generation and heat demand, future electricity demand patterns are shifting due to electrification and increased adoption of EVs. Large-scale EV charging introduces peak loads and affects daily load profiles, which may interfere with the availability of electricity for the SHTS. A BESS could absorb excess solar power during the day and release it for heat production or EV charging. However, implementing a BESS involves high CAPEX and space requirements. In practice, the performance of the SHTS may differ from the modeled results due to forecasting uncertainties and shifting electricity demand. Still, the flexibility of the SHTS enables it to adapt to changing conditions, helping the system perform reliably in real-world conditions.

Financing and public priorities

Financing and prioritization of SHTSs depend heavily on public relevance. Public investments in sustainable infrastructure often compete with other high-priority needs, such as affordable housing, healthcare, or education. Showing that an SHTS can contribute to long-term cost reductions, emission reductions, and efficient integration of renewables is, therefore, essential to gain public and political support.

Moreover, questions may arise about who bears the cost of implementation. Will this be just the grid operator, or is there a contribution from municipalities, homeowners, or housing associations? Creative financing structures could help lower the entry barrier for adoption and share the costs between stakeholders. Since the SHTS may appear complex to those unfamiliar with the subject, transparency regarding its functioning and cost-effectiveness will be crucial for aligning public opinion and ensuring social acceptance.

Practical Relevance

Beyond its analytical value, the SHTS model offers practical opportunities for supporting local energy planning. By incorporating neighborhood-specific heat demand profiles as input, the model can be used to explore which configurations are most suitable for different neighborhoods. For instance, areas with demand profiles with relatively high peaks or low solar potential may benefit more from higher storage capacity or larger HPs or e-boilers, whereas other locations may optimize self-consumption with a different configuration.

This enables grid operators, municipalities, or housing associations to use the model as a planning tool to guide local energy strategies. It can provide advice on how an SHTS could support sustainability goals and translate abstract energy ambitions into realistic design choices that reflect what is feasible in a given neighborhood.

5.4. Real-Life Implementation Challenges

While simulation results demonstrate strong technical and economic potential, implementing the SHTS concept in real-life urban settings presents a range of complex spatial and financial challenges.

Spatial integration and urban constraints

A major challenge lies in integrating the system physically into existing urban neighborhoods. These areas often lack sufficient space to accommodate a TTES, particularly when required storage volumes reach approximately 3.500 kWh. Under the assumption of perfect mixing, this corresponds to a tank volume of about 100 m^3 . This corresponds to a cylindrical tank of approximately 5 m in both diameter and height. However, to assess realistic sizing requirements, a stratified tank model was developed, as elaborated in Appendix A. The stratified tank model shows that the perfect mixing assumption overestimates usable storage. Therefore, tank volumes must be increased to ensure reliable performance under real-world conditions.

Successful deployment also hinges on how visibly and practically the SHTS can be integrated into the neighborhood. This includes visible elements such as the TTES, local infrastructure modifications, or assets like the HP and e-boiler. It also requires ensuring safe access for maintenance, compliance with noise regulations, and minimizing negative aesthetic effects in residential areas.

This visibility creates both an opportunity and a challenge: it can promote awareness of the energy transition, but may also lead to resistance if residents feel insufficiently involved. Actively engaging citizens early in the planning process, along with clear communication, can help build trust and increase social acceptance. The upcoming "Wet Collectieve Warmtevoorziening" (WCW) introduces a new pricing structure aimed at more transparency for DHN. This may result in lower heat prices because the SHTS could help avoid grid congestion and reduce infrastructure investments. This strengthens the case for financial investments from grid operators. Such cost reductions could help improve public acceptance of the system, even when

the SHTS is prominently visible in the neighborhood. Ensuring that residents understand not just how the system works, but how it contributes to their daily lives and sustainability goals, will be key for the successful implementation of an SHTS.

Societal value and stakeholder benefits

Financially, the SHTS operates within the energy infrastructure, so households themselves are unlikely to notice any direct changes in comfort or daily operation. The system operates in the background, creating value for multiple stakeholders. The electricity grid operator benefits from reduced solar feed-in during peak hours, which helps mitigate local congestion without the need for costly grid reinforcements. Simultaneously, the DHN operator gains access to a low-cost, locally produced heat source.

Beyond these benefits, the system also delivers significant societal value. By supporting local energy balancing and increasing renewable self-consumption, the SHTS contributes directly to climate and sustainability goals. The societal value of congestion relief, though not reflected in economic indicators, represents a meaningful reduction in societal costs and should be accounted for in future decision-making.

Ultimately, the real-life success of an SHTS will depend not only on its technical performance but also on how well it can be integrated within the physical, social, economic, and organizational structures in neighborhoods.

Conclusion

Local electricity grids face rising pressure from peak feed-in, due to increasing levels of solar panels and electrification in residential areas. This thesis explored the potential of an SHTS to address this challenge by converting surplus solar-generated electricity into usable heat. The SHTS aims to reduce grid congestion and improve the performance of local energy supply systems at the neighborhood scale.

The main research question guiding this study was: *Under what conditions does the implementation of a Smart Heat Transfer Station (SHTS) improve the performance of energy supply systems in neighborhoods?*

To address this question, a comprehensive simulation model was developed that integrates an HP, e-boiler, TTES, and rooftop solar panels into a coordinated system. Using a simulation model, the study explored a wide range of configurations, applied realistic control strategies, and evaluated both technical and economic performance indicators.

The findings show that the SHTS can enhance local energy system flexibility and reduce electricity feed-in during peak solar production hours. By transforming surplus solar-generated electricity into heat, it reduces real-time grid feed-in and enables flexible use of electricity. In doing so, it alleviates pressure on the electricity network and reduces the need for costly grid reinforcements.

The SHTS also contributes to reduced carbon emissions by lowering heat provision through district heating. When operated under favorable conditions, it enables the DHN operator to access low-cost, locally produced heat. Meanwhile, households experience no reduction in comfort or service quality, as the system operates in the background.

Part of the research was the development and application of a rule-based control strategy. The control logic prioritized operation during moments of excess solar-generated electricity, combined with enforced minimum runtime conditions and incorporated forecasting logic. Results showed that, under this logic, the SHTS performed reliably and achieved consistent reductions in grid feed-in, providing heat, and thus provided a valuable baseline for future optimization studies.

The capacity of the SHTS assets is critical to the system's performance. In particular, the size of the TTES strongly influenced how much heat could be captured and how flexibly the system could respond to demand. Additionally, the e-boiler played a key role in the amount of grid feed-in, whereas the heat pump was effective at charging the tank during hours of low electricity prices.

Economically, the system demonstrated favorable outcomes under current pricing and tax conditions. NPV and LCOH outcomes indicated that investing in an SHTS can be viable, particularly in specific configurations. In addition, while the system provides high value to electricity grid operators, they currently play no financial role in its implementation. This creates a mismatch between where the value lies and where the investment and risk lie. By improving collaboration through incentives or regulation, there are clear opportunities to strengthen cooperation and make the business case even more attractive for the adoption of the SHTS.

The results of this thesis indicate that the SHTS improves the performance of neighborhood energy supply systems most effectively under several related conditions and depends on the availability of local solar-generated electricity. The TTES capacity should be as large as practically feasible within the built environment to buffer fluctuations between supply and demand. In addition, a medium-sized e-boiler and HP are recommended. This corresponds to a TTES capacity of 35% of the average daily heat demand. The HP and e-boiler are sized at 10% and 31% of the maximum grid feed-in capacity with a conventional

HTS, respectively. When these conditions are met, the SHTS significantly reduces the amount of excess solar-generated electricity fed back into the grid, lowers carbon emissions, and delivers heat reliably and cost-effectively.

In summary, this thesis concludes that an SHTS is a technically viable, economically promising solution for neighborhoods with high solar penetration. Its greatest strength lies in its ability to reduce grid feed-in during peak hours, thereby directly contributing to congestion management, an increasingly pressing issue in the energy landscape.

While further work is needed to refine control strategies and resolve spatial and legal barriers, this case study provides strong evidence that smart, flexible systems like the SHTS can play a vital role in future energy systems. By turning surplus solar generation into locally usable heat, the SHTS reduces grid congestion, enhances renewable self-consumption, and supports broader energy transition goals. As the energy transition evolves, scalable and realistic solutions will be essential, and this thesis shows that the SHTS is one of them.

abla

Recommendations

While the developed simulation framework has proven valuable in assessing the performance and feasibility of an SHTS, several opportunities remain to extend and deepen this research. These recommendations target both future academic exploration and practical implementation.

A key direction for future work involves integrating more advanced control strategies. The current model relies on rule-based logic, including a basic form of forecasting to coordinate HP operation based on historical demand and future solar forecasts. Although effective to a degree, this approach remains limited and will not be optimal for dynamic market conditions, weather, and demand variability. Future studies are encouraged to implement predictive or optimization-based control algorithms, such as Model Predictive Control or learning-based control methods. These methods can better optimize the control logic and forecasts, thereby improving overall system efficiency.

Another relevant path to consider is scaling the model to another level. While this study focused on 300 households, larger-scale deployment could introduce new opportunities and/or complexities. Besides that, investigating the aggregated behavior of multiple SHTS units and their interaction with local infrastructure could yield valuable insights.

Another recommendation is to improve the modeling of end-user behavior. The current setup relies on a generalized heat demand profile. Using actual behavioral data could enhance the accuracy of demand-side simulations. Involving users could promote acceptance and more flexible energy use.

This study centered on TTES as the primary energy buffer. While suitable for heat storage, it is not necessarily the optimal option, particularly in space-constrained settings. Emerging alternatives such as phase change materials and thermochemical storage solutions could be worth further investigation. BESS provides a nice way to store electrical energy and offer flexibility. Future research could explore hybrid configurations that combine the efficiency of thermal storage with electrical storage, such as a BESS.

In this study, electricity pricing was modeled dynamically over a single year, but then repeated identically for subsequent years. In reality, however, policy instruments such as net metering, changing political priorities, and fluctuations in CO_2 pricing can have a significant impact on the financial viability of SHTS. Conducting a series of policy analyses would therefore be valuable in assessing the robustness of the SHTS concept across multiple future scenarios.

In addition, implementation depends not only on technical feasibility but also on overcoming legal and spatial barriers. Legal constraints and a lack of visual and spatial integration can delay implementation. Addressing these issues requires transparency between stakeholders. Future research could explore legal frameworks and spatial integration options that can support the deployment of SHTSs.

Finally, future research could explore the business case for SHTSs from the perspective of DHN operators. An impact analysis between a 'base case' of a conventional HTS and a scenario with an SHTS could clarify its economic effects. This includes potential savings due to avoided grid congestion and limited infrastructure reinforcements. Such avoided costs could serve as a basis for financial compensation from the grid operator, improving the attractiveness of SHTS for DHN operators.

In summary, while this study has laid a strong foundation for simulating and evaluating SHTSs, future research should prioritize improving control intelligence, scaling, diversifying technology options, and addressing legal complexities. Together, these steps will be crucial in unlocking the full potential of flexible, decentralized energy infrastructure within the evolving energy landscape.

- [1] Statistics Netherlands (CBS). Nearly three-quarters of the Dutch population use smart devices. Accessed: 2025-01-30. 2021. URL: https://www.cbs.nl/en-gb/news/2021/48/nearly-three-quarters-of-the-dutch-population-use-smart-devices.
- [2] Statistics Netherlands (CBS). Renewable electricity share up by 20 percent in 2022. Accessed: 2025-01-30. 2023. URL: https://www.cbs.nl/en-gb/news/2023/10/renewable-electricity-share-up-by-20-percent-in-2022.
- [3] International Energy Agency (IEA). *The Netherlands 2024: Energy Policy Review*. Accessed: 2025-01-30. International Energy Agency, 2024. URL: https://iea.blob.core.windows.net/assets/2b729152-456e-43ed-bd9b-ecff5ed86c13/TheNetherlands2024.pdf.
- [4] National Renewable Energy Laboratory (NREL). *Integrating Variable Renewable Energy Into the Grid:* Key Issues. Accessed: 2025-01-30. National Renewable Energy Laboratory (NREL), 2024. URL: https://www.nrel.gov/docs/fy25osti/91019.pdf.
- [5] Omais Abdur Rehman et al. "Enabling Technologies for Sector Coupling: A Review on the Role of Heat Pumps and Thermal Energy Storage". In: *Energies* 14.24 (2021). ISSN: 1996-1073. DOI: 10. 3390/en14248195. URL: https://www.mdpi.com/1996-1073/14/24/8195.
- [6] Dr Ahmed et al. "Modelling Techniques Used in The Analysis of Stratified Thermal Energy Storage: A Review". In: *MATEC Web of Conferences* 225 (Jan. 2018), p. 01015. DOI: 10.1051/matecconf/201822501015.
- [7] Alfa Laval. *District Heating*. Accessed: 2025-02-10. 2025. URL: https://www.alfalaval.us/industries/hvac/district-heating/.
- [8] ARANER. What is a Water-to-Water Heat Pump? Accessed: 2025-01-30. 2025. URL: https://www.araner.com/blog/what-is-a-water-to-water-heat-pump.
- [9] Atriensis. *Emissiefactoren 2024 bekend*. Accessed: 2025-03-29. 2024. URL: https://atriensis.nl/emissiefactoren-2024-bekend/.
- [10] Belastingdienst. *Energiebelasting*. Accessed: 2025-05-16. 2024. URL: https://www.belastingdienst.nl/wps/wcm/connect/bldcontentnl/belastingdienst/zakelijk/overige_belastingen/belastingen_op_milieugrondslag/energiebelasting/.
- [11] Angelique Biemans et al. Netimpact Woningen met Warmtepomp op Basis van Slimme Meterdata. Accessed: 2025-02-10. Rijksdienst voor Ondernemend Nederland, Netbeheer Nederland, Techniek Nederland, 2025. URL: https://www.rvo.nl/sites/default/files/2025-01/Rapport-Netimpact-woningen-met-warmtepomp.pdf.
- [12] Martin Bloemendal. SET3205 Heat Storage HT-ATES. Lecture slides for SET3205 Heat Storage. 2024
- [13] Lisa Brand et al. "Smart district heating networks A simulation study of prosumers' impact on technical parameters in distribution networks". In: *Applied Energy* 129 (2014), pp. 39–48. ISSN: 0306-2619. DOI: https://doi.org/10.1016/j.apenergy.2014.04.079. URL: https://www.sciencedirect.com/science/article/pii/S0306261914004425.
- [14] Wim-Paul Breugem. SET3205 Heat Storage LHTES. Lecture slides for SET3205 Heat Storage. 2024.
- [15] Qi Chen et al. "Energy storage to solve the diurnal, weekly, and seasonal mismatch and achieve zero-carbon electricity consumption in buildings". In: *Applied Energy* 312 (2022), p. 118744. ISSN: 0306-2619. DOI: https://doi.org/10.1016/j.apenergy.2022.118744. URL: https://www.sciencedirect.com/science/article/pii/S0306261922002008.
- [16] Stanislav Chicherin et al. "Method for Assessing Heat Loss in A District Heating Network with A Focus on the State of Insulation and Actual Demand for Useful Energy". In: *Energies* 13.17 (2020). ISSN: 1996-1073. DOI: 10.3390/en13174505. URL: https://www.mdpi.com/1996-1073/13/17/4505.

[17] Stanislav Chicherin et al. "The First Fifth-Generation District Heating and Cooling System in Kaza-khstan: Planning and Design". In: *Energies* 17.23 (2024). ISSN: 1996-1073. DOI: 10.3390/en17236 169. URL: https://www.mdpi.com/1996-1073/17/23/6169.

- [18] D. Christensen and C. Hancock. Evaluating Air-Source Heat Pumps for Cold Climates: A Study of Heating System Performance in Minnesota. Tech. rep. Golden, CO, USA: National Renewable Energy Laboratory (NREL), 2014. URL: https://www.nrel.gov/docs/fy14osti/60135.pdf (visited on 01/28/2025).
- [19] Islington Council. Connections Guidance: Connecting to Bunhill Heat and Power. Tech. rep. Accessed: 2025-01-30. Islington Council, 2019. URL: https://www.islington.gov.uk/~/media/sharepoint-lists/public-records/energyservices/information/adviceandguidance/201920 20/20190828connectionsguidancepart21.pdf.
- [20] Abdulrahman Dahash, Annette Steingrube, and Mehmet Elci. "A Power-Based Model of a Heating Station for District Heating (DH) System Applications". In: May 2017. DOI: 10.3384/ecp17132415.
- [21] DeWarmteTransitieMakers. Internal report/documents. Unpublished internal report/document. 2025.
- [22] Jan Dusek. "R290 Heat Pumps Dominate the ISH 2023 Show in Germany". In: Natural Refrigerants (2023). Accessed: 2025-02-03. URL: https://naturalrefrigerants.com/r290-heat-pumps-dominate-the-ish-2023-show-in-germany/.
- [23] Eneco. Eneco Tariefblad Warmte & Koude 2025. Accessed: 2025-04-20. 2024. URL: https://www.eneco.nl/-/media/eneco-nl/files/voorwaarden/voorwaarden_stadswarmte/enecotariefblad-warmte--koude-2025.pdf.
- [24] Energie-Nederland. Facts & Figures on the Energy Transition. https://www.energie-nederland.nl/en/topics/energy-transition/facts-figures/. Accessed: 2025-01-24. 2021.
- [25] Dandelion Energy. Open-Loop vs. Closed-Loop Geothermal Systems. Accessed: 2025-01-30. 2020. URL: https://dandelionenergy.com/open-loop-vs-closed-loop-geothermal-systems.
- [26] U.S. Department of Energy. *Air-Source Heat Pumps*. Accessed: 2025-01-30. 2025. URL: https://www.energy.gov/energysaver/air-source-heat-pumps.
- [27] American Council for an Energy-Efficient Economy (ACEEE). *Electrification Retrofits: Overcoming Barriers to Implementation*. Tech. rep. Accessed: 2025-01-29. American Council for an Energy-Efficient Economy, 2022. URL: https://www.aceee.org/sites/default/files/pdfs/b2206.pdf.
- [28] American Council for an Energy-Efficient Economy (ACEEE). Large Heat Pumps for Commercial Buildings. Accessed: 2025-01-30. 2024. URL: https://www.aceee.org/sites/default/files/proceedings/ssb24/pdfs/20240722163117609_2816fba1-a426-4e5a-8e9e-464d1f9a2422.pdf.
- [29] European Commission. *EU Emissions Trading System (EU ETS)*. Accessed: 2025-05-12. 2023. URL: https://climate.ec.europa.eu/eu-action/eu-emissions-trading-system-eu-ets/about-eu-ets_en.
- [30] European Commission Joint Research Centre. More coordination needed for renewable deployment to prevent grid congestion. Accessed: December 3, 2024. May 2024. URL: https://joint-research-centre.ec.europa.eu/jrc-news-and-updates/more-coordination-needed-renewable-deployment-prevent-grid-congestion-2024-05-27_en.
- [31] Eurostat. Energy consumption in households. Accessed: 2024-01-29. 2024. URL: https://ec.europa.eu/eurostat/statistics-explained/index.php?title=Energy_consumption_in_households.
- [32] EV Range Insights. How Vehicle-to-Grid (V2G) Technology Is Revolutionizing the EV Ecosystem in 2024. Accessed: 2024-12-21. 2024. URL: https://www.evrange.com/ev-range-insights/how-vehicle-to-grid-v2g-technology-is-revolutionizing-the-ev-ecosystem-in-2024?utm_source=chatgpt.com.
- [33] Gaslicht.com. Verschillen stadswarmte, gasaansluitingen en vaste energiecontracten. Accessed: 2025-05-20. 2024. URL: https://www.gaslicht.com/nieuws/verschillen-stadswarmte-gasaansluit ingen-en-vaste-energiecontracten.
- [34] G. Glenk and S. Reichelstein. "Economics of converting renewable power to hydrogen". In: *Nature Energy* 4.3 (2019), pp. 216–222. DOI: 10.1038/s41560-019-0326-1.

[35] Alvaro Gonzalez-Castellanos, Priyanko Guha Thakurta, and Aldo Bischi. *Congestion Management via Increasing Integration of Electric and Thermal Energy Infrastructures*. Tech. rep. 100RES 2020 – Applied Energy Symposium (ICAE). Pisa, Italy: Skolkovo Institute of Science and Technology, 2020. URL: https://arxiv.org/pdf/2101.00835.

- [36] Alvaro Gonzalez-Castellanos, Priyanko Guha Thakurta, and Aldo Bischi. "Congestion management via increasing integration of electric and thermal energy infrastructures". In: 100% Renewable: Strategies, technologies, and challenges for a fossil free future. Applied Energy Symposium (ICAE). Pisa, Italy, Oct. 2020. URL: https://arxiv.org/pdf/2101.00835v1.
- [37] E. Guelpa et al. "Reduction of supply temperature in existing district heating: A review of strategies and implementations". In: *Energy* 262 (2023), p. 125363. ISSN: 0360-5442. DOI: https://doi.org/10.1016/j.energy.2022.125363. URL: https://www.sciencedirect.com/science/article/pii/S0360544222022459.
- [38] Philipp Andreas Gunkel et al. Variability in electricity consumption by category of consumer: the impact on electricity load profiles. 2022. arXiv: 2210.03524 [eess.SY]. URL: https://arxiv.org/abs/2210.03524.
- [39] Mirjam Harmelink et al. Datarapport Beleidsnota Warmte: Impact van Warmteoplossingen op het Energiesysteem. Tech. rep. Bijlage bij de Beleidsnota Warmte en het Warmteprogramma. Gemeente Utrecht, 2025. URL: https://utrecht.bestuurlijkeinformatie.nl/Agenda/Document/13b91c41-cc55-4bb5-a0c5-45e6239ebbca?documentId=78aa14a3-8a5d-4616-b69e-24261acc7ea8&agendaItemId=ee8eea6c-93ba-42f4-8300-4b201890174b.
- [40] Roman J. Hennig, Laurens J. de Vries, and Simon H. Tindemans. "Congestion management in electricity distribution networks: Smart tariffs, local markets and direct control". In: *Utilities Policy* 85 (2023), p. 101660. ISSN: 0957-1787. DOI: https://doi.org/10.1016/j.jup.2023.101660. URL: https://www.sciencedirect.com/science/article/pii/S0957178723001728.
- [41] B.A.L.M. Hermans et al. "Model Predictive Control of Vehicle Charging Stations in Grid-Connected Microgrids: An Implementation Study". In: *Applied Energy* (2024). Accessed: 2025-02-10. DOI: 10.1016/j.apenergy.2024.123210. URL: https://doi.org/10.1016/j.apenergy.2024.123210.
- [42] International Energy Agency. *Electricity Grids and Secure Energy Transitions*. Accessed: 17-12-2024. 2023. URL: https://iea.blob.core.windows.net/assets/ea2ff609-8180-4312-8de9-494bcf21 696d/ElectricityGridsandSecureEnergyTransitions.pdf.
- [43] International Energy Agency. Renewables 2022: Analysis and Forecast to 2027. Accessed: December 5, 2024. 2022. URL: https://iea.blob.core.windows.net/assets/ada7af90-e280-46c4-a577-df2e4fb44254/Renewables2022.pdf.
- [44] Joint Research Centre, European Commission. *Photovoltaic Geographical Information System*. htt ps://re.jrc.ec.europa.eu/pvg_tools/en/. Accessed: 2025-05-19. 2025.
- [45] Min-Hwi Kim et al. "Energy Performance Investigation of Bi-Directional Convergence Energy Prosumers for an Energy Sharing Community". In: *Energies* 14.17 (2021). ISSN: 1996-1073. DOI: 10. 3390/en14175544. URL: https://www.mdpi.com/1996-1073/14/17/5544.
- [46] Elke Klaassen, Jasper Frunt, and Han Slootweg. "Assessing the impact of distributed energy resources on LV grids using practical measurements". In: *Proceedings of CIRED 2015 23rd International Conference on Electricity Distribution*. June 2015.
- [47] Alexis Koulidis. SET3205 Heat Storage TTES and PTES. Lecture slides for SET3205 Heat Storage. 2024.
- [48] David Kröger, Milijana Teodosic, and Christian Rehtanz. "Modeling and contribution of flexible heating systems for transmission grid congestion management". In: *Electric Power Systems Research* 234 (2024), p. 110830. ISSN: 0378-7796. DOI: https://doi.org/10.1016/j.epsr.2024.110830. URL: https://www.sciencedirect.com/science/article/pii/S0378779624007168.
- [49] Maunu Kuosa et al. "Study of a district heating system with the ring network technology and plate heat exchangers in a consumer substation". In: *Energy and Buildings* 80 (2014), pp. 276–289. ISSN: 0378-7788. DOI: https://doi.org/10.1016/j.enbuild.2014.05.016. URL: https://www.sciencedirect.com/science/article/pii/S0378778814004083.

[50] T. Lenhart et al. "Comparison of two different approaches to sensitivity analysis of a distributed hydrological model". In: *Physics and Chemistry of the Earth, Parts A/B/C* 27 (9–10 2002), pp. 645–654. URL: https://swat.tamu.edu/media/90104/2002_lenhart-eckhardt-fohrer-frede_comparison-two-approaches-sensitivity-analysis-pce.pdf.

- [51] Hao Li et al. "Enhancing partial load efficiency of air source heat pump heating systems: A comprehensive review of magnitude, influencing factors, and improvement strategies". In: *Journal of Building Engineering* 97 (2024), p. 110715. ISSN: 2352-7102. DOI: https://doi.org/10.1016/j.jobe.2024. 110715. URL: https://www.sciencedirect.com/science/article/pii/S2352710224022836.
- [52] X. Luo et al. "Overview of current development in electrical energy storage technologies and the application potential in power system operation". In: *Applied Energy* 137 (2015), pp. 511–536. DOI: 10.1016/j.apenergy.2014.09.081.
- [53] L. Lyons et al. Clean Energy Technology Observatory: Heat Pumps in the European Union 2022 Status Report on Technology Development, Trends, Value Chains and Markets. Tech. rep. Luxembourg: Publications Office of the European Union, 2022. DOI: 10.2760/372872. URL: https://publications.jrc.ec.europa.eu/repository/handle/JRC130874.
- [54] Gabin Mantulet. Carbon Price Forecast under the EU ETS. Tech. rep. ICE Institute of Climate Economics, 2023. URL: https://dlowejb4br3l12.cloudfront.net/publications/executive-briefing/carbon-price-forecast-under-eu-ets.pdf.
- [55] Jacob Maxa, Andrej Novikov, and Mathias Nowottnick. "Thermal Peak Management Using Organic Phase Change Materials for Latent Heat Storage in Electronic Applications". In: *Materials* 11 (Dec. 2017), p. 31. DOI: 10.3390/ma11010031.
- [56] MOOI Noord-Holland. Warmte Overdracht Station Amsterdam. Accessed: 2025-02-10. 2025. URL: https://www.mooinoord-holland.nl/mooinoord-holland-inzendingen/warmte-overdracht-station-amsterdam/.
- [57] Netbeheer Nederland. Handboek Spanningskwaliteit in Nederland. Accessed: 2025-01-30. Netbeheer Nederland, 2016. URL: https://www.netbeheernederland.nl/sites/default/files/2024-02/handboek_spanningskwaliteit_2016_v1.1.pdf.
- [58] Nederlandse Emissieautoriteit. *Tarieven CO2-heffing*. Accessed: 2025-03-29. 2025. URL: https://www.emissieautoriteit.nl/onderwerpen/tarieven-co2-heffing.
- [59] NederlandVvE. Steeds meer conflicten binnen VvE's door verduurzaming en onderhoudsplannen. 2025. URL: https://nederlandvve.nl/vve-nieuws/steeds-meer-conflicten-binnen-vves-door-verduurzaming-en-onderhoudsplannen/ (visited on 01/28/2025).
- [60] HeatNet NWE. Netherlands HeatNet NWE: Low-Temperature District Heating in North-West Europe. Tech. rep. Accessed: 2025-01-29. Interreg North-West Europe, 2024. URL: https://vb.nweurope.eu/media/5541/netherlands_heatnet-nwe_lt-wp11_final.pdf.
- [61] Keith O'Donovan, Basak Falay, and Ingo Leusbrock. "Renewables, storage, intelligent control: how to address complexity and dynamics in smart district heating systems?" In: Energy Procedia 149 (2018). 16th International Symposium on District Heating and Cooling, DHC2018, 9–12 September 2018, Hamburg, Germany, pp. 529–538. ISSN: 1876-6102. DOI: https://doi.org/10.1016/j.egypro.2018.08.217. URL: https://www.sciencedirect.com/science/article/pii/S1876610218305137.
- [62] Rijksdienst voor Ondernemend Nederland (RVO). *Aardgasvrij Wonen en Werken*. https://www.rvo.nl/onderwerpen/aardgasvrij. Accessed: 2025-01-24. 2024.
- [63] P. Pardo et al. "A review on high temperature thermochemical heat energy storage". In: *Renewable and Sustainable Energy Reviews* 32 (2014), pp. 591–610. DOI: 10.1016/j.rser.2013.12.014.
- [64] Zsuzsanna Pató. *Gridlock in the Netherlands*. Accessed December 2024. Regulatory Assistance Project (RAP), Feb. 2024.
- [65] Planbureau voor de Leefomgeving (PBL). Eindadvies basisbedragen SDE++ 2025. https://www.pbl.nl/system/files/document/2025-02/pbl-2025-eindadvies-sde-plus-plus-2025-5472.pdf. Accessed: 2025-05-19. 2025.
- [66] Renewable Energy Installer. "Refrigerants in Heat Pumps: Evolution and Environmental Impact". In: Renewable Energy Installer (2023). Accessed: 2025-02-03. URL: https://www.renewableenergyinstaller.co.uk/2023/10/refrigerants-in-heat-pumps-evolution-and-environmental-impact/.

[67] DNE RESEARCH. Nationaal Warmtepomp Trendrapport 2024—2025. Accessed: 2025-02-22. 2024. URL: https://warmte-pompen.nl/nationaal-warmtepomp-trendrapport-2024-2025-gepublice erd/.

- [68] DNE RESEARCH. *Nationaal Warmtepomp Trendrapport 2025*. Accessed: 2025-06-30. 2025. URL: https://www.dutchnewenergy.nl/nationaal-warmtepomp-trendrapport/.
- [69] Hanna van Sambeek et al. De rol van slimme apparaten bij netcongestie op het laagspanningsnet: Een analyse van flexibiliteitsmogelijkheden, interoperabiliteit en beleidsopties. Tech. rep. TNO 2024 R12069. TNO, Nov. 2024. URL: https://publications.tno.nl/publication/34643334/VCEVgiNu/TNO-2024-R12069.pdf.
- [70] Ioan Sarbu and Emilian Stefan Valea. "Energy Savings Potential for Pumping Water in District Heating Stations". In: Sustainability 7.5 (2015), pp. 5705–5719. ISSN: 2071-1050. DOI: 10.3390/su7055705. URL: https://www.mdpi.com/2071-1050/7/5/5705.
- [71] Julia Sborz, Andreza Kalbusch, and Elisa Henning. "A Review on Domestic Hot Water Consumption in Social Housing". In: *Water* 14.17 (2022). ISSN: 2073-4441. DOI: 10.3390/w14172699. URL: https://www.mdpi.com/2073-4441/14/17/2699.
- [72] F. Schlosser et al. "Large-scale heat pumps: Applications, performance, economic feasibility and industrial integration". In: Renewable and Sustainable Energy Reviews 133 (2020), p. 110219. ISSN: 1364-0321. DOI: https://doi.org/10.1016/j.rser.2020.110219. URL: https://www.sciencedirect.com/science/article/pii/S1364032120305086.
- [73] Statistics Netherlands (CBS). Over half of electricity production now comes from renewable sources. Accessed: 2025-05-12. 2024. URL: https://www.cbs.nl/en-gb/news/2024/39/over-half-of-electricity-production-now-comes-from-renewable-sources.
- [74] TenneT. Generation Adequacy Electricity: Summary. Accessed: 2025-01-30. TenneT, 2024. URL: ht tps://netztransparenz.tennet.eu/fileadmin/user_upload/Company/Publications/Technical_Publications/Dutch/Summary_Generation_adequacy_electricity.pdf.
- [75] TenneT. Investment Plan 2024: Netopland. Accessed: 2025-01-30. TenneT, 2024. URL: https://tennet-drupal.s3.eu-central-1.amazonaws.com/default/2024-04/IP2024_Netopland_17-4-2024.pdf.
- [76] TenneT. Netcapaciteitskaart Congestiemanagement. Accessed: 2025-01-27. 2025. URL: https://www.tennet.eu/nl/de-elektriciteitsmarkt/congestiemanagement/netcapaciteitskaart.
- [77] TNO. TNO-2024-R11165. Tech. rep. Accessed: 2024-12-21. TNO, 2024. URL: https://publications.tno.nl/publication/34643172/0QzXXhpm/TNO-2024-R11165.pdf.
- [78] TU Delft. SET3205 Heat Storage: Tank Assignment 1. TU Delft SET3205 course. 2025.
- [79] Bureau Européen des Unions de Consommateurs (BEUC). How to Make District Heating Fit for Consumers. Accessed: 2025-01-30. BEUC The European Consumer Organisation, 2021. URL: https://www.beuc.eu/sites/default/files/publications/beuc-x-2021-044_consumer_rights_district_heating.pdf.
- [80] Urban Sustainability Directors Network (USDN). Connecting Existing Buildings to District Heating Networks Technical Report. Accessed: 2025-02-10. 2016. URL: https://www.usdn.org/uploads/cms/documents/161214_-_connecting_existing_buildings_to_dhns_-_technical_report_00.pdf.
- [81] Phil Vardon. SET3205 Heat Storage BTES. Lecture slides for SET3205 Heat Storage. 2024.
- [82] Ruben Verbruggen, Wytze van der Gaast, and Marc Londo. "Social acceptance of district heating: evidence from the Netherlands". In: Sustainability Science 18 (2023). Accessed: 2025-01-29, pp. 1201–1218. DOI: 10.1007/s11625-023-01452-8. URL: https://link.springer.com/article/10.1007/s11625-023-01452-8.
- [83] Thijs J.H. Vlugt and Mahinder Ramdin. Engineering Thermodynamics: Refrigeration & Heat Pump Fundamentals. ME45075. 2024. URL: https://www.tudelft.nl.
- [84] Qian Wang and Sture Holmberg. "Combined Retrofitting with Low Temperature Heating and Ventilation Energy Savings". In: *Energy Procedia* 78 (2015). 6th International Building Physics Conference, IBPC 2015, pp. 1081–1086. ISSN: 1876-6102. DOI: https://doi.org/10.1016/j.egypro.2015.11.055. URL: https://www.sciencedirect.com/science/article/pii/S1876610215017877.

[85] Warmte365. Door de warmtepompgroei stijgt de elektriciteitsvraag in sommige wijken tot 50 procent. Accessed: 2024-12-21. 2023. URL: https://www.warmte365.nl/nieuws/door-de-warmtepompgroei-stijgt-de-elektriciteitsvraag-in-sommige-wijken-tot-50-procent-65A9ACB1.html.

- [86] Warmte365. Individuele warmtepomp blijkt voordeliger dan buurtwarmtepomp. 2025. URL: https://www.warmte365.nl (visited on 01/28/2025).
- [87] WarmteprofielenGenerator. WarmteprofielenGenerator. https://warmteprofielengenerator.nl/. Accessed: 2025-01-22. 2025.
- [88] Werkgroep Emissiefactoren Warmtenetten. *Duurzaamheidsrapportage Warmtenetten 2021*. Accessed: 2025-05-12. 2021. URL: https://co2emissiefactoren.nl/media/sources/Duurzaamheidsrapportage_warmtenetten_2021.pdf.
- [89] Wolf GmbH. Types of Heat Pumps. 2025. URL: https://www.wolf.eu/en-de/advisor/types-of-heat-pumps (visited on 01/28/2025).
- [90] Michael Wolinetz and Jonn Axsen. "Cross-Country Comparison of Hourly Electricity Mixes for EV Charging Profiles". In: ResearchGate (2020). Accessed: 2024-12-21. URL: https://www.researchg ate.net/publication/341454431_Cross-Country_Comparison_of_Hourly_Electricity_Mixes_ for_EV_Charging_Profiles.
- [91] World Business Council for Sustainable Development. Renewable Industrial Heat Navigator Brief: Thermal Energy Storage. https://www.wbcsd.org/wp-content/uploads/2025/02/Renewable-industrial-heat-navigator-brief_Thermal-energy-storage.pdf. Accessed: 2025-05-19. 2025.
- [92] World Nuclear Association. Carbon Dioxide Emissions from Electricity. Accessed: 2025-05-12. 2023. URL: https://world-nuclear.org/information-library/energy-and-the-environment/carbon-dioxide-emissions-from-electricity.
- [93] Zhaowei Xu et al. "Investigation on the efficiency degradation characterization of low ambient temperature air source heat pump under partial load operation". In: *International Journal of Refrigeration* 133 (Oct. 2021). DOI: 10.1016/j.ijrefrig.2021.10.002.
- [94] Tinghao Zhang et al. Flow Rate Control in Smart District Heating Systems Using Deep Reinforcement Learning. 2019. arXiv: 1912.05313 [eess.SY]. URL: https://arxiv.org/abs/1912.05313.
- [95] Zonneplan. *Bidirectioneel laden: alles wat je moet weten*. Accessed: 2024-12-21. 2024. URL: https://www.zonneplan.nl/laadpaal/bidirectioneel-laden.



Thermal Stratified Tank Model

Within this thesis, the model assumes a perfectly mixed TTES, which reduced the complexity of the energy balance and potentially overestimates usable energy. In reality, stratification effects cause thermal layering. To address this, a stratified tank model was implemented to evaluate the performance and sizing of the TTES more realistically.

The tank was modeled as a vertically stratified volume, divided into layers. Each layer maintains its own temperature and energy balance based on the inflow and outflow of heat, shown in figure A.1. Heat inflow from the heat pump and e-boiler are injected at the top layer. Outflows are extracted from the top layer as well. The return flow, is inserted in the bottom layer of the tank.

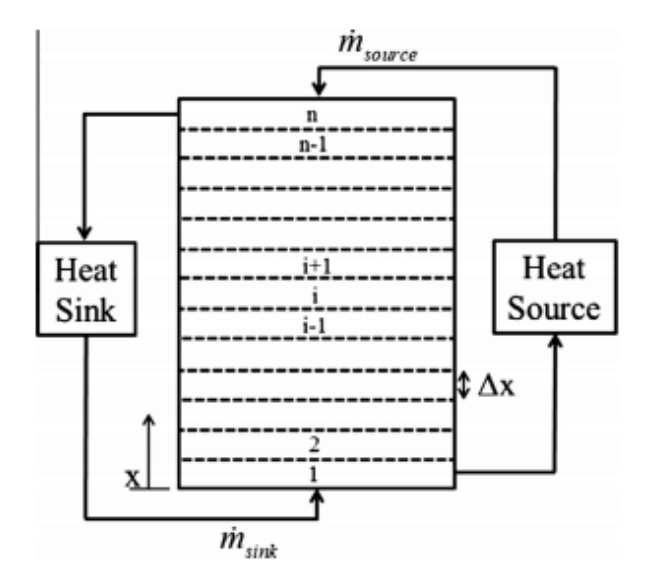


Figure A.1: Multi-Node modeling of stratified thermal energy storage tank [6]

The tank is assumed to be cylindrical with a height that is twice the diameter, to minimize the outer surface area, and thus losses to the surrounding [20].

Heat inflow and outflow are modeled based on heat supply and demand data. The incoming water temperature out of the heat pump and e-boiler are fixed at $T_{\text{source}} = 70^{\circ}\text{C}$ and the return temperature is $T_{\text{return}} = 40^{\circ}\text{C}$. Mass flows are calculated from energy flows using:

$$\dot{m}_{\rm in} = \frac{Q_{\rm in}}{c_w(T_{\rm source}-T_{\rm top})}, \quad \dot{m}_{\rm out} = \frac{Q_{\rm demand}}{c_w(T_{\rm top}-T_{\rm return})} \tag{A.1}$$

Let m be the mass of a single layer and T_i^t the temperature of layer i at time t. The general form of the energy balance for the top, middle, and bottom layers are given below.

Top Layer:

$$\begin{split} T_0^{t+1} &= T_0^t + \frac{\Delta t}{m c_w} \Big[\dot{m}_{\text{in}} c_w (T_{\text{source}} - T_0^t) + \delta_- \dot{m} c_w (T_0^t - T_1^t) \\ &- U A_1 (T_0^t - T_{\text{amb}}) - \frac{A_1 \lambda_{\text{eff}}}{\Delta z} (T_0^t - T_1^t) \Big] \end{split} \tag{A.2}$$

Intermediate Layers:

$$\begin{split} T_{i}^{t+1} &= T_{i}^{t} + \frac{\Delta t}{mc_{w}} \Big[\delta_{+} \dot{m} c_{w} (T_{i-1}^{t} - T_{i}^{t}) + \delta_{-} \dot{m} c_{w} (T_{i}^{t} - T_{i+1}^{t}) \\ &- U A_{\text{side}} (T_{i}^{t} - T_{\text{amb}}) - \frac{A_{\text{side}} \lambda_{\text{eff}}}{\Delta z} \left[(T_{i-1}^{t} - T_{i}^{t}) - (T_{i}^{t} - T_{i+1}^{t}) \right] \Big] \end{split} \tag{A.3}$$

Bottom Layer:

$$\begin{split} T_N^{t+1} &= T_N^t + \frac{\Delta t}{mc_w} \Big[\dot{m}_{\text{out}} c_w (T_{\text{return}} - T_N^t) + \delta_+ \dot{m} c_w (T_{N-1}^t - T_N^t) \\ &- U A_1 (T_N^t - T_{\text{amb}}) - \frac{A_1 \lambda_{\text{eff}}}{\Delta z} (T_{N-1}^t - T_N^t) \Big] \end{split} \tag{A.4}$$

Flow Direction

The variables δ_+ and δ_- are binary switches indicating the direction of net mass flow:

$$\delta_{-} = \begin{cases} 1 & \text{if } \dot{m} < 0 \\ 0 & \text{otherwise} \end{cases}, \quad \delta_{+} = \begin{cases} 1 & \text{if } \dot{m} > 0 \\ 0 & \text{otherwise} \end{cases}$$
 (A.5)

The simulation uses a time step that can be specified to adjust the accuracy. Euler forward integration is applied to update the temperature profile for each layer over time.

The results consists of temperature profiles per layer, mass, and heat flows in/out, and can be used to assess the performance of the tank.

Heat Transfer Coefficient and Coefficient of Conduction

A constant heat transfer coefficient of 0.5 W/m^2K is used to calculate thermal losses to the environment. This is a representative of typical insulation performance for thermal storage systems [78]. Thermal conduction between layers in the stratified storage tank is governed by a conduction coefficient of 0.5847 W/mK [78].

Results

Simulations show that, under theoretical charging and discharging conditions, a stratified tank produces and absorbs less usable heat than a perfectly mixed tank. Figure A.2 shows the temperatures plotted against time. The charging and discharging moments of the tank can be identified. Figure A.3 shows the theoretical heat in and output, the corresponding mass flow, and the resulting real heat in and output. The maximum combined input flow rate is limited to 6 kg/s, which is the result of two inflow sources, the heat pump and the e-boiler, each contributing up to 3 kg/s.

Temperature Profile with Heat Demand Considered

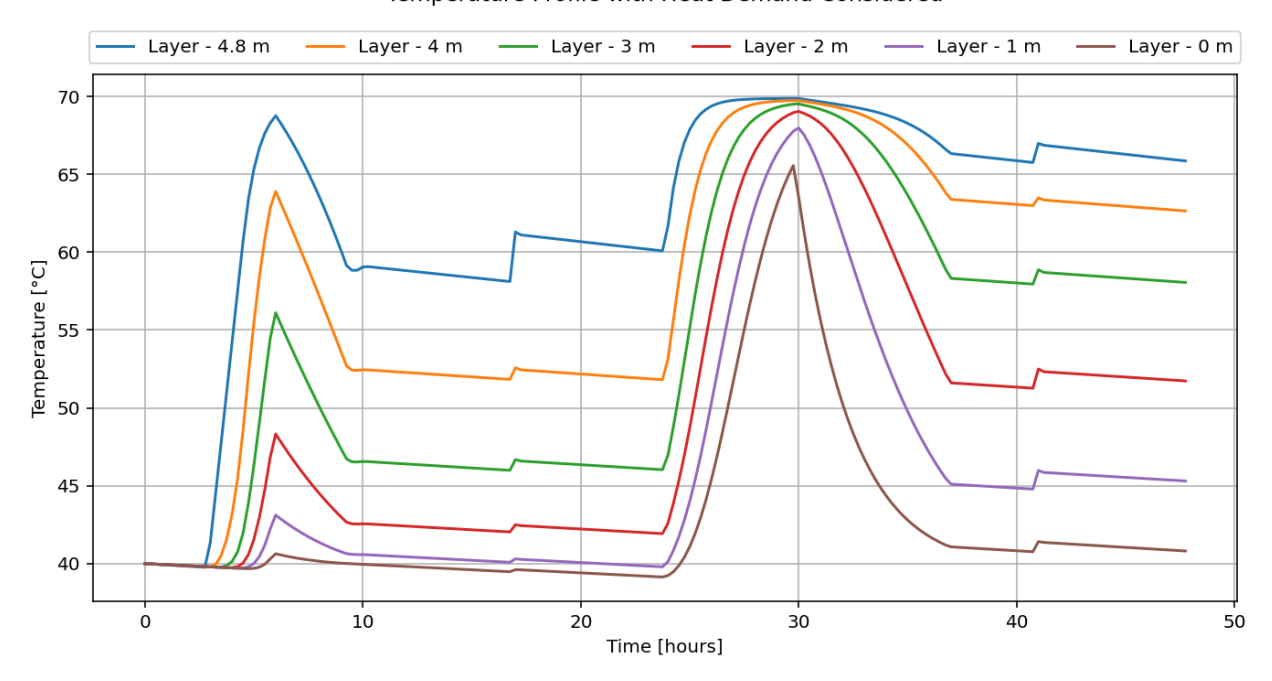


Figure A.2: Thermal layers in the tank model, during charging and discharging

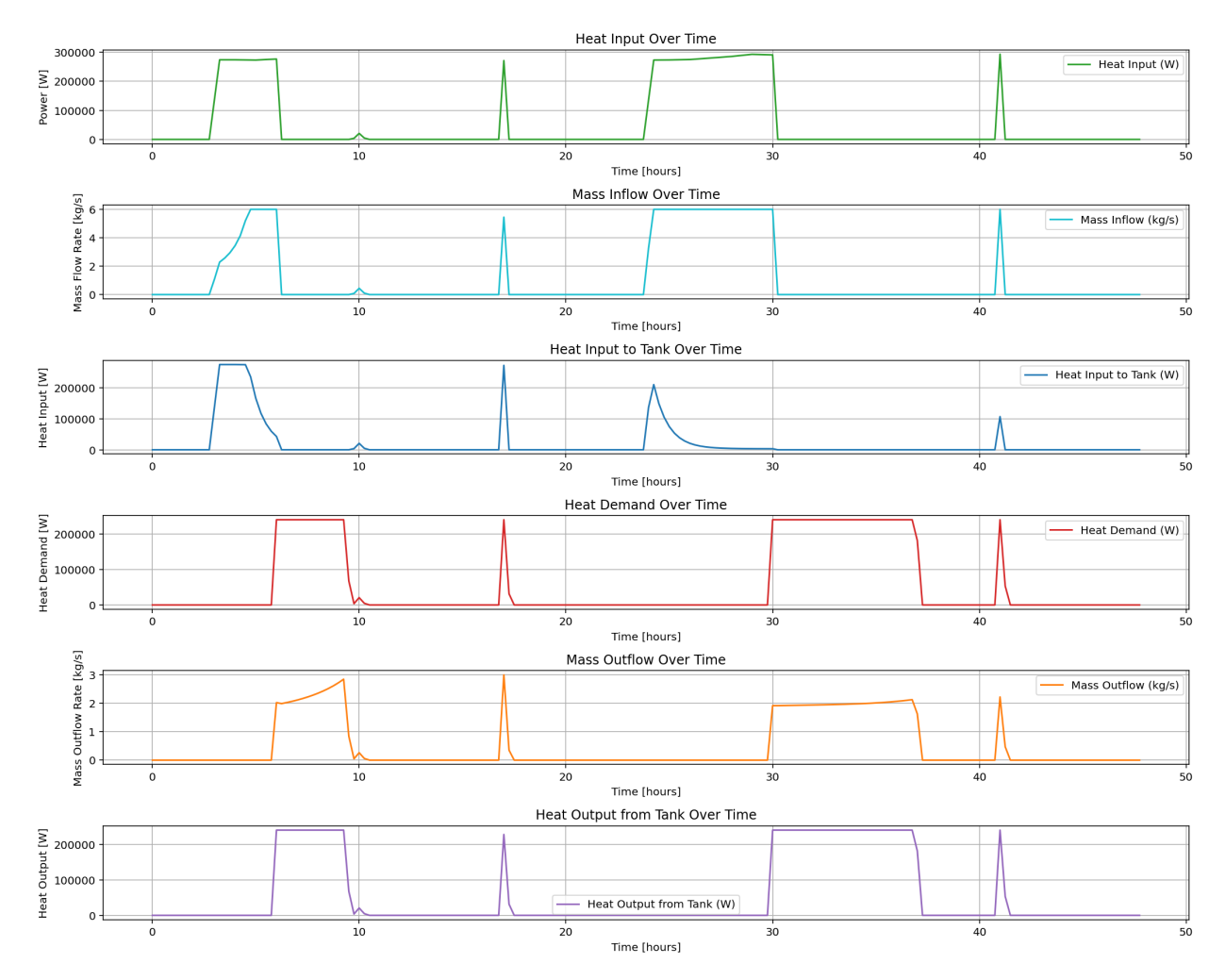


Figure A.3: Energy and mass flows within the tank model, during charging and discharging

The maximum flow velocity within the tank is a limiting factor in the charge and discharge performance. The plots show that the temperature in the upper layers increases rapidly during charging, and this rise eventually slows down. This is due to the reduction in temperature difference between the incoming hot water and the top layer of the tank. As ΔT decreases, the effectiveness of heat transfer decreases significantly, limiting the amount of heat that can be delivered to the tank.

During discharging, relatively fewer limitations were observed. This is because discharging draws from the top layer, where temperatures are highest, and returns cooler water to the bottom of the tank. The resulting temperature difference remains large enough to enable effective heat extraction, even with the restricted mass flow rate of 3 kg/s.

In practice, this means that designing a TTES for a dynamic thermal system requires careful consideration of stratification effects. It will be necessary to increase the TTES size, optimize flow rates, or apply mixing within the tank to manage temperature differences between temperature layers.